
1174

TRANSPORTATION RESEARCH RECORD

Rail Replacement and Maintenance Management

TRANSPORTATION RESEARCH BOARD
NATIONAL RESEARCH COUNCIL
WASHINGTON, D.C. 1988

Transportation Research Record 1174

Price: \$13.00

Editor: Naomi Kassabian

Production: Harlow A. Bickford

mode

3 rail transportation

subject area

40 maintenance

Transportation Research Board publications are available by ordering directly from TRB. They may also be obtained on a regular basis through organizational or individual affiliation with TRB; affiliates or library subscribers are eligible for substantial discounts. For further information, write to the Transportation Research Board, National Research Council, 2101 Constitution Avenue, N.W., Washington, D.C. 20418.

Printed in the United States of America

Library of Congress Cataloging-in-Publication Data
National Research Council. Transportation Research Board.

Rail replacement and maintenance management.

p. cm.—(Transportation research record, ISSN 0361-1981 ; 1174)

ISBN 0-309-04714-5

1. Railroads—Rails—Congresses. 2. Railroads—Track—Maintenance and repair—Congresses. I. National Research Council (U.S.).

Transportation Research Board. II. Series.

TE7

[.H5 no. 1174TF258]

380.5 s—dc20

[625.1'7]

89-3431

CIP

Sponsorship of Transportation Research Record 1174

**GROUP 3—OPERATION, SAFETY, AND MAINTENANCE OF
TRANSPORTATION FACILITIES**

Chairman: James I. Taylor, University of Notre Dame

Maintenance Section

Committee on Railway Maintenance

Chairman: Albert J. Reinschmidt, Association of American Railroads

Secretary: William B. O'Sullivan, Federal Railroad Administration

David M. Coleman, Ronald H. Dunn, Amir N. Hanna, Thomas B.

Hutcheson, Robert A. Kendall, Richard G. McGinnis, Willis H. Melgren,

Guenther W. Oberlechner, Ernest T. Selig, William J. Semioli, Harry E.

Stewart, Vincent R. Terrill

Elaine King, Transportation Research Board staff

The organizational units, officers, and members are as of December 31, 1987.

NOTICE: The Transportation Research Board does not endorse products or manufacturers. Trade and manufacturers' names appear in this Record because they are considered essential to its object.

Transportation Research Record 1174

Contents

Foreword	v
<hr/>	
Branchline Rail Replacement Strategies <i>D. E. Staplin and T. R. Wells</i>	1
<hr/>	
Fatigue Analysis of the Effects of Wheel Load on Rail Life <i>R. K. Steele and M. W. Joerms</i>	13
<hr/>	
Rail Testing: Strategies for Safe and Economical Rail Quality Assurance <i>Oscar Orringer</i>	28
<hr/>	
Production Processes To Yield Superior Rail Steel <i>W. H. Hodgson and R. R. Preston</i>	43
<hr/>	
Manufacture and Properties of Deep Head Hardened Rail <i>H. Yoshitake, Y. Makino, K. Sugino, H. Kageyama, T. Suzuki, K. Fukuda, and T. Miyata</i>	50
<hr/>	
In Situ Rail Head Rectification on British Railways <i>P. Leech</i>	57
<hr/>	
Technical and Financial Appraisal of a Contemporary Repair Technique for Rails and Crossings <i>R. S. Johnson</i>	60
<hr/>	
Examination of Methods To Achieve Rail Lubrication <i>Douglas B. Tharp</i>	78
<hr/>	
Report from FAST—Recent Test Experiences <i>R. P. Reiff</i>	81
<hr/>	

Foreword

Rail, among all track components, is a railroad's most valuable asset. Maintenance-of-way officers, therefore, must make rail acquisition, renewal, and maintenance decisions in the most effective way. Fortunately, the results of investigations into several decision-assisting methods, more improvements in the manufacture of rail steels, and the emergence of novel techniques for prolonging rail life are now available to provide additional management options.

A symposium, Rail: Replacement Strategies and Maintenance Management, was sponsored by the Transportation Research Board Committee on Railway Maintenance in June 1987 at the University of Illinois, Urbana-Champaign. The purpose of this symposium was to provide a forum in which several of these new approaches could be brought to the attention of track maintenance managers and subjected to a critical review. To a marked extent, this goal was realized by the participants during the program. A wider segment of the track maintenance management community will be reached through the publication and distribution of these papers. Nevertheless, the final measure of this symposium's usefulness will be the extent to which its revealed wisdom is actually applied to help maintenance-of-way officers meet their responsibilities for the care of an important corporate investment.

Special recognition is given to William B. O'Sullivan, secretary of the Committee on Railway Maintenance, for his work in assembling the papers contained in this Record. Mr. O'Sullivan oversaw the peer review of these papers and collected the final manuscripts for publication.

Branchline Rail Replacement Strategies

D. E. STAPLIN AND T. R. WELLS

To increase profitability, railroads need to improve their capital budgeting processes, which include capitalized maintenance projects such as rail that have traditionally been based on historical funding levels. The Association of American Railroads, through its Track Maintenance Research Committee, has developed a model for financial analysis of rail replacement projects, the Rail Performance Model. Use of this model has been demonstrated for mainline cases. In this paper its use to analyze branchline relays, including the transfer of used rail from one location to another, is described.

The pace of change in the rail industry has accelerated just as it has in many other traditional U.S. businesses. A trip down the Monongahela and Ohio River valleys past the silent steel mills brings one to grips with the enormity of what has happened and continues to happen to the U.S. economy.

The rail industry is struggling to cope with the changes to its traditional customers and attempting to learn to be more competitive in a deregulated environment in other markets. An earlier trend to large mergers, such as the CSX Corporation, has now been followed by downsizing. Regional and shortline railroads have sprung up from branchlines spun off by large carriers.

As always, the industry is concerned about its rate of return. CSX, for example, experienced an average return on invested capital of approximately 6.5 percent from 1982 through 1986. Return on shareholder equity averaged 9 percent, exclusive of special charges (1). In a regulated environment blame for a low rate of return was usually laid at the doorstep of the rule-making agencies. Under deregulation it is no longer possible to stand pat and point a finger. Therefore, it is doubtful if a "business-as-usual" atmosphere would now exist even if the domestic steel industry was still experiencing 100 million ton-years or Detroit was making 10 million automobiles.

Under depreciation-accounting guidelines adopted by the regulatory agencies in the early eighties, large-scale maintenance-of-way programs such as rail relays, crosstie replacement, and surfacing were freed from having an immediate impact on earnings. But the change from operating to capital expense was soon followed by the realization that steel and wood products could not be purchased with "earnings." Cash was and is still the preferred medium of exchange, and the increasingly competitive atmosphere has made cash scarce. There is a tendency today to view large capital replace-

ment programs in the same light as capital additions and betterments.

Meanwhile, out on the line-of-road chief engineers, division engineers, and roadmasters can now see the need for track improvement projects just as clearly today as they could in the past regardless of what name the accountant attaches to the dollars or what competitive conditions are like. What is needed is a medium by which both the maintenance engineers and the financial officers can feel comfortable about the allocation of maintenance funds.

Fortunately, in the late seventies a largely volunteer group under the auspices of the Association of American Railroads (AAR) began to prepare for the day when maintenance dollars would come under the same scrutiny as funds for a new yard. The Track Maintenance Research Committee, as it has come to be known, has developed an economic model for rail replacement known as the Rail Performance Model (RPM) (2). Although largely developed for heavy tonnage mainline situations, the RPM can be and has been modified for branchline use. This discussion will concern the use of the economic framework of RPM for making decisions on branchline rail replacement, giving an explanation of how the inputs to the economic and engineering framework of RPM can be developed for the branchline case.

Branchlines are a source of great interest for three reasons:

1. Large-scale upgrading programs have greatly eliminated jointed rail from heavy-tonnage, high-speed mainlines. CSX and other major railroads generally lay more than 80 percent of such routes with continuous welded rail (CWR). The replacement of jointed rail on these lines is nearly complete. This removes a potential source of secondhand rail for branchlines.
2. Concentration of joint elimination programs on mainlines has resulted in postponement of programs for branchlines. Unfortunately, restricted budgets now often do not permit a large-scale assault on these lines similar to that mounted on the mainlines in the seventies and early eighties.
3. The regional and shortline carriers often consist only of what would be considered branchlines by the large carriers.

RAIL REPLACEMENT PROCESS

At the risk of putting the cart before the horse, it seems prudent to examine the way in which rail is replaced before examining why. Some of the methods described here are used by all railroads regardless of size. Rail replacement programs

D. E. Staplin, CSX Rail Transport, P.O. Box 45052, Jacksonville, Fla. 32232-5052. T. R. Wells, CSX Rail Transport, 500 Water Street, Jacksonville, Fla. 32202.

can be divided into a source-and-use classification much like a crash-flow analysis.

Source

There are four main sources of rail. The most obvious is new rail purchased from steel companies. A second source would be used or secondhand rail purchased in the marketplace. Although this is perhaps not an important source for large railroads, it may well be the only source for a shortline. A third source is secondhand rail made available from track retirements. Finally, secondhand rail can frequently be reclaimed from a use site. Sometimes this rail can be used as is and other times it must be processed. This could include cropping out damaged ends or an internal flaw. Some railroads straighten rail that has been bent in service due to poor support or other surface breakdowns. Although inventory could be considered a source, it is always derived from one of the other four.

Use

Large replacement programs constitute the main use of rail. Both new and secondhand rail are installed out-of-face over a significant distance, generally more than 5 or 6 mi for a large railroad. Often these relays reach 40 mi in length. Such programs use large mechanized gangs and since about 1960, most of the rail laid in this manner has been continuously welded.

A second form of replacement is the patch program, used when local conditions dictate a smaller quantity but at least several rail lengths. Typical examples include replacement due to curve wear, corrugations, an epidemic of engine burns (which occur frequently where trains must stop to pick up and set off and are also common near the entrances and exits of passing sidings), and replacement of joints left in a track from wreck panels. The normal unit of such programs would be one or more ribbons of CWR (1,400+ ft), although some roads use jointed rail on higher-degree curves to allay fears of buckled track and for ease of transposing. This type of program is also seen occasionally for replacing rail on bridges. Rail utilized may be secondhand, new standard, or new premium.

A third major use of rail is for spot replacement, one rail or less at a time. The reasons for this are usually compelling, because such spot work is very labor intensive. The main reasons include fatigue cracks (or breaks), chipped or battered ends in joints, bent rails, and engine burns. In CWR territory, field welding of the replacement is common. In cold regions joint bars must sometimes be applied first until weather condi-

tions moderate and the weld or welds can be made without fear of adverse thermal stress patterns.

A fourth major use of rail is for new trackage, often in yard or industry locations, for which secondhand rail is used.

Finally, there is a catch-all miscellaneous category. Wreck panels, road crossing programs, and switch material all require rail, as do bonded insulated joints.

As a final consequence, the rail replacement process will generate scrap. Unless inventories are built up or depleted, the amount of scrap generated from relays (measured in lineal units) must equal the new and secondhand purchased rail plus the rail utilized from retirements.

Case Study

Before its consolidation into a single CSX road, the Seaboard System Railroad sources and uses for a typical year were as shown in Table 1.

It may be noted that 394 mi of source rail produces total use of 731 mi, which appears to be unbalanced. The reason for this is that rail reclaimed from the relay of the source material (394 mi less 24 mi of construction rail) cascades into other relays, a process that will be discussed next. In reality cascading creates an internal source that accounts for another 337 mi of rail.

CASCADING OF RAIL

Branchlines are often the recipients of rail relay through a process called cascading, which is the removal of rail and its relay to an area of lesser use. From the standpoint of the RPM, this cascading often occurs before the point of optimum life, when only a single stage of use is considered.

History

Almost from the start, railroads have been made up of lines with widely varying service demands. Annual tonnage, axle loading, speed, track geometry (curvature), and service class (passenger, bulk, merchandise, etc.) varied widely. Often lines having higher annual tonnages were also operated at higher speeds. Although the reduction of intercity passenger trains on most routes has reduced the concern for speed somewhat, freight axle loads have pushed higher. Some hint at the diversity of line characteristics today can be seen in Figure 1, which shows CSX track and traffic conditions for 1986 as reported in the Annual Report to the Interstate Commerce

TABLE 1 SEABOARD SYSTEM RAILROAD: SOURCES AND USES OF RAIL

Source of Rail		Use of Rail (program type) (mi)					
Type	Miles	Large Relays	Curve and Miscellaneous Patch	Single Replacements	Construction	Switch and Other	Wreck Panels
New	224	205	10		4	5	
New premium	80	30	40			10	
Secondhand purchase	40	40					
Retirements	50	30			20		
Secondhand	NA	210	70	30	10	10	7
Total	394	515	120	30	34	25	7

SOURCE: CSX Internal Records.

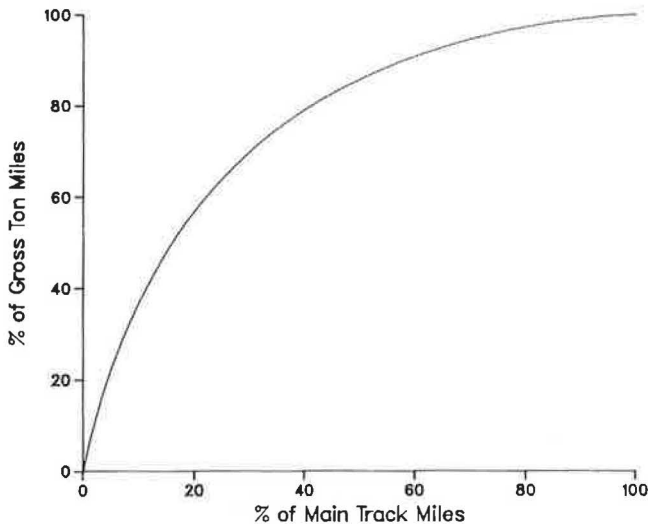


FIGURE 1 CSX track and traffic distribution.

Commission (3). Just focusing on annual tonnage as a factor, 66 percent of all gross ton-miles is carried on only 27 percent of the track and 95 percent of all gross ton-miles is carried on 58 percent of the main tracks.

Improvements in Rail Design

As service requirements increased, rail was improved. Design improvements first concentrated on heavier, stiffer sections to improve ride quality. Improved cross-section design reduced local stresses such as those at the head web fillet junction. Longer rolled lengths produced fewer joints. Better drilling patterns and continuous welding improved the joint area itself.

Better steel also contributed to rail endurance. Higher yield strengths, improved hydrogen elimination, and cleaner grain structure are significant examples.

Natural Process

The tendency of service demands to be concentrated and the steady introduction of improved rails made cascading a natural process. The introduction of control-cooled rail, for example, was a very important factor in increasing the margin of safety for high-speed passenger traffic. Today railway maintenance officers would cringe at the thought of running 100 mph on jointed 100-lb non-control-cooled rail. Earlier maintenance engineers reaped the benefit of using the displaced 100-lb rail for branchlines laid with 60- and 70-lb rail.

Cascading Today

Improvements in rail technology have vastly increased reliability of rail. Installation of CWR on lines with heavy traffic has improved reliability and safety. Still, cascading remains a valid process for several reasons.

First, as Figure 1 indicates, there is still a variety of lines to be maintained. Even the downsizing trends will not eliminate this variety, especially when yard mileage is considered. Considering the tendency of shortlines to be formed when

medium- and low-density lines are spun off, there may exist in the future a market for large railways to buy new rail and sell the released secondhand rail to their smaller partners.

A second reason for cascading is that rail manufacturing technology is still improving. Medium- and high-strength rails, continuous casting, and longer lengths have all become widely available in the last 10 years.

Maintenance officers are also becoming better informed for decision making. It is now known that the Weibull distribution can be used to model the occurrence of fatigue defects in rail (4). The increase in rates of failure causes the maintenance cost to escalate. Maintenance costs related to wear and joint conditions also worsen with time and use. Cost control, then, can be a very important reason for cascading rail. Figure 2 shows an example of reducing annual rail defects (and therefore costs) by cascading. As noted in the preceding section, earlier engineers did not upgrade the railroads totally. CSX, a composite of at least six major railroads, still has nearly 50 percent of its total trackage laid with jointed rail. Moreover, as shown in Figure 3, there is still much lightweight rail in the mainlines and branchlines. Inclusion of sidings and yards would make the percentage of lightweight rail much higher.

GENERAL ECONOMIC FRAMEWORK

At CSX, the Engineering Department staff was challenged to prove that removing welded rail and relaying it on a branchline was cheaper than simply waiting and buying new rail for that line. The RPM was used for this analysis. Cascading, it was reasoned, was economical if the present value of moving the welded rail (and associated future maintenance cost) was less than the total optimum (lowest) life-cycle costs for both the new and secondhand relay sites. These optimums for the sites assumed buying new rail and running it until scrap value was reached. To perform this analysis, specific candidate sites must be identified along with their history (tonnage and defects) and all related maintenance costs.

The general economic concept is shown in Figure 4. Premature replacement in the new rail territory will result in a higher

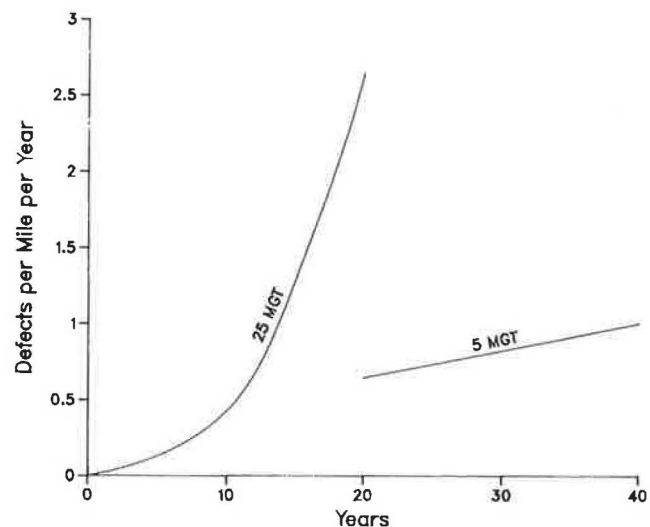


FIGURE 2 Rail cascade impact on yearly defects.

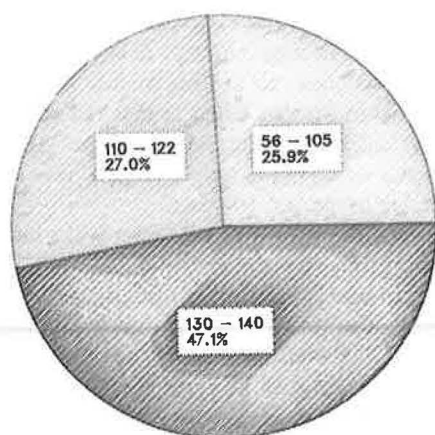


FIGURE 3 CSX transportation: weights of rail in main and branch track (rail weight in pounds per yard).

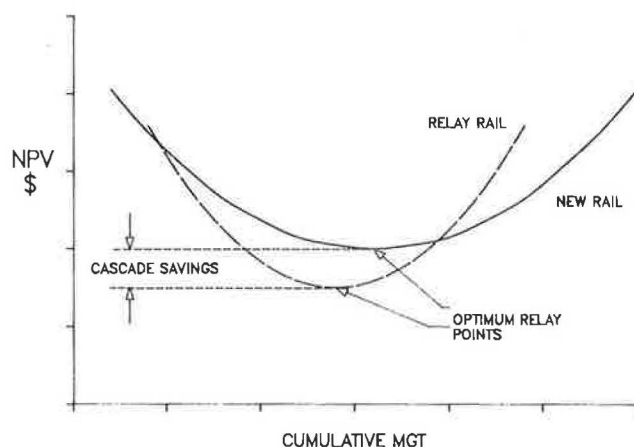


FIGURE 4 Economics of rail cascading.

net present value of costs compared with the optimum relay point. The optimum net present value can be maintained, however, if the railroad receives more than scrap value for the released rail. This seems plausible because the rail is still usable. Even though secondhand rail would cost more to maintain than new rail if both were laid at the same time, the secondhand rail site may receive the benefits of being rid of the existing, troublesome rail sooner or at a lower total cost. It is these benefits that offset the increased costs of maintenance. There may even be specialized cases in which the cascading process eliminates a costly maintenance problem in new rail territory. On CSX, for example, rail welded years ago by the oxyacetylene method is experiencing high rates of weld fa-

tigue. By cascading this rail (rewelding in the process) it is often possible to kill two birds with one stone, so to speak.

PRACTICAL EXAMPLES OF CASCADING

With the diversity of line characteristics and rail conditions on even a medium-sized road, the possible combinations for cascading are seemingly infinite. There are three general cases that draw in many of the site-specific possibilities.

Main to Branch

The most common example is that which has already been discussed—new rail laid on lines of heaviest use, which releases rail for branchlines experiencing high maintenance costs. Table 2 gives a relative idea of the financial stakes involved, using CSX as a hypothetical example. The reason a higher average life might be expected if rail is cascaded may be clearer after the next example.

Tangent to Curve

Often patch rail must be installed where a local condition such as curvature causes more rapid deterioration than that in adjoining rail. On high-tonnage lines this situation may warrant use of a premium rail. On medium- and lower-tonnage lines another alternative exists. Were new rail to be laid at such locations, say a curve, premium grades could not be justified. Suppose that the hypothetical life of new standard rail in this branch curve regime is 300 million gross tons (MGT) before scrapping. It may be possible to take rail from a mainline with 350 MGT and get another 250 MGT on the curve for a total life of 600 MGT. If side (high rail) or vertical (low rail) head wear is the condemning factor, such an example is entirely feasible. Thus the possibility of life extension through cascading is significant.

Transposing rail is a special subcase on which there are many opinions but little hard data. The authors encourage future work in that area.

Branch and Curve to Industry and Yard Tracks

All maintenance officers have had the experience of being on inspection and finding rail recently laid in track that is only marginally better than scrap. The classic reply to the inquiry that this generates is, "You should have seen what was here before!" Often this reply makes perfect sense. CSX in the past 5 years has averaged approximately 150 track-mi of curve patch annually. Premium rail and better lubrication may

TABLE 2 CSX HYPOTHETICAL NEW RAIL REQUIREMENTS

Case	Total Traffic (million gross mi)	Avg Total Life of New Rail (MGT)	New Rail Required Annually (track-mi)	Cost of New Rail Purchases at \$400/Ton (\$ millions)
Lay only new rail	291,984	500	584	50.2
Cascade	291,984	700	417	35.8
Difference		200	167	14.4

reduce this in the future, but it is not yet possible to estimate the net requirement. It is clear that significant mileage will still be involved and that disposal of this rail will also be necessary.

The normal case is that the released material is welded, of a heavy section, and contains one or more of the following defects: side wear, flattened head (vertical wear), plastic flow, and corrugation or other surface defects. If only mainline and branchline use is considered, this rail would be scrapped.

Consider Figure 3 and the 25 percent of the railroad still laid with lightweight rail or those miles and miles of yard track. This track needs relief from terrible joint conditions and girder strength to support relatively slow-moving loads. Consider the 56-lb rail that is laid in an elevator track to support 100-ton covered grain hoppers. Rail that is scrap for mainline replacement purposes is traded for rail that is scrap for another purpose. The relief that this "near-scrap" rail gives in some deplorable back track will cause a roadmaster to drag a released ribbon for miles. Truly, this is a case of the frog turning into a prince.

VALUE OF RAIL

Rail installation is one railroad activity in which the ratio of material value to labor costs is high. In an economic or budget analysis the price of the rail and associated fasteners needs to be given careful consideration. Rail that is purchased has a well-defined value, but as has been shown (Table 1), it may account for less than 50 percent of rail actually used. Is the rest automatically free? Rail already on the property is an asset and therefore must have some sort of value. To overcome this problem most railroads have an internal or "book" value for secondhand rail. Often it is based on an accounting convenience, which bears only a coincidental resemblance to economic values. To make sound economic decisions on branchline relays, realistic values must be established.

Economic Value as Determined by RPM

With the RPM, it is possible to estimate the value of existing rail being replaced by new rail. The analysis is based on traffic

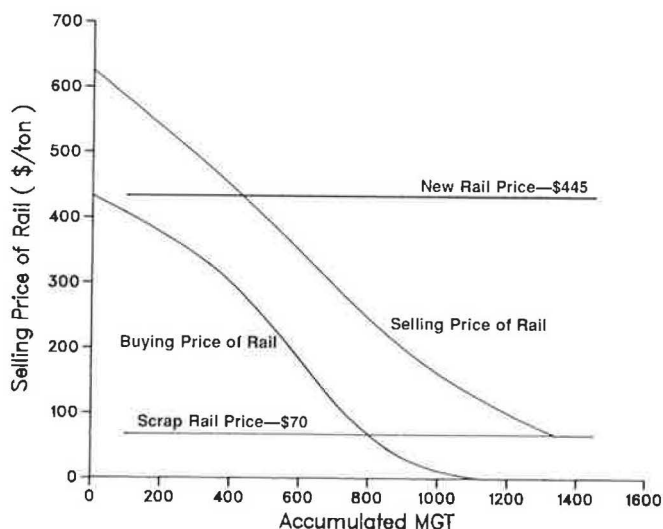


FIGURE 5 Minimum selling price needed to replace existing rail.

characteristics of the particular site and the fatigue history of the present rail. Figure 5 shows the concept of a "selling" value for rail in track (5). It is the minimum price that the owner would have to receive to be able to purchase and install new rail in replacement for the existing rail. The basis for the comparison is running the existing rail to scrap value. As the tonnage accumulates and the condition of the existing rail worsens (maintenance costs go up), the owner would have to receive less and less to persuade him to replace the rail because he is getting closer to the point when he will have to do so anyway.

This concept is extremely useful if a railroad is considering selling secondhand rail. It could prove especially beneficial for setting prices if the sale of rail to shortlines is considered. It is also useful in analyzing cascade opportunities, as will be seen in a later section.

Another curve produced by the RPM is termed the "buy" value curve. This curve shows the price the railroad could afford to pay for rail of comparable quality for use at that specific location (5). If a railroad is buying rail of a known defect and tonnage history for a specific use, it has a powerful tool to ensure value in its purchase.

Market Value of Rail

The existing market for new rail is relatively well defined and understood. The market for secondhand rail is relatively small and not well defined or understood. Moreover, recent abandonments due to consolidation and downsizing have changed that market.

Secondhand rail suitable for use in main tracks carrying any appreciable traffic is very scarce and commands a high price, usually between 60 and 70 percent of new. Because railroads usually find this sort of rail valuable for internal use, they rarely sell it. Normally it becomes available from a large abandonment where it cannot be immediately used and the time value of money to carry the inventory cannot be justified. Another source is through liquidation proceedings such as the Rock Island bankruptcy. The price is quoted "as is," which usually means with bolt holes. The price to the site at which the rail will be used must include any processing, such as cropping. Thus, if 132-lb rail is purchased for \$275/ton, cropping costs \$5/rail, and scrap sells for \$80/ton, the net price of rail ready for welding is almost \$300/ton, exclusive of freight.

Lighter weights of secondhand rail naturally command a lower price. Often this is in the range of 30 to 40 percent of new on a per-ton basis. Several years ago, 100-lb rail was scarce and brought a relatively high price for construction of yard and industrial facilities. Sections of 90- and 85-lb weights were more commonly available and therefore less valuable. With downsizing, 100-lb material is now commonly available and lighter weights probably do not bring a large premium over scrap. CSX will no longer weld rail under 100 lb/yd.

If relay rail is purchased to be used as jointed rail, care needs to be exercised over the drillings to ensure compatibility with existing rail. Purchasers can expect to pay a premium for drillings that are not common if they must obtain them to match their own.

Alternative Uses

There are classes of relay rail that do not fit easily into either of the previous uses. Earlier in this discussion, it was indicated that CSX is often happy to install worn, heavy weights of rail in sidings and yards. From the perspective of the RPM, this rail is not fit to install in a main or branch track and therefore has a value near scrap. From a market standpoint, who would be willing to buy this rail? A major railway would usually have this class of rail available on its own property. A contractor would not pay the same price per ton (and therefore a higher price per foot of track) for 100-lb rail when the lighter rail is perfectly adequate for a siding. Yet, if the railroad is willing to use the rail, how can it be claimed to have only scrap value?

There is another approach that considers the railway's alternatives. First, the railroad will never accept lower than scrap value, so that price becomes the floor. Although the worn heavier weights cannot be sold at sidetrack prices (per ton), the railroad might be able to sell them at the same price per foot. Then the buyer could afford to buy the heavier rail because there would be no price premium. If the railroad has lighter weights of rail in its stock that could have been used wherever the worn heavy rail was installed, an opportunity cost is assessed for the weight differential when this lighterweight rail is scrapped. More cash could be generated by scrapping the heavier rail. An example of such a calculation is as follows:

Given that the market price of 100-lb relay rail is \$160/ton and the market price of scrap rail is \$80/ton,

Calculate

1. Value of 132-lb siding rail if railroad has no surplus of siding-grade rail:

$$\begin{aligned}\text{Price} &= \$160/\text{ton} \times (100/132) \\ &= \$121/\text{ton}\end{aligned}$$

2. Value of 132-lb siding rail if railroad has surplus siding-grade rail:

$$\begin{aligned}\text{Price} &= \$121/\text{ton} + \$80/\text{ton} \times [(132 - 100)/(132)] \\ &= \$140/\text{ton}\end{aligned}$$

Under a surplus condition, the value of the 132-lb siding rail could be as high as \$140/ton or 75 percent above scrap. If a railroad needed siding-class rail of all weights, the value of the 132-lb rail of that class would drop to \$121/ton or 51 percent over scrap. Two cautions must be exercised in connection with these values. By laying heavier weights of rail in sidings, the railroad may have to spend more cash for fittings. Frequently, surplus tieplates are readily available for 100-lb rail but not for 132-lb rail. Buying new tieplates at \$4.50 each would add an additional \$90 to \$102/ton to the cost of installing the 132-lb siding rail. A second caution has to do with the buying and selling prices of rail. A railroad can earn market values for its secondhand rail if it sells directly to the end user. Often the railroad sells this rail to a broker, who must earn a profit. If the market value of 100-lb rail is \$160/ton, the carrier may realize only \$120 to \$130/ton by selling to a broker. Inventory carrying costs must also be considered whenever the rail is held, whether by a carrier or a dealer.

Summary

The three methods of valuing rail mentioned can be used to solve particular problems. There may also be cases in which rail value can be determined by using more than one method. Good economics dictates that the highest alternative price should set the value.

Traditional methods of grading and valuing rail have included measuring head and side wear, plastic flow, and examination of surface condition. The methods outlined here would be satisfactory for estimating purposes, but inspections should be included before buying or selling actually occurs. The best decisions can be made with sound inspection and when the history of the rail and future use are both known. Because the market for secondhand rail is relatively small, it is also suggested that relay economics be tested by using a range of values. The chances of estimating the value with precision are low because of potential price variability if there is no firm quote on the table.

CASCADE ANALYSIS WITH THE RPM

The RPM calculates optimum rail life by using expected future maintenance, relay, and other pertinent costs and treating them with the accepted financial analysis tool of net present value (NPV). This method is used by analysts to incorporate time factors into an economic analysis. The NPV method will be reviewed briefly as a beginning of the concepts underlying the RPM and cascade analysis.

Net Present Value in the RPM

In the NPV concept, cash in hand today is valued more than cash in hand at a future time. As an example, if \$1,000 were put in a savings account today and earned 5 percent per year, next year there would be \$1,050 in the account. In the following year, there would be approximately \$1,103 in the account. Reversing the logic a bit, if it were desired to have \$1,100 in 2 years, approximately \$1,000 would need to be deposited today. The RPM uses this logic of discounting future expenditures to today's cash equivalent in testing rail relay strategies. This enables comparisons to be made between alternatives on an "apples for apples" basis.

The RPM estimates the necessary cash maintenance requirements for rail into the future. It then calculates what it would take to finance that maintenance by putting a fixed sum of money in a high-yield account. High yield refers to what a company feels it needs to earn on capital investments before they are made. These investments, usually internal to the company, have earnings that are above what is traditionally seen in savings accounts, certificates of deposit, and bonds. For example, today the individual investor can buy various financial instruments in the established market with earnings of 5 to 10 percent per year. Many companies feel that a project is not worth investing in unless it returns 15 percent. If a company is cash poor, it may raise that threshold as a means of determining its spending priorities. A company's threshold is

typically higher than market investments because of the higher likelihood that the benefits from an expenditure will not be realized.

Early versions of the RPM keyed on the rate of defect formation as the means to estimate future rail maintenance costs. As further research quantified other maintenance problems, and therefore maintenance expenditures, they were incorporated into the model. The prediction of defects shows that they can be expected to grow in number as the rail gets older, meaning that annual maintenance expenses also grow. Maintenance expense that grows as an item gets older is a common occurrence but predicting the type of growth requires research.

Rail defect formation was first used in the RPM to predict future maintenance costs because maintenance-of-way engineers began asking at what point it is more economical to replace rail than to fix defective and broken rail. Many believed that defect formation may be an explosive situation, resulting in defect occurrences over a period of a year or two followed by dramatic growth to unacceptable levels. Analysis of defect trends now shows that over a long period, defect occurrences do grow, but rarely in an explosive manner. From year to year, there may be wide variances in defect occurrences; an upswing in occurrence may make it appear as if the defect growth were explosive. Figure 6 shows the number of defect occurrences on a branchline for which a cascade analysis was performed.

Because defect occurrences may take a random pattern from year to year, trend lines over several years are needed. Overlaid on Figure 6 is an example trend line from which costs associated with the defect occurrences can be assigned in each year, representing the expected maintenance costs. Over the years, the maintenance costs increase as the defect occurrences increase. There is an optimal year when an out-of-face rail relay is more economical than continued increased maintenance costs. The RPM tests for the year in which the optimum occurs, which is the year with the lowest NPV.

The NPV that will be referred to in the upcoming text includes all predicted future rail maintenance costs plus the

costs of rail relay, adjusted for time. The time adjustment is the discounting process described previously in which future costs are reduced by the annual discount rate for each year into the future in which they will occur. Rail relay costs are estimated on the basis of the cost of rail; other track material (OTM); labor associated with installation, including fringes; other overhead; and project costs, such as rail welding and transportation. Rail maintenance costs hinge primarily on costs of defects, although other costs, including tie and surfacing costs and rail wear, have been experimented with in various versions of the RPM. The RPM also includes tax effects in the calculations. Although no details will be given here, in past years the tax effects reduced the theoretical cost to do maintenance and relay rail by approximately 50 percent. This is mentioned because NPV values may be quoted that will be significantly below the cash outlay to relay rail.

RPM for Cascade Analysis

Cascade analysis was initiated at CSX when the economy of rail relay on secondary lines was in question. Quite an expenditure is made to move rail from one site to another in order to minimize new rail purchases. Several questions were asked—for example, does a secondary line ever justify a rail relay, and if it does, is it truly economical to cascade instead of buying new rail? Earlier the RPM had been used to develop rail section standards and guidelines for premium rail use at CSX. Benefits of rail replacement extend many years into the future. On the lighter-density lines, heavy modern sections, if laid new, could be expected to last 50 years or more. Some results of the RPM suggest that in certain branchline situations, a low-maintenance CWR may never need a relay after installation; instead, ongoing maintenance after a relay is the most economical.

However, branchlines are rarely endowed with heavy, good-quality rail that can be expected to last forever. Instead, many have lightweight rail with poor joint conditions and other maintenance problems. Use of the RPM allows an evaluation as to when a rail replacement would be the most economical from an investment point of view.

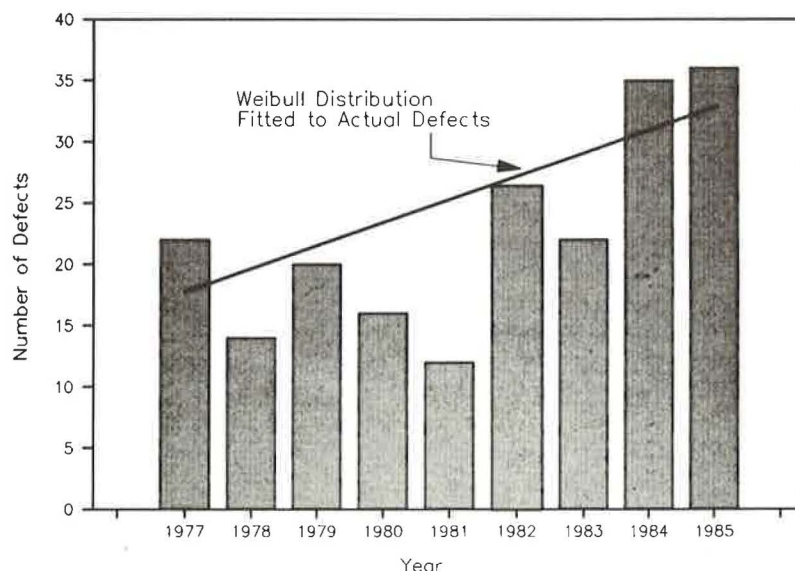


FIGURE 6 Rail defect trending.

The RPM was developed by looking at rail replacement on high-density mainlines, typically with 20 MGT of traffic annually. Despite this intent in its development, the model can be used for lighter-density lines, and various versions have been made to handle branch- or light-density lines. To properly evaluate a lighter-density line, a longer time horizon to estimate the life of the replacement rail is needed than for heavy-density lines.

The typical reason for branchline relay is jointed rail burdening the line with much more track maintenance costs than welded rail. On lines with poor rail, more attention to maintaining joints, such as tightening bolts and replacing bars; decreased tie life in the joint areas; potentially more surfacing costs; and potentially shorter surfacing cycles result in higher maintenance costs. The RPM in the various analyses shows that the higher maintenance costs associated with jointed rail shorten the economic life of that rail.

Because rail has a long life, the time effects on expenditures for maintenance have a very dramatic impact on the value rail has for a particular site. In a heavy-density line with a high level of defect occurrences, the value of rail could be as low as that of scrap. But by transferring that rail to a site that has a fraction of the traffic of a heavy-density line, defect occurrences can also be expected to lessen. Defect occurrences are expected to go down on an annual basis because they occur as a direct result of use. If a branchline is close to justifying new rail, it most likely can afford to pay a reduced price for secondhand rail that can cut out most of the maintenance costs of the existing rail.

To perform the cascade analysis with the RPM, two track sites need to be chosen that will be rail relay candidates in the next couple of years. One site should be a new rail site, where the service requirements call for the best materials. The other site should be a branchline site, in which it seems logical to use secondhand materials.

At CSX, a special version of the RPM was developed to analyze cascade economics. In that version, an economic analysis is done first on the heavy-density line that is used as the new rail site. The model is run assuming that the rail in track will stay there until it is considered scrap for that site. This is a key assumption for valuing the rail during the years before it is considered scrap.

Choice of Cascade Sites

As discussed earlier, the further into the future that money is needed, the less money today that has to be saved to cover the future expense. For rail, the cost to relay is a large component of the total cost and one that occurs all at once. If the rail relay cost occurs over the next couple of years, it will be the major component of the NPV; the other major component is the annual maintenance cost. On the other hand, if the best time to relay rail is decades in the future, the NPV component for the relay will be relatively small.

This means that when the NPVs for various sites are considered, those sites with relays in the current or next few years will have the largest NPVs, whereas the sites with relays deferred for several years will have lower NPVs. Taking that analogy a little further, when one site is analyzed, the NPV the year after the relay will be the lowest, because the rail relay is

a past expenditure, which is not included in future costs. On the other hand, in the year of relay, the NPV will be the highest, because cash is needed immediately to fund the project.

When evaluating a site in which new rail is being considered, the larger railroads will hope to use the released rail on lighter-density lines, or possibly to sell the rail. The question then arises as to the value that the rail needs to make it worth removing before it is scrap. This value of rail can either be its sale price or its internal value for cascade purposes.

The RPM was used to produce various sale prices of rail in the years preceding the optimal year of relay, when the rail is considered scrap. The analysis consists of calculating the NPV to relay the rail this year (no consideration for the optimal time for relay) and that for rail relay in the optimal year. If the optimal year is in the future, the NPV to relay in the current year must be lowered to match the NPV of the optimal year, or there will be an economic loss. To do this, it is assumed that the rail is worth more than scrap and that the extra value above scrap will be treated as a credit against the relay, lowering the NPV. A calculation is made to determine how much extra value the rail has to contain to equal the optimal NPV. This procedure then assumes that because the NPV for relay this year and the optimal year are the same, the railroad is indifferent to relay timing.

The extra value calculated to bring an NPV down to the optimal NPV is prorated over the tons of rail that would be removed from track. This proration is added to the scrap value of the rail to arrive at a price per ton that the railroad needs to realize to make the relay worthwhile. Figure 5 shows the selling price, which is the value the railroad needs to get for rail, at the various points during the rail life.

Because installation costs are included in the rail relay analysis, the railroad will have to get more money for recently replaced rail than the price of the material alone. This reflects the cost of undoing work recently completed. Obviously, during the period of time that the railroad would need to sell the rail for more than the cost of new rail, there is no reason to expect that rail to be relayed for cascading. Once the selling price of the rail becomes less than the cost of new rail, the rail can be considered available for cascade. As a practical matter, most railroads probably would not consider rail available for relay until its selling price was significantly less than the value of new rail.

It must be kept in mind that the value of rail at one site can be different than the value of identical rail at another site. The purpose of cascading is to reduce total costs of relay and maintenance. The special CSX version of the RPM used in the cascade analysis can produce a table of rail selling prices from the new rail site and read them into an analysis for a branchline. This was done for one example to see whether there are economies of cascading. The result showed a considerable drop in NPV for rail maintenance of the two sites together when rail was cascaded from one site to another site. The alternative tested was new rail at both sites.

Example of Cascade Analysis

The RPM used actual data from both sites to estimate the expected maintenance costs in the future. The new rail site was

a high-speed line carrying several passenger and piggyback trains a day, plus a medium to heavy volume of other traffic, for a total of 43 MGT per year. The track consisted of relatively old welded rail with over 600 MGT of traffic on it. Its defect rate was still low—less than one defect per mile per year—with little evidence that the rate would suddenly grow. This site was considered for relay with the idea of producing good quality relay rail and with a concern over future problems with oxyacetylene welds. Otherwise, relay of the line would not have made good sense economically.

The branchline considered handled about 12 MGT a year of traffic; a good portion of that was unit coal trains. This line had 100-lb jointed control-cooled rail. The defect rate was rising on the line, and tie and surfacing work were on short cycles because of joint conditions. Maintenance levels on the line were relatively high and were expected to continue to grow.

On the branchline, the RPM was used to see whether the site could support a rail relay. The analysis showed that a new rail relay program would be justified in about 5 years. This analysis confirmed that expected maintenance costs were too high to expect to maintain the line without rail replacement. The NPV of relaying the branchline was noted, and a second analysis feeding the used rail characteristics from the new rail site was used. In this analysis, it was assumed that the year the rail was removed from the new rail line would be the year that it was laid in the light-density line. This means that the cost to the branchline to buy the rail would be down each year that it waited to buy it, because the rail's selling price would fall every year on the new rail site.

When this analysis was done, the optimal time for relay was still about 5 years into the future, but the NPV of this strategy was noticeably below that of the first strategy, as shown in Figure 7. Although it may be surprising that the time of the relay was coincidentally in the same year instead of earlier, it must be remembered that over time the selling price of the relay rail is going down faster than the rise in maintenance costs on the branchline. There does come a point when the rise in maintenance costs exceeds the drop in price of the rail, which is the point at which the cascade should be performed.

Timing

To further demonstrate that cascading can be beneficial, more work was done with the CSX version of the RPM to see what value should be placed on relay rail available for branchline use. Because the relay rail gets more use at its original site, its value on the branch site falls. The "buy" line in Figure 8 illustrates this concept. During the years in which the selling price exceeds the buying price, cascading relay rail to the branchline site would not be economical. In this example, after 500 MGT, there does come a point when the branchline buying price and the new-rail selling price are equal. Then for the following several years, a gap develops, because the branchline buying price exceeds the new-rail selling price. Eventually, the rail can be expected to require so much maintenance, even on the branchline, that it will be considered scrap, at which point it does not pay to cascade it. Figure 8 shows this point being reached at about 1,500 MGT.

Theoretically, the most beneficial time for the railroad to cascade is when the difference between the branch site's

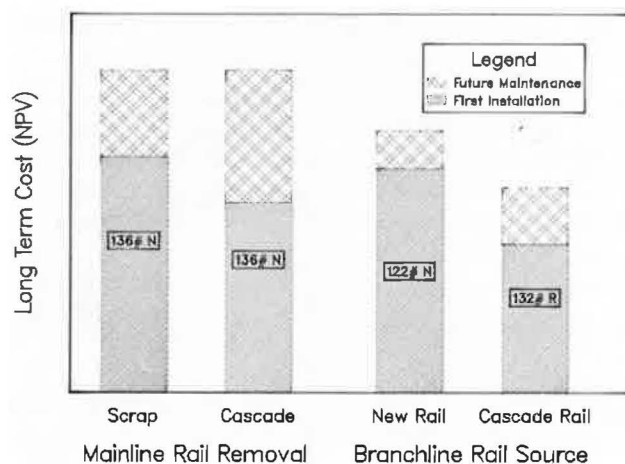


FIGURE 7 Rail cascade cost example.

buying price and the new-rail site's selling price is the maximum. In Figure 8 the maximum buy-sell differential appears to be between 1,000 and 1,200 MGT. A precise mathematical solution is possible but has not yet been incorporated into the model.

An explanation is in order for why rail can have a higher value for a branchline than a higher-density mainline. The NPV calculation by the RPM includes both maintenance and relay costs. Because a time discount is made for a future cost, transferring rail with relatively high maintenance to a light-density line will lower the use-related annual maintenance costs substantially. For example, if rail is transferred from a 25-MGT line to a 5-MGT line (i.e., the traffic falls 80 percent), as shown in Figure 2, the annual maintenance levels are expected to decrease 80 percent. Likewise, the future increase in maintenance costs related to use on the branchline will be expected to be 20 percent of the high-density line costs. With these assumptions, the rail-related maintenance costs expected in one year on the high-density line would now be spread over 5 years on the branchline. The NPV of the costs spread over 5 years is significantly less than if they occurred in the current year. As a result the maintenance component of the RPM NPV substantially drops. When the maintenance component of NPV falls, the value of the rail for use on the branchline rises.

Other Considerations

The preceding discussion describing cost impacts of cascading reveals that there are significant economies. A major assumption underlying this analysis is that the branchline receiving cascaded rail is expected to be operated for many years into the future. In the railroad environment today where many are downsizing, the possibility of divestiture of a branchline may preclude it from having a rail relay performed. Because newly formed carriers enjoy reduced unit labor costs, improved labor productivity, or government-sponsored funds, or all three, it may be more efficient to have them perform the work. If the Class I railroad did the work before the sale, the selling price added to the property might not recoup the expenditure.

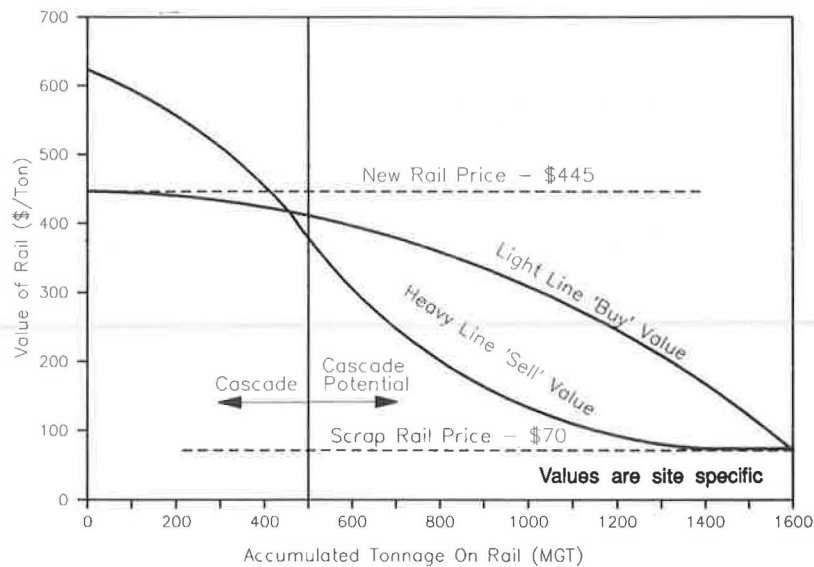


FIGURE 8 Rail cascade values from heavy to light tonnage lines.

RPM ON BRANCHLINE CASES

Analysts looking at the economics of branchline relays may lack hard data on the source of the rail to be used. In the case of a shortline, the rail may have been purchased from another railroad or supplier. It may have been part of the inventory when the property was purchased. In these cases, cascade analysis is not relevant and the RPM can be used to evaluate the potential relay site directly. The analyst will often be without hard data for some key inputs, but this does not mean that all is lost.

Areas of High Sensitivity in RPM

Fortunately there is help available for the analyst by using the RPM (6). Table 3 gives input parameters with their corresponding degrees of sensitivity. The degree of sensitivity is a measure of the impact on the output (results) of a change in a particular input.

Branchlines represent an interesting challenge for choosing a discount rate. The default value in RPM is established near the industrywide cost of capital. Applying this to projects of low to average risk in the rail industry, such as new rail relays, is acceptable. Applying it to branchlines may be dangerous unless other provisions for risk are made. Relays on mainlines have little risk because the commodities carried are diverse. On branchlines, the cargo may be limited to only a few customers or a few commodities. There is a much greater chance of a radical change that could render the anticipated benefits of the rail replacement useless. Financial experts should be consulted, but a one- or two-point increase in the discount rate would be acceptable if no other information is available.

An alternative approach to hiking the discount rate would be to use high and low estimates for traffic or benefit levels so that the results of a major change could be anticipated. As mentioned elsewhere, the same approach to estimating the

fatigue history of the rail should be taken where hard data are not available.

Not shown in Table 3 but discussed in a previous section is the input price of rail. The methods outlined provide a framework for estimating the value of rail that yields a wide variation in prices depending on the rail quality and intended use. First cost has significant impact in a discounted cash flow, and therefore input rail values are also highly sensitive.

If rail to be used for relay has a known defect and tonnage history, the Weibull parameters can be determined for use in the RPM either through graphic plotting or use of a computer model such as WIBPAC (7). If the history is not known, then several options are open:

1. Expert opinion: If the analyst is familiar with Weibull parameters from rail defect data, a reasonable range of values may be estimated based on the type of rail, age, wheel load history (if available), and wear. Weibull slopes typically range between 2.0 and 4.0, with the average slightly above 3. The characteristic life ranges from 500 MGT to over 3,000 MGT, with an average near 1,500 MGT. In general, the more inferior the design and chemistry, the higher the slope and the lower the characteristic life. Inferior track support conditions would also result in higher slopes and lower characteristic lives. A "best case-worst case" approach should be considered.

TABLE 3 RPM PARAMETER SENSITIVITY

Category	Parameter	Relative Sensitivity
Economic	Discount rate	High
	Derailment cost	Medium
	Depreciation method	Medium
	Defect repair cost	Low
	Gang costs	Low
Engineering	Weibull slope	High
	Characteristic life	Medium
	Inspection reliability	Medium
Traffic	Tonnage rate	Medium
	Previous tonnage	Medium

2. Use of similar type rail where data are available would certainly provide an estimating vehicle; care would have to be taken to ensure that any differences in past use were considered. Again, a range of values should be used.

3. If only recent tonnage and defect histories are available, a regression on the defect rate per million gross tons could be attempted. Making better predictions in this case is a current priority of the Rail Working Group of AAR's Track Maintenance Research Committee.

4. The Rail Working Group, in conjunction with a research team from George Washington University, has developed a Bayesian model that will predict future defect probabilities if some recent tonnage history and defect information are known. An alternative model has also been developed by the Santa Fe Railroad.

Defect records should be examined closely to determine whether it is appropriate to include all data in an analysis. If rail with a history of weld failures were to be rewelded and laid in a branchline, the weld failure history should be excluded from future projections. If rail with a history of joint failures is cropped, welded, and relayed, future projections should not be made with historical joint failure data.

A second problem arises in making defect projections on lines with very high failure rates. The Weibull distribution assumes that a rail can fail only once (no multiple defects) and that it is removed from the population upon failure. Inspection and detection of cracked or broken rails lead to the introduction of replacement rails. Often no history of these rails is known. In time, these rails may also fail, but to lump their statistics with those of the original rail is technically incorrect. The RPM assumes that replacement rails have a use history similar to that of the original rail. In a main track, this may be a valid assumption because there is usually a conscientious attempt to match wear patterns. On branch tracks, especially lower-tonnage ones, this assumption is tenuous at best. The failure history must be closely scrutinized. Perhaps a regression would give a better explanation of future trends than a Weibull plot, especially if there has been a high failure rate for an extended period of time.

Other Areas of Concern

The RPM contains a matrix of cost savings for replacing joints with CWR. The pretax savings for branchlines discounted at 6 percent are approximately \$14,000 for 1 track-mi. Moreover, the timing of these savings is spread evenly over the future years. This matrix was designed as an average case, which may well understate the condition of some deteriorated branchline rail.

Not only the rail can cause maintenance headaches, but the other fittings as well. Many lighter weights of rail have joint bars that are obsolete in design. Skirted bars with spike notches cut out are especially famous for quarter cracks. If the spike holes have been used, poor anchorage will often result in severe cocking of and damage to the joint ties. If the rail does run and these spike holes are not used, the bars often hit spikes of an adjacent tie with similar results.

With poor anchorage, there is increasing risk of pull-aparts, broken center bars, and chipped rail ends. The joints them-

selves are often mechanically worn, making it impossible to keep them tight. The surface deteriorates as a result of poor joint conditions.

Tieplates are often of the small, single-shoulder variety that have inadequate bearing area. This type of tieplate tends to rotate, causing an irregular gauge. Small plates have also been known to curl up under heavy axle loads, which accelerates tie deterioration.

Unless rail support is reasonably well maintained, lightweight sections are prone to becoming surface bent, including in the lateral direction. Often this accentuates rock and roll, not to mention gauge problems.

The deterioration mechanisms described here result in track that will not dependably support regular use, especially where heavily loaded equipment is involved.

In the long term, maintaining such a line would likely result in escalating costs. There may even be cases where repair material is no longer available from internal stocks and must be purchased. Maintenance savings from 10 to 50 percent higher than those calculated by the RPM are possible on branch and industry track with extremely poor rail. It is even possible that derailments other than those due to broken rails will be saved by relay. A future modification of the RPM will permit the user to identify site-specific problems. Currently it is recommended that the analyst consider those items not included in the model in a separate analysis.

Derailed costs are shown (Table 3) to be of medium sensitivity. They are based on experience with averages. Although average costs are used in the model, the deviation from average is considerable, and railway management tends to be averse to risk as a result. The concern over expensive mainline accidents raises the sensitivity of this variable for those territories. On branchlines, incidents tend to be much less costly and the analysis therefore is less sensitive. Site-specific traffic should be considered for relay analyses, however, because there are branchlines that carry high volumes of chemicals and other potentially dangerous commodities. On very light tonnage lines, the number of derailments may be a more important factor than average expense. In that case the default value for the probability of a derailment given a rail failure may need to be changed.

The RPM does not include any savings for transportation. Under normal conditions, work rules do not permit running-time reductions to be turned into hard dollar savings. The branchline (or shortline) case may be an exception. Raising speeds from 10 or 25 mph to 25 or 40 mph may well result in productivity gains if local schedules can be rearranged. For example, a 10-mi branchline will take more than 2 hr to serve at FRA Class 1. Improving the running speed to 25 mph would cut the service time in half because of over-the-road movement. Reliability of service could be important to any carrier.

User's Guide to RPM

As noted earlier, the prospective analyst can obtain the RPM User's Manual (6). By so doing, inputs to RPM can be researched ahead of time. Some of the inputs assume that welded rail will be installed, but jointed rail can also be handled. A shortline is likely to be in a better position to

estimate costs than a large carrier. Current default values are more pertinent to large railroads.

CONCLUSION

The RPM provides the basic economic framework for evaluating branchline rail relays. Although special programming improves the productivity of these analyses, the standard version available from the AAR Research and Test Department is entirely adequate for the job.

The RPM can handle branchline analysis as part of a cascade program or as a stand-alone. Rail values must be carefully thought out in the stand-alone case.

For railroads with the proper variation in line use, cascading has been demonstrated to provide substantial benefits compared with a strategy of relaying only new rail. This finding affirms what maintenance engineers have believed and practiced for years. The model goes on, however, to provide a means of ranking expenditures and making more nearly optimal relay decisions.

Several input items to the RPM need careful consideration because of their sensitivity. One of these is the price or value of rail, especially relay rail. The RPM is capable of valuing rail if adequate history of use is available. Market value and alternative use provide other avenues if insufficient history exists.

Interest (discount) rates or traffic type and volume, or both, need to be considered as a package because of potential large variations in actual benefits from those projected within the RPM framework. Higher discount rates can be used to reduce uncertainty. Using input ranges instead of single values for sensitive variables will also accomplish the task.

Finally, branchline relays may involve benefits above and beyond those calculated directly by the RPM. Lines that have suffered from extremely poor rail conditions are likely to show benefits exceeding those predicted by using default values in the model.

It is apparent from working with the RPM that those railroads with efficient records of traffic, rail defect data, and maintenance costs will find themselves in an enhanced position to take advantage of its capabilities. In an increasingly competitive environment, those firms with the best decision-making apparatus will be the survivors.

REFERENCES

1. *CSX Corporation 1986 Annual Report and Form 10K*. CSX Corporation, Richmond, Va., 1987, pp. 4, 17.
2. T. R. Wells and T. A. Gudiness. *Rail Performance Model: Technical Background and Preliminary Results*. Report R-474. Association of American Railroads, Chicago, 1981, pp. 1-8.
3. *Annual Report to the Interstate Commerce Commission for 1986*. CSX Corporation, Jacksonville, Fla., March 1987, pp. 72-72A, 85, 90, 98.
4. P. M. Besuner, D. H. Stone, K. W. Schoeneberg, and M. A. De Herrera. *Probability Analysis of Rail Defect Data*. Presented at Heavy Haul Railways Conference, Perth, Western Australia, 1978.
5. T. R. Wells. *Rail Performance Model: Evaluating Rail*. Presented at the 1983 Annual Conference of the American Railway Engineering Association, Chicago, March 1983.
6. D. D. Davis. *Rail Performance Model—User's Manual*. Report R-654. Association of American Railroads, Chicago, 1987, p. 76.
7. R. A. Armstrong. *User's Guide to the Program: WIBPAC for the Analysis of Rail Failure Data*. Report R-513. Association of American Railroads, Chicago, 1982, pp. 1-3.

Fatigue Analysis of the Effects of Wheel Load on Rail Life

R. K. STEELE AND M. W. JOERMS

To obtain a proper assessment of wheel-load effects on rail fatigue life, both crack initiation and growth behavior must be considered. In order to do this, a small-crack growth model has been added to the three-dimensional initiation model PHOENIX. The combined model appears to make reasonable predictions in general agreement with observations from the Facility for Accelerated Service Testing (FAST). Exercise of the model suggests that modest increases in wear rate tend to lengthen crack initiation life but slightly shorten crack growth life. Total fatigue life (to 20 percent transverse defect) has been found to be approximately proportional to wheel load raised to the power of -2 . If strong tensile stresses exist in the rail, fatigue life can be shortened greatly. However, the wheel-load dependency would be reduced somewhat (power of -1.5). The ramifications of introducing many heavier wheel loads are expected to be (a) a higher ratio of service failures to detected defects due to more rapid crack growth and (b) a larger number of detected defects. The ensuing loss of rail integrity can be balanced by taking a number of steps, including utilizing premium rail metallurgies with a more conformal contact profile, programming grinding to simulate wear, and adopting a rail performance approach to nondestructive inspection. In this approach actual detected defect and service failure experience acts to control inspection strategy.

The continuing thrust of railroad operations toward heavier wheel loads calls into question the ability of rail to resist the heavier loads. A proper understanding of the effects of heavier wheel loads on rail performance cannot be obtained without consideration of other factors such as wheel-rail profile, improved strength and cleanliness of rail steel, and wear, that is, grinding.

The fatigue defect [shell/transverse defect (TD)], which forms internally within the rail head under the influence of the contact and residual stresses, is particularly amenable to fatigue analysis. Furthermore, some reliable experimental data (1) are available by which to gauge the correctness of a fatigue analysis. For these reasons and because the shell/TD has a high likelihood of causing a service failure with appreciable derailment potential (2), this paper will focus on that defect system.

As in all fatigue analyses, some caution must be exercised in defining fatigue life. Fatigue failures are characterized by a life distribution rather than by a single "life." Thus, the percentile of the population failed must be specified when life is calculated. Also, because of uncertainties about actual environmental conditions (i.e., loading, support, material), the fatigue analysis is more suited to illustrating expected trends in behavior than providing exact life estimates.

BACKGROUND

Fatigue fractures are frequently viewed as involving two processes: (a) initiation and (b) growth. During the initiation phase, the material is considered to remain "sound" (without a recognizable crack) until a crack opens within some small microstructural entity such as an individual metal grain. Growth processes then enlarge the crack, eventually to the point at which structural failure may occur.

The development of fatigue cracks in rail under the influence of wheel and rail contact stresses has been modeled by Chipperfield and Blickblau (3), Leis and Rice (4), Zarembski (5), and Lieurade et al. (6), among others.

The approach utilized by Chipperfield and Blickblau is based on opening and shear mode linear elastic fracture mechanics. They do not incorporate into their calculation those residual stresses that can exist within the rail. Their analysis predicts that a shell will initiate at approximately one-half the depth at which shells actually develop (i.e., $1/4$ to $3/8$ in.). The analysis does, however, predict the correct size for the shell (10 mm) when the TD first appears. However, they do not address the issue of why some shells do not turn into TDs.

The analyses of Leis and Rice and of Lieurade et al. are based on calculations of equivalent strain range determined from three-dimensional stresses, including the service-induced residual stresses. Neither analysis appears to treat growth of the shell or development of the TD. Both appear to predict shell occurrence at approximately the correct depth.

Even though the analyses appear to be similar in nature, each suggests a very different estimate of wheel-load dependence. The Leis-Rice analysis suggests that a 50 percent increase in wheel load will produce about a 50 percent decrease in life when measured in million gross tons (MGT), with no residual stresses considered or about a 23 percent decrease in life if observed service-induced residual stresses are included. On the other hand, Lieurade et al. state that "service life can be reduced by a factor of 1,000 when p_0/k (contact stress/yield strength) changes from 4.5 to 6, a 33 percent increase in contact stress. Usually Hertzian contact stress is proportional to wheel load raised to about the one-third power (7), so a 33 percent increase in pressure is approximately the equivalent of a 135 percent increase in wheel load. It is not clear whether the factor of 1,000 applies to cycles of loading or to MGT as the units of service exposure. On the basis of very limited revenue service data from sites that are not necessarily equivalent (1), the Leis-Rice estimate appears somewhat low and the Lieurade et al. estimate, very high.

Rather interestingly, the approach used by Zarembski also predicts a high dependency of rail life on wheel load, similar

in fact to that reported by Lieurade et al. However, the Zarembski method uses only uniaxial stresses and ignores the three-dimensional nature of contact stress. Furthermore, it does not incorporate the service-induced residual stresses, and therefore predicts maximum fatigue damage to occur at the rail head running surface rather than internally, where shells are actually observed to form.

Yet the computational approach used by Zarembski is simple in concept and straightforward in operation, which allows high computational efficiency. Thus, over the course of the last 4 years, both the Association of American Railroads (AAR) and the Transportation Systems Center (TSC) of the U.S. Department of Transportation have modified this approach to incorporate three-dimensional stresses, including service-induced residual stresses. Perlman et al. and Steele have described the results of exercising both versions of the model. The AAR version is called PHOENIX; its computational approach is described in the appendix.

FATIGUE MODEL

PHOENIX is primarily a crack initiation model that uses the following stress systems:

1. Contact stresses calculated for Hertzian contact without the presence of surface tractions;
2. Three-dimensional residual stresses, specifically those found experimentally by Schilling and Blake (10) to be typical [similar residual stress distributions, reported by Groom (11), are shown in Figure 1];
3. Uniaxial beam bending stresses and head-on-web (HOW) bending stresses (12); and
4. Uniaxial stresses caused by the deviation of the rail temperature from the neutral temperature or by rail creep.

The basic rail steel fatigue characteristics are those reported by Fowler (13) in the form of constant stress amplitude or life (i.e., S/N) data. The fact that many tests were run at each stress amplitude level allows an estimation of the S/N relationships at a number of life percentiles. The reaggregation of all of Fowler's longitudinal S/N data is shown in Figure 2.

The rail surface region becomes work hardened under repeated action of passing wheels, which also improves fatigue resistance (14). The model has been modified to accept the variation of hardness from the running surface inward and to pick appropriate fatigue (S/N) characteristics to use at each level of hardness.

Wear (or grinding) can be simulated by the computational removal of surface material while the work-hardening and residual-stress gradients remain fixed with respect to the current surface. This simulation is valid when the rate of wear is small compared with the rate at which the surface work-hardens. Typically this is done incrementally at 10-MGT intervals during damage calculation.

PHOENIX calculates the service exposure in MGT to produce the very first manifestation of a fatigue crack (shell) beneath the running surface of the rail. This first manifestation would not be observable, however, except by fortuitous destructive sectioning right at the point of initiation. At the stress levels at which initiation is calculated to occur, the life to

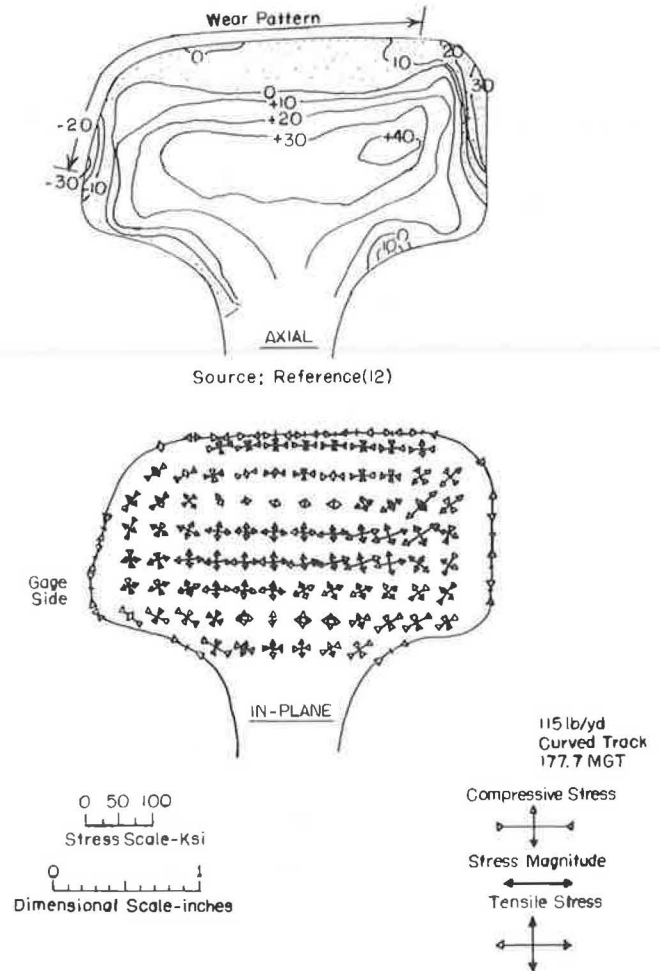


FIGURE 1 Axial and in-plane residual stresses in a service-worn rail (12).

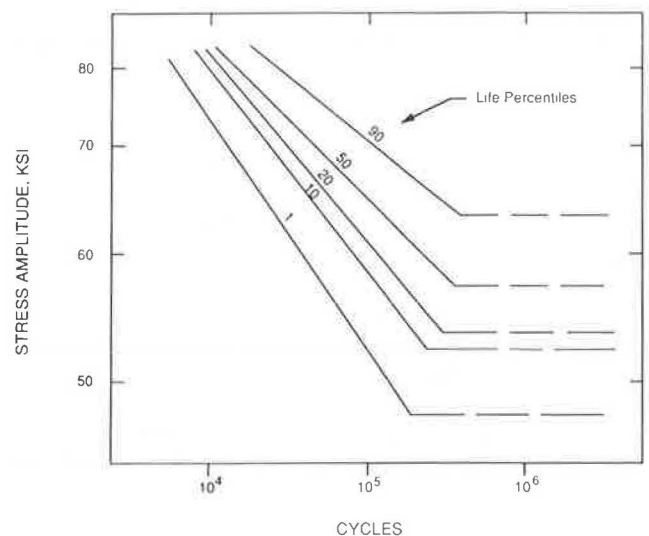


FIGURE 2 Reaggregated S/N data for standard carbon rail.

macroscopic crack initiation would be expected (15) to be a large part (perhaps 90 to 95 percent) of total life. Thus initiation life alone may, in most cases, be adequate for engineering estimates.

However, when an estimate of structural integrity is sought, some knowledge of the likelihood of finding the defect must enter into consideration. Because the ability to find a defect nondestructively depends on the size of the defect, the growth behavior needs to be established.

The growth of the shell and its subsequent turning into a TD have been treated analytically by Hearle and Johnson (16) and by Farris et al. (17, 18). However, the rigorous computation is far too complex to be incorporated into PHOENIX at this time. Thus, a simpler, interim modeling approach treating TD growth alone has been developed, which is compared in Figure 3 with actual growth. This approach makes the tacit

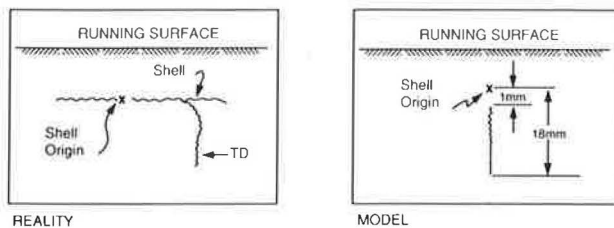


FIGURE 3 TD growth from shell versus modeled growth.

assumption that the period of shell growth before the development of a TD (1 mm in radius) is small compared with the total service exposure life and can be neglected in making engineering judgments.

Following from the work of Orringer et al. (19), the growth relationship has been taken as

$$da/dN = C \Delta K_{\text{eff}}^n / (1 - R) \quad (1)$$

where

- da/dN = crack growth rate,
- a = crack radius,
- N = cycles of loading,
- C = 10^{-11} in./cycle,
- R = stress ratio (minimum stress divided by maximum stress),
- n = slope of logarithmic plot of da/dN versus ΔK , and
- ΔK_{eff}^n = effective stress intensity range,

$$\Delta K_{\text{eff}}^n = (\Delta K_I^2 + \Delta K_{II}^2)^{1/2} \quad (2)$$

where the subscripts I and II refer to the crack opening and vertical shear modes, respectively. The incorporation of a shear contribution into the growth analysis was necessary because early trials of the growth model using only the opening mode stress intensity revealed growth periods far longer than observed to be reasonable. The limitations of blending opening and shear modes, specifically as shown in Equation 2, have been discussed by Besuner (20).

In the analysis, the TD is treated as a penny-shaped crack embedded in an infinite solid so that the relationship between stress intensity and stress and crack radius is simply

$$\Delta K_{\text{eff}} = 1.13 \Delta \sigma_{\text{eff}}(a)^{1/2} \quad (3)$$

Strictly speaking, Equation 3 is not the correct formulation, because the transverse crack does not grow in a self-similar fashion, that is, retaining its circular shape, by the same radial growth from its origin in all directions. The non-self-similar growth behavior is shown in Figure 4 (21). This asymmetry of growth results from the difference between the steady (residual) stresses above the defect origin (compression) and those below it (tension). Nevertheless, the lower portion of the crack front remains approximately circular and is centered on the TD origin (at the shell) for crack sizes up to approximately 10 to 15 percent of the rail head cross-sectional area. However,

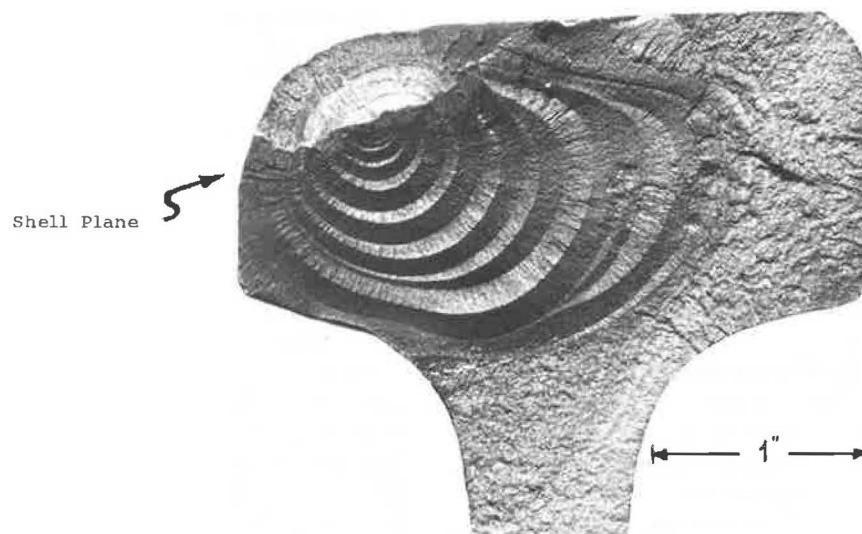


FIGURE 4 TD originating from a shell, showing progressive growth rings.

the area of the TD is generally about 60 percent that of a circle whose radius extends from the TD origin to the lower crack front.

The Mode I live (varying) stresses result from beam bending, HOW bending, temperature variation, and downgrade rail creep (caused by train braking and tractive effort in climbing grades) along the track. Beam bending is calculated for a rail supported on a continuous foundation such that as a wheel passes, the rail head at a specific point will experience about five times the stress in compression than the maximum that will occur in tension (reverse bending). Maximum reverse bending occurs when the wheel is approximately 5 ft from the point of maximum compression flexural stress. The HOW stresses are calculated for the rail head acting as an independent beam supported continuously by the web of the rail. They are superimposed on the beam-bending stresses, tending to produce a tension peak at the bottom of the rail head when the wheel is directly above (Figure 5). Their effect is most acute when the track structure is stiff.

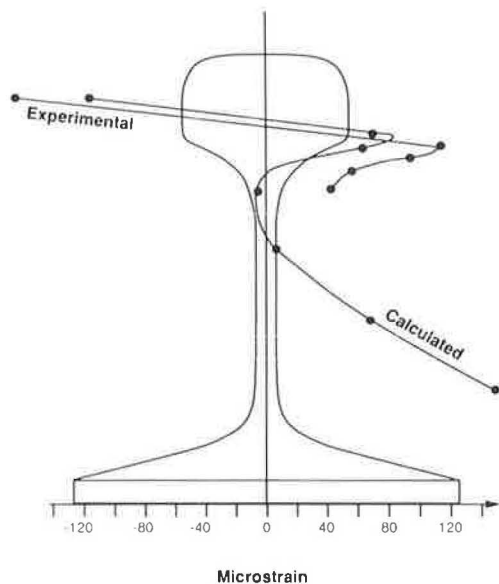


FIGURE 5 Head-on-web bending strains for rail on stiff track.

The Mode II stresses result from beam shear (maximum at the neutral axis of the rail), HOW shear (maximum approximately at the mid-height of the rail head), and contact shear, which reaches its maximum, in the absence of surface tractions, approximately 0.1 to 0.15 in. beneath the surface. In calculation of the HOW shear, the head is treated as a beam supported across its entire width when in reality it is supported only over the central third of its width. Thus, the HOW shear stress contribution may be overemphasized. The relationship of the bending-induced shears is shown in Figure 6. Interestingly, below the depth of maximum contact shear (0.1 to 0.15 in.), the contact shear amplitude is approximately 27 percent of the vertical (compression) stress at each point (7). This relationship has been used to simplify the calculation. All shear stresses are treated as being fully reversed and are added algebraically together.

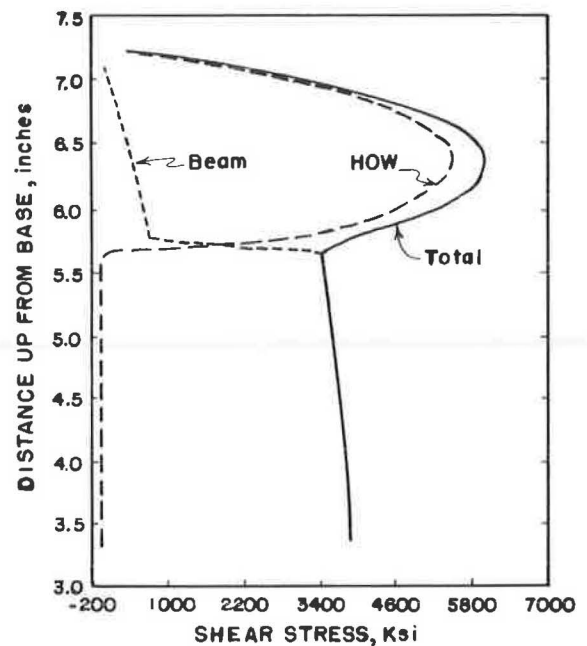


FIGURE 6 Beam and HOW shear stress distribution.

The calculation of the growth curve proceeds incrementally from the integrated form of Equation 1, that is,

$$a_f = a_i / [a_i C' (1.13 \Delta \sigma_{eff})^n \Delta N + 1] \quad (4)$$

where

- $C' = C / (1 - R)$;
- a_i, a_f = crack radii at the beginning and end of interval ΔN , respectively; and
- ΔN = number of cycles of loading for each block of the load spectra.

As the crack grows into regions of different stress, the level of stress is adjusted to be that calculated to exist at the position of the crack tip as if no crack actually existed there.

The crack growth characteristics of rail steel are taken to be those described by Scutti (22); they are shown in Figure 7. Although the typical slope n of the data trend is near 4, some variation is apparent.

RESULTS

Before a look at the combined effects of shell initiation and transverse crack growth, the predictions of the crack growth model need to be examined for agreement with observed crack growth behavior. Regrettably, the only known growth information for small TDs (from a few percent up to 10 to 15 percent) is that reported (1) for a defect in a 4-degree curve at the Facility for Accelerated Service Testing (FAST). Failure of the rail occurred late in a rather cold February, suggesting the presence of thermal tension stress.

To model this behavior, the following conditions have been specified as inputs into both the initiation and growth parts of

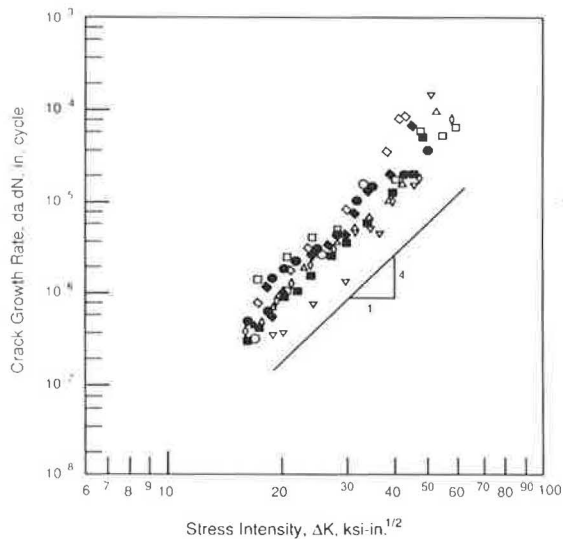


FIGURE 7 Crack growth behavior of rail steel (22).

the model (the initiation model is used to locate the depth of the origin of the TD):

Rail section: 115 lb/yd;
Track stiffness μ : 5,000 psi;
Wheel load (average): 32.2 kips [32.2 kips is the vectorial sum of the typical average FAST wheel load (30.3 kips) and a typical lateral load (11 kips)];
Load spectra: FAST type;
Wheel diameter: 36 in.;
Rail crown radius: 5 in., 20 in.;
S/N characteristics: reaggregated;
Life percentile: 5th;
Residual stresses: standard (Figure 8);
Thermal stresses: 0, +15 ksi.

Before examination of the results of the parametric exercise, a few words are necessary about the variation in rail crown

radius. When wheels run on rail in tangent track, the contact zone on new rail is generally near the center of the rail head, just slightly to the gage side. At that position the worn rail crown radius is about 20 in. (23). However, when the rail is in a curve, the wheel "footprint" extends all the way from the gage face to about one-half the distance from the center to the field side of the rail head (Figure 9). Thus, it is not clear what crown radius should be used in the analysis. Over the shell defect, the radius of curvature of the worn rail varies continuously from less than an inch to about 20 in. near the center of the rail head (Figure 10).

Nor is it clear how much of the vertical wheel load is partitioned from the ball of the rail to the gage face. Curving model analysis (23) for the FAST worn-wheel and worn-rail profiles suggests that under unlubricated conditions nearly 50 percent of the vertical load can be carried on the gage face. Under lubricated conditions, this is calculated to drop to about 35 percent. This pattern is shown in Figure 11.

Yet another concern is that PHOENIX makes the contact stress calculation for the crossed cylinder contact configuration (wheel profile radius = ∞). However, the worn wheel rolling on the worn rail represents a more conformal situation. For this case, the wheel profile radius at the point of contact typically is not infinity but more nearly about 5 in. greater than the rail profile radius at that point (24, 25). Thus, a large number of different wheel and rail profile contact arrangements could produce the same contact stress. This is shown in Figure 12, which has been prepared from the work of Kumar and Singh (26) for a 36-in. diameter wheel. Here a 5-in. rail profile crown radius in contact with a 10-in. wheel profile radius yields a contact stress of about 200 ksi (33-kip wheel load). The same contact stress could be achieved with an approximately 9-in. rail crown radius in contact with a 35-in. wheel profile radius. The equivalent crossed cylinder configuration would have a 12-in. rail crown radius.

In recognition of all these uncertainties, the contact situation for curving (with flanging) has been treated by including both the 5- and the 20-in. rail crown radii in the calculations. The results of these calculations are shown in Figures 13 and 14.

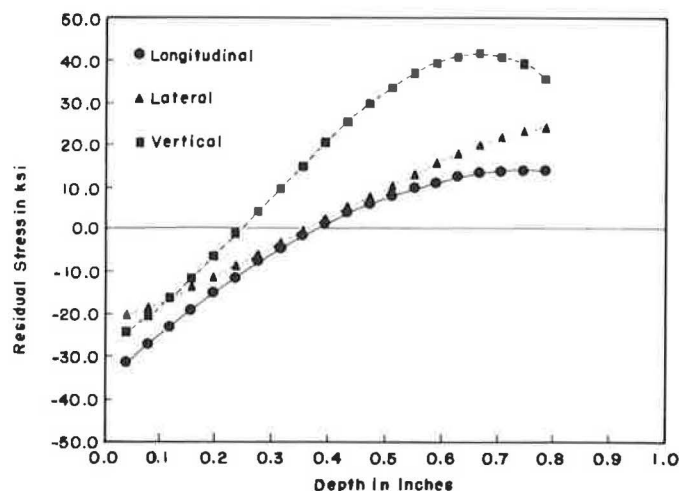


FIGURE 8 Residual stress profiles used in PHOENIX.

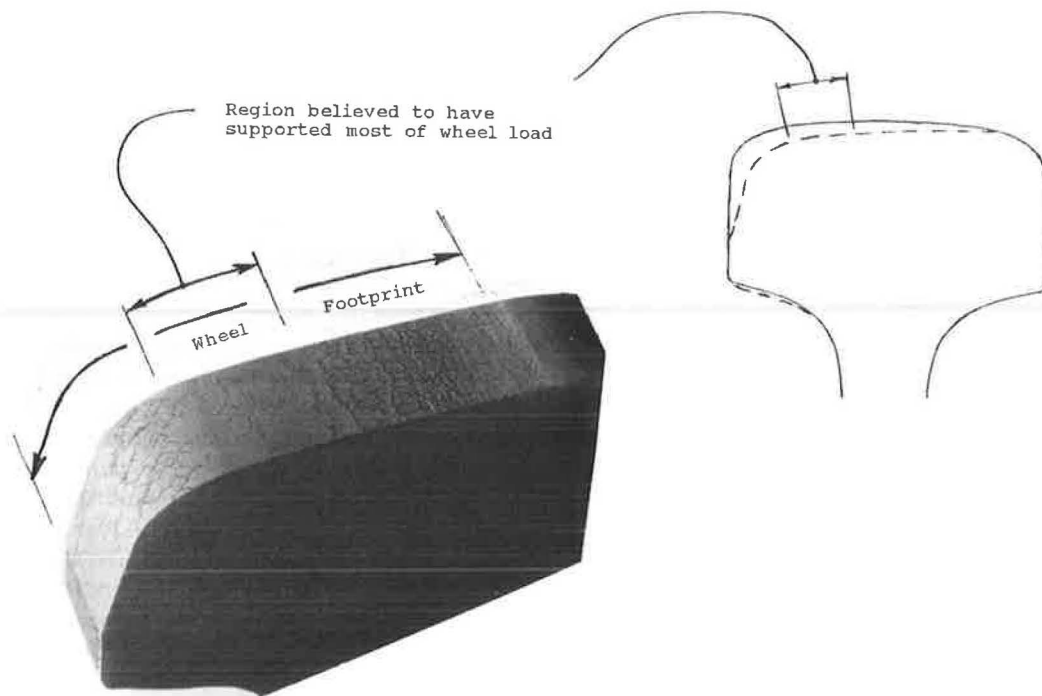


FIGURE 9 FAST failed rail (4-degree curve/gage face and tread).

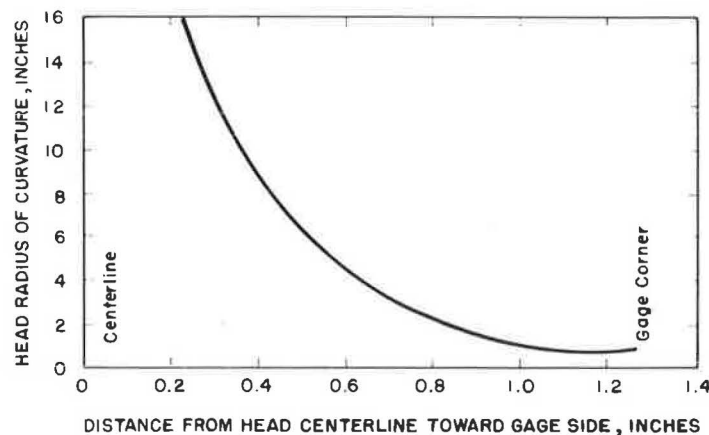


FIGURE 10 Variation of FAST worn rail crown radius of curvature across gage side half of rail head.

With all shear stress contributions included and no thermal stress, both the 5- and the 20-in. rail crown radii lead to significantly shorter predicted crack growth lives than that actually observed. However, if the model were to overemphasize the contribution of the HOW shear, the two different crown radii would cause the life prediction to bracket the observed behavior; that is, with the 5-in. (crossed cylinder) crown radius, the model predicts too short a life, whereas with the 20-in. (crossed cylinder) crown radius, the model predicts too long a life.

With the +15-ksi static stress included to represent the likelihood that a thermal stress would occur in February, the predicted growth behavior for the 20-in. crown radius (with no load partitioning) is much closer to that observed. The thermal stress does not have much of an effect until the defect radius

reaches 5 mm (20-in. crown radius) and 10 mm (5-in. crown radius).

The initiation life and initiation depth also yield some clues about the appropriateness of the predictions. As can be seen in Figure 4, the depth of initiation was about 0.35 in. and the total service exposure had been estimated to be about 180 MGT (1). Remarkably, the 20-in. crown radius without HOW shear but with a +15-ksi tensile thermal stress leads to an initiation-life prediction of 174 MGT (total life \approx 220 MGT) and a depth of initiation of 0.32 in.—which is not very far from what was actually observed.

The same contact stress calculated to exist with a 20-in. crown radius (crossed cylinders) could also result from an 8-in. crown radius in conformal contact with a 14-in. wheel profile radius (Figure 12). The wear pattern and the head

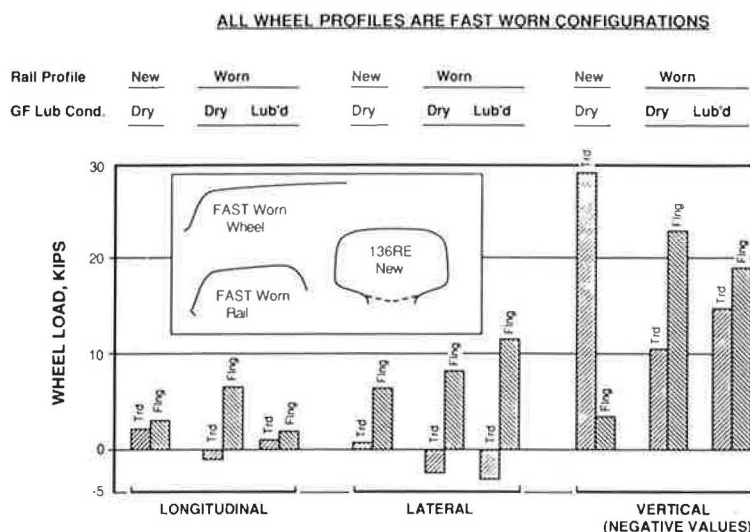


FIGURE 11 Effect of flange contact and lubrication state on wheel force distribution on high rail of curve.

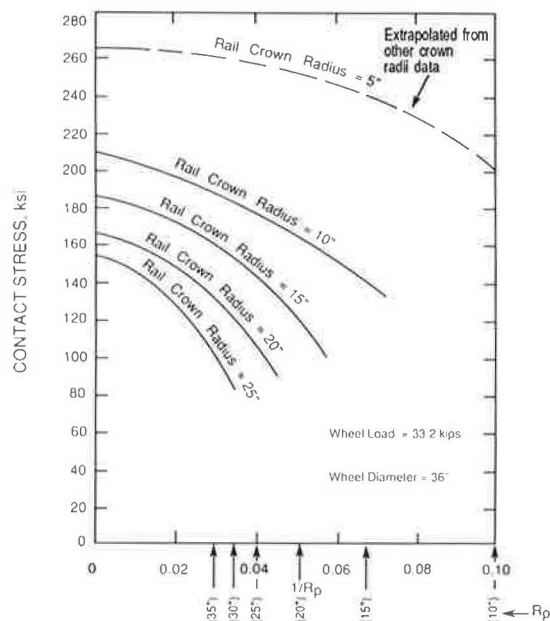


FIGURE 12 Variation of contact stress with reciprocal of wheel profile radius.

check-free zone about $\frac{1}{2}$ in. toward the gage face from the rail head center (Figure 9) do suggest that this location was the predominant wheel loading path. At that point, Figure 10 indicates that the rail crown radius should be near 6 to 7 in.

There remain uncertainties about (a) the actual load on that path (how much is partitioned to the gage face), (b) the wheel profile radius at contact, (c) the thermal stress level imposed during initiation and growth, and (d) the actual fatigue characteristics of the failed rail. Thus, in the remainder of the analysis to be described here, the HOW shears will be included to provide a conservative estimate of crack growth behavior.

Figures 15 and 16 show the effect of track stiffness on crack growth for a heavier rail section (136 lb/yd), again with the

components of shear stress turned off one at a time. When the TD is small, the contact shear stresses have the dominant effect. With all shear stresses operative, reducing the track stiffness by a factor of 5 shortens the crack growth life at any specified crack size by a factor of about 2.

The FAST Defect Initiation and Growth Experiment results can also serve as a basis for checking the validity of the crack growth calculations. Orringer et al. (19) have reported the FAST growth behavior of a number of TDs transplanted from revenue service into FAST tangent track. At small defect sizes in the range of 10 to 20 percent, the area growth behavior appears to be linear, ranging from a low near 0.25 percent/MGT to a high near 1.3 percent/MGT. (A linear relationship of defect area with MGT implies that for a circular defect, the rate of crack front movement decreases with increasing MGT as the defect becomes larger.) These 0.25- and 1.3-percent slopes (converted to radial growth) are shown in Figure 16 at 11 percent defect size. They are arbitrarily positioned at 45 MGT to allow slope comparisons. The steeper of the two slopes is very close to the slope of the calculated growth curve, where contact and HOW shears at least are operative. This encourages belief that the transverse crack growth computation method is appropriate.

Lest one become too confident of that, though, a significant caveat must be noted: transverse crack growth behavior can depend strongly on where the crack initiation part of the model positions the "center" of the TD. Figure 17 shows what can happen if the ultimate tensile strength used in the initiation calculation is too low. Specifically, increased wheel load can be calculated to initiate a shell at much greater depth (a different position in the residual stress field) so that the crack growth is actually less rapid. When initiation occurs at the same (or only slightly different) depth, the heavier wheel loads increase the rate of crack growth, shortening the growth period by about 35 percent for the 18 percent increase in wheel load from 33 to 39 kips.

Crack growth behavior is extremely sensitive to the value of the power term n (Equation 1). Although the typical value

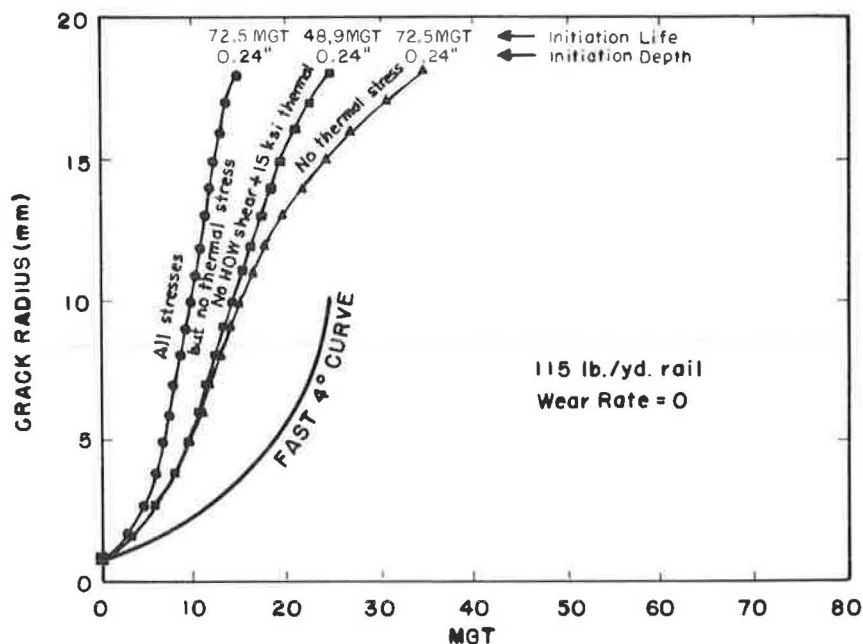


FIGURE 13 Comparison of predicted and observed transverse crack growth behavior (5-in. crown radius).

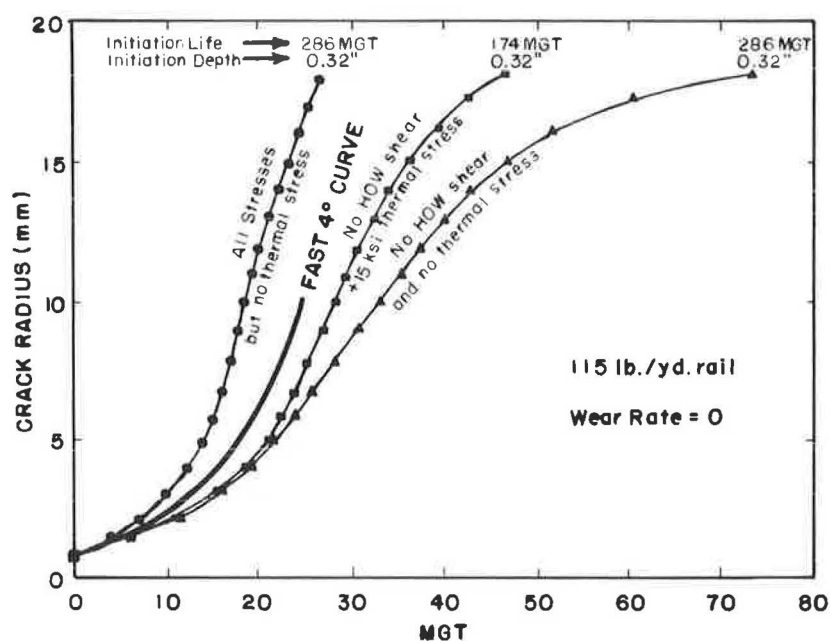


FIGURE 14 Comparison of predicted and observed transverse crack growth behavior (20-in. crown radius).

appears to be near 4 (Figure 7), some variation does occur. Figure 18 shows the very large variation in crack growth behavior that would be expected for relatively small variations in the value of n .

The last two paragraphs have exemplified how much the modeler of fatigue processes is at the mercy of his uncertainty of material properties as well as of environmental characteristics.

With these caveats in mind, initiation and growth can be combined to examine quantitatively the trends to be expected

from variations in wheel load. Because most revenue service track is less stiff than that at FAST, and to simulate a realistic support environment leading to relatively rapid crack growth, a track stiffness of 1,000 psi was selected. The life predictions (both initiation and total life to 20 percent TD size) are shown as a function of wear rate in Figure 19. The service lives calculated here are based on a common residual stress pattern (Figure 8) for all three wheel loads. In fact, that pattern and magnitude of stresses would be a function of wheel load. A rail subjected to only 19-kip wheel loads would be expected to

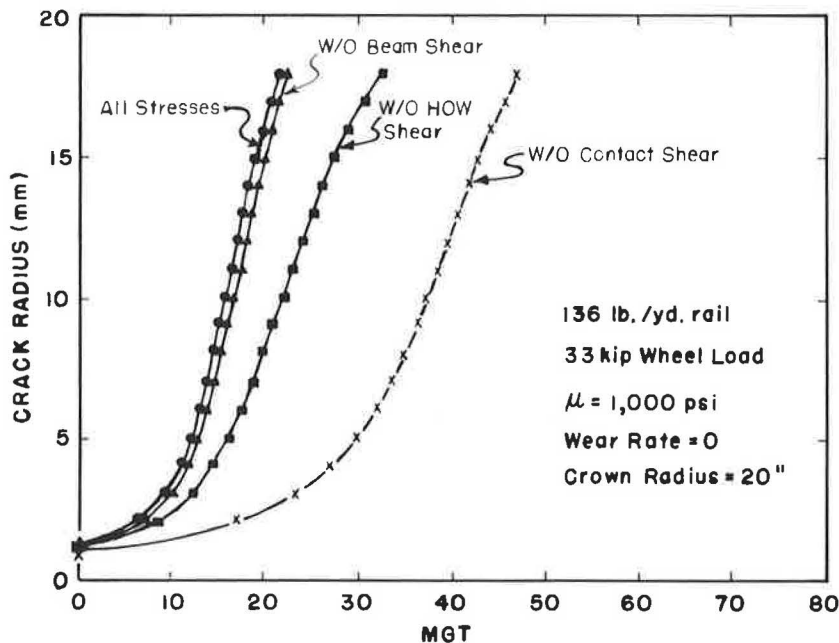


FIGURE 15 Contribution of different shear stress systems to growth behavior: $\mu = 1,000$ psi.

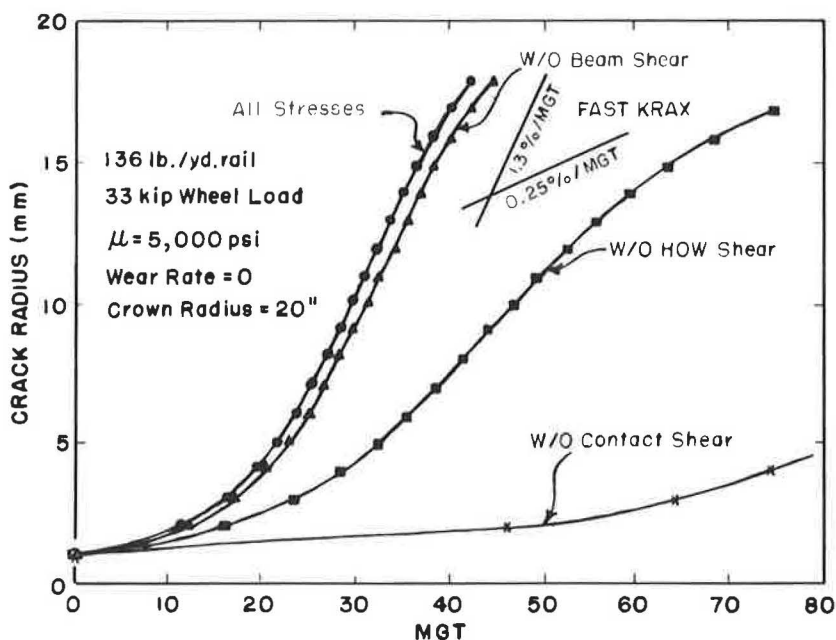


FIGURE 16 Contribution of different shear stress systems to growth behavior: $\mu = 5,000$ psi.

exhibit less plastic flow and therefore lower residual stress levels with a less well-developed pattern. A rail exposed to only 39-kip wheel loads would be expected to have a somewhat more pronounced residual stress pattern than that used in the analysis as well as somewhat higher stress levels.

Increasing the wear rate is calculated to have two effects. It tends to lengthen the initiation life; a flatter (larger-radius) rail crown curvature tends to enhance the life benefit of an increased wear rate (9). However, it tends to shorten the growth

life. The effects of the wear rate are more noticeable at the lower wheel loads. Overall, the effect of increasing the wear rate is to increase the total life. Considering initiation of the shell alone, the effect of the wear rate on life is predicted to be even more pronounced with higher-strength rail. This is shown in Figure 20, which also shows that fatigue life improvement attributable to the use of a high-premium rail will be expected to be about a factor of 2 at zero wear rate. However, it will be closer to a factor of 2.5 at a wear rate near 1.6 mm/100 MGT.

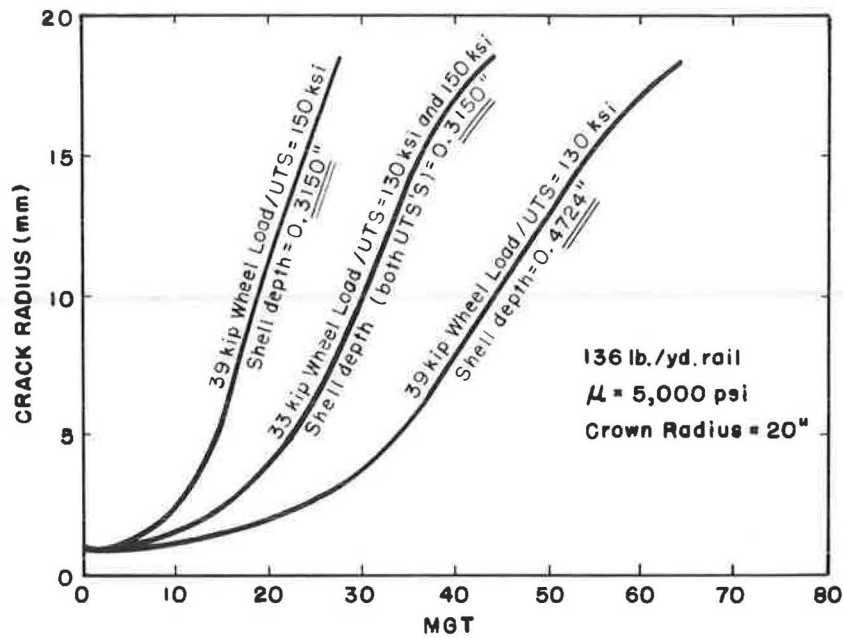


FIGURE 17 Effect of ultimate tensile strength on calculation of crack growth behavior.

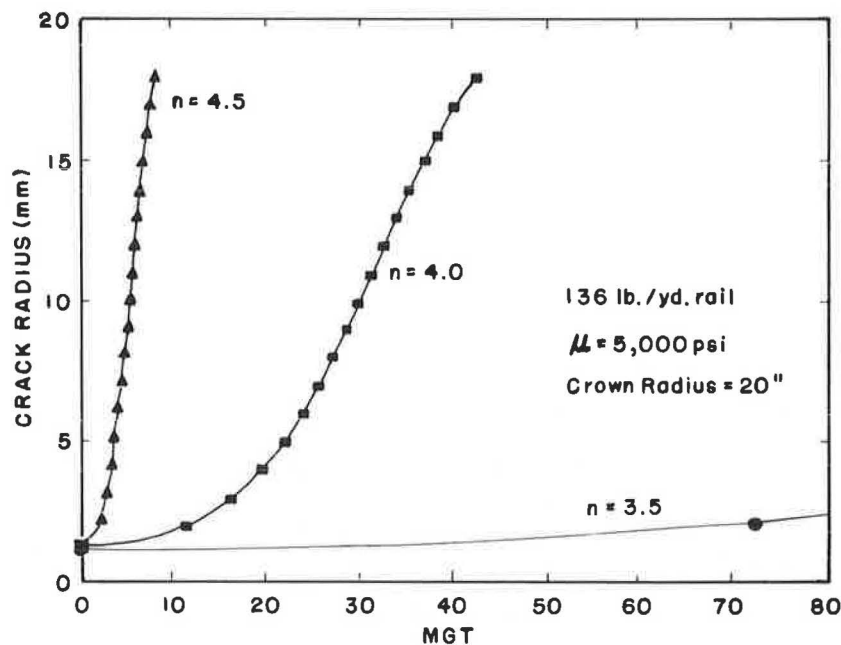


FIGURE 18 Effect of crack growth exponent on crack growth behavior.

The wheel-load dependence may be seen more clearly if the data are plotted as shown in Figure 21. Here the total life to 20 percent TD size is given for both the standard residual stress case and for the case in which a 15-ksi steady tension stress has been imposed along the rail. The latter situation can develop during a cold period or from the creep of rail down a grade. A revenue service typical wear rate of 1 mm/100 MGT was used in the calculation. In both cases, the following relationship applies:

$$\text{Service life (5th percentile, MGT)} \propto (\text{wheel load})^m \quad (5)$$

where m is -2 for the standard case. The 15-ksi tension has reduced expected service life significantly (about 50 percent). It also has reduced the value of m to -1.5 , that is, it has decreased the wheel-load dependence somewhat.

DISCUSSION

The combined initiation-and-growth model used here appears to produce believable initiation-and-growth predictions, at least on a comparative if not an absolute basis. The wheel-load dependence predicted ($m = -1.5$ to -2) is in close agreement

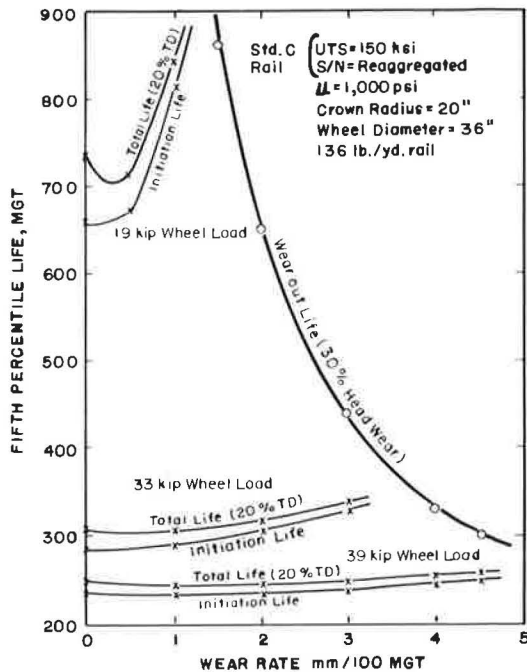


FIGURE 19 Effect of wear rate on 5th-percentile fatigue life of standard carbon rail at different wheel loads.

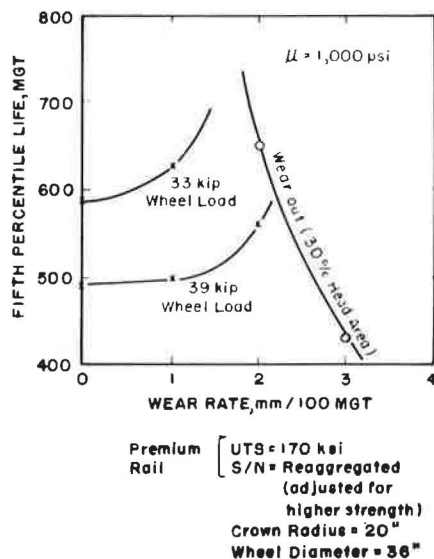


FIGURE 20 Effect of wear rate on 5th-percentile initiation life of premium rail steel (320 BHN).

with an analysis of revenue service rail failure behavior made by Steele and Reiff (1). Both of these predictions are then in closer agreement with the predictions of Leis and Rice (4) than with the calculations of Zarembski (5) and of Lieurance et al. (6).

However, before the reader becomes too convinced of infallibility, he should be aware that the model also makes some other predictions that may or may not be reasonable. Specifically, the initiation model interprets compression acting along the rail as beneficial in prolonging shell initiation life. Thus,

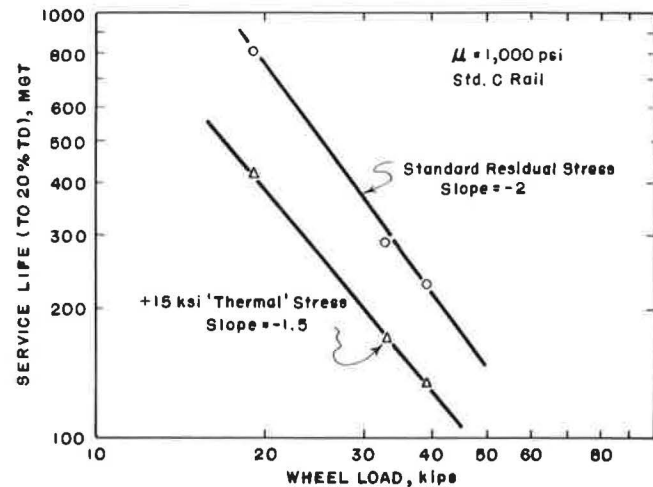


FIGURE 21 Service life as a function of wheel load with and without additional "thermal" stress component.

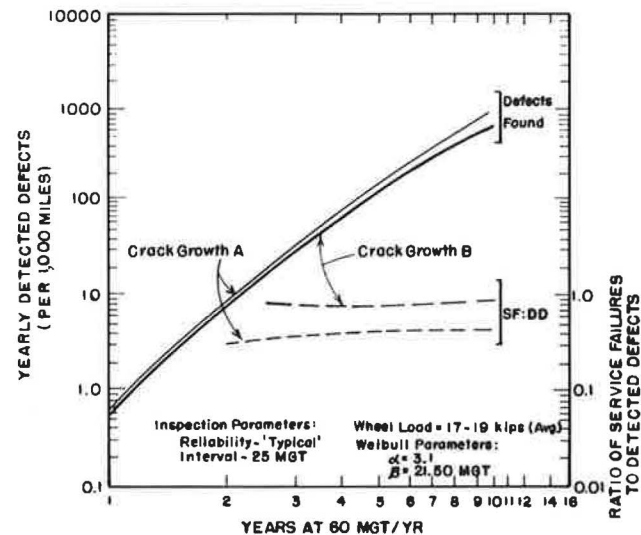


FIGURE 22 Variation of detected defects and ratio of service failures to detected defects with service exposure for two different crack growth behaviors.

soft track and light rail sections are calculated to have slightly longer initiation lives, with all other parameters (especially crown radius) kept constant. There are some field defect data (1), the exact wheel loadings and wear rates for which are not really known, that suggest that lighter rail sections have poorer rail head defect fatigue service lives. However, there are also published rolling load test data (27) to suggest that the level of flexural stress (and by inference rail section and track stiffness) has little effect on shell initiation.

The ramifications of the projections of decreased rail fatigue life made in this paper for heavier wheel loads will be felt most keenly in the increased likelihood of service failure occurrence. The relationship between rail failure behavior and rail integrity has been treated by Davis et al. (28). Specifically, the effects of increased crack growth rate and higher initiation rate have been considered, albeit separately. Were no other changes to occur, reducing the crack growth period by 50 percent would be expected to approximately double the ratio of

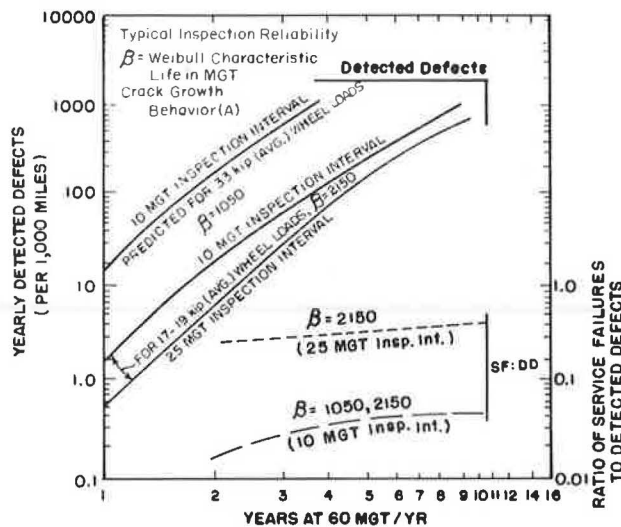


FIGURE 23 Predicted effect of increased average wheel load on detected defects and ratio of service failures to detected defects.

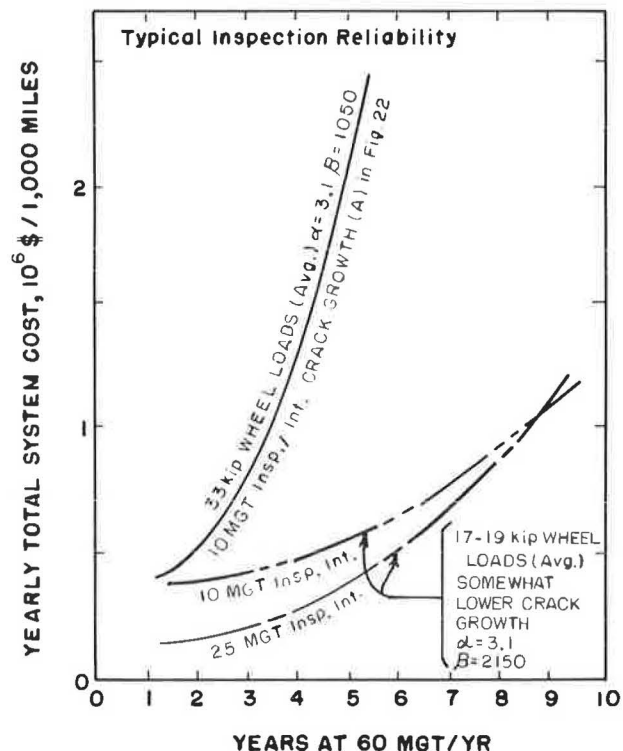


FIGURE 24 Predicted effect of increasing average wheel load from 17 to 19 kips to 33 kips on yearly total system cost.

service failures to detected defects. This is shown in Figure 22 for a 60-MGT/year line (17- to 19-kip wheel loads) with inspections at 25-MGT intervals. Changing from all 17- to 19-kip wheel loads to all 33-kip wheel loads (keeping crack growth behavior fixed) would not alter the ratio of service failures to detected defects (Figure 23) at a fixed inspection interval. But the number of detected defects would increase by a factor of 8 to 9 for a fixed inspection interval of 10 MGT.

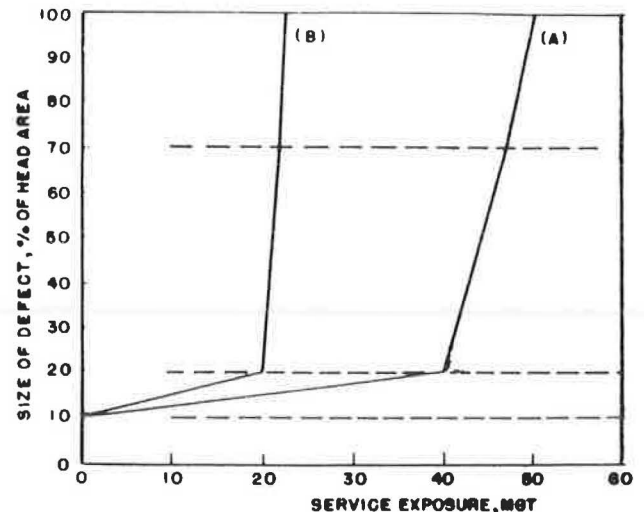


FIGURE 25 Crack growth behavior used for 17- to 19-kip (B) and 33-kip (A) wheel loads.

The cost analysis performed by Moore (27) did not include 39-kip wheel loads, but examination of the differences in costs between all 17- to 19-kip wheel loads and all 33-kip wheel loads is enlightening. Figure 24 gives the calculated yearly total system costs for 33- and 17- to 19-kip wheel loads. The crack growth behavior used for the 33-kip wheel loads was that shown by curve A in Figure 25. For 17- to 19-kip wheel loads, the crack growth rate used was somewhat slower, requiring 60 MGT instead of 45 MGT to reach 70 percent size. This is not as slow as the fatigue analysis in this paper suggests that it should be at the lower wheel loads. But the results are appropriate enough to illustrate the large cost penalties for an approximately 80 percent increase in wheel load.

Thus, the projections of this analysis and the analyses made by Moore (27) suggest that significant increases in yearly total system cost will occur with the introduction of large numbers of heavier wheel loads, unless changes are made in any or all of the following parameters:

- Rail metallurgy and running surface design,
- Rail maintenance practice (i.e., grinding), and
- Rail nondestructive inspection (NDI).

Improvements in rail metallurgy (rail with a Brinnell Hardness Number of 300) and rail head manufactured profile may be expected to provide very effective compensation for heavier wheel loads (23). But their introduction may be slow because of the substantial track mileage that would need to be replaced. In contrast, rail grinding and NDI are practices easily applied to in-track rail to preserve integrity. Grinding, which both reconfigures the rail contact surface and simulates wear, can alter the defect initiation Weibull parameters, especially increasing the characteristic life, 8. The use of a rail performance (i.e., rail integrity) guideline for rail defect inspection can achieve lower total system cost through improved management of existing inspection resources. As wheel loads increase and cause more rapid crack growth, more sensitive inspection techniques will offer significant cost advantage and will allow the same level of integrity to be achieved under more adverse conditions without increasing the number of rail inspections.

SUMMARY

A means of performing transverse crack growth calculations (1- to 18-mm radius) has been incorporated into the three-dimensional fatigue initiation model PHOENIX. In order to reproduce observed crack growth rates at small defect size, the inclusion of a shear mode contribution to stress intensity has been necessary. The complete model has been exercised for conditions simulating the FAST environment, with results close to those actually observed experimentally. Projections made for revenue service conditions (softer track) suggest that the influence of wheel loads on fatigue life is dependent appreciably upon wear rate. Large tensile (thermal) stresses reduce expected life significantly (about 50 percent). Generally,

$$\text{Service life (MGT)} = (\text{wheel load})^m$$

where m is -1.5 to -2 . Although heavier wheel loads can be expected to reduce rail fatigue life, the problem can be managed satisfactorily by improving rail metallurgy and design, rail repair practice, rail inspection strategy, or all three.

REFERENCES

1. R. K. Steele and R. P. Reiff. Rail: Its Behavior and Relationship to Total System Wear. *Proceedings, Second International Heavy Haul Railway Conference*, Association of American Railroads et al., Sept. 1982, pp. 227-276.
2. R. K. Steele. Requirements for the Reliability Assessment of Railroad Rail in Service. *Railroad Track Mechanics and Technology*, 1978, pp. 303-322.
3. C. G. Chipperfield and A. S. Blickblau. Modeling Rolling Contact Fatigue in Rails. *Rail International*, Vol. 15, No. 1, 1984, pp. 25-31.
4. B. N. Leis and R. C. Rice. Rail Fatigue Resistance—Increased Tonnage and Other Factors of Consequence. *Proceedings, Second International Heavy Haul Railway Conference*, Association of American Railroads et al., Sept. 1982, pp. 99-117.
5. A. M. Zaremski. *Effect of Increasing Axle Loads on Rail Fatigue Life*. AAR Report R-485. Association of American Railroads, Washington, D.C., June 1981.
6. H. P. Lieurade, R. Y. Deroche, B. Deboile, and R. Conti. A Study of the Shelling Mechanism of Rails. Report RE 1302. Presented at Second International Symposium on Contact Mechanics and Wear of Rail/Wheel Systems, University of Rhode Island, Kingston, July 8-10, 1986.
7. T. G. Johns, K. B. Davies, P. M. McGuire, and S. G. Sampath. *Engineering Analysis of Stresses in Railroad Rail*. Report DOT-TSC-1038. Battelle Columbus Laboratory, June 1977.
8. A. B. Perlman, D. Y. Joeng, and O. Orringer. Rail Flaw Growth Investigations. *AREA Bulletin* 688. Vol. 83, 1982, pp. 536-550.
9. R. K. Steele. The Consequences of Truly Effective Lubrication Upon Rail Performance. ASME Paper 84-WA/RT-17. Presented at the Winter Meeting, American Society of Mechanical Engineers, New Orleans, La., 1984.
10. G. C. Schilling and G. T. Blake. *Measurement of Triaxial Residual Stresses in Railroad Rail*. AAR Report R-477. Association of American Railroads, Washington, D.C., March 1981.
11. J. J. Groom. *Final Report on Task 2: Residual Stress Determination*. Report DOT-TSC-1426. Battelle Columbus Laboratory, Nov. 1979.
12. S. G. Sampath, D. R. Albeck, J. C. Kennedy, B. N. Leis, and R. C. Rice. *Analysis of Service Stresses in Rails*. Report DOT-TSC-1663. Battelle Columbus Laboratory, Sept. 1982.
13. G. J. Fowler. *Fatigue Crack Initiation and Propagation in Pearlitic Rail Steels*. Ph.D. dissertation. School of Engineering and Applied Science, University of California, Los Angeles, 1976.
14. A. J. McEvily and K. Minakawa. *Metallurgical Evaluation of FAST Rail Steels*. Report DOT-TSC-1551. University of Connecticut, Storrs, Aug. 1981.
15. G. E. Dieter. *Mechanical Metallurgy*, 2nd ed. McGraw-Hill, New York, 1976, pp. 414-415.
16. A. D. Hearle and K. L. Johnson. Mode II Stress Intensity Factors for a Crack Parallel to the Surface of an Elastic Half-Space Subjected to a Moving Point Load. *Journal of the Mechanics and Physics of Solids*, Vol. 33, No. 1, 1985, pp. 61-81.
17. T. N. Farris, L. M. Keer, and R. K. Steele. The Effect of Service Loading on Shell Growth in Rails. *Journal of the Mechanics and Physics of Solids*, Vol. 35, No. 6, 1987, pp. 671-700.
18. T. N. Farris, L. M. Keer, and R. K. Steele. *Life Prediction for Unstable Shell Growth in Rails*. AAR Report R-655. Association of American Railroads, Washington, D.C., March 1987. (Also to be published in the *Journal of Engineering for Industry*.)
19. O. Orringer, J. M. Morris, and D. Y. Jeong. Detail Fracture Growth in Rails: Test Results. *Theoretical and Applied Fracture Mechanics*, Vol. 5, 1986, pp. 63-95.
20. P. M. Besuner. *Fracture Mechanics Analysis of Rails with Shell-Initiated Transverse Cracks*. In *Rail Steels—Developments, Processing and Use*, ASTM STP-644, American Society for Testing and Materials, Philadelphia, Pa., 1978, pp. 303-329.
21. M. J. Wisnowski. *Description of a Failed Rail from FAST*. AAR Report R-371. Association of American Railroads, Washington, D.C., Feb. 1980. (Also published as Report TTC/TM-98.)
22. J. J. Scutti. *Fatigue Properties of Rail Steel*. MS thesis. Massachusetts Institute of Technology, Cambridge, 1982.
23. R. K. Steele and D. H. Stone. Developments in Railroad Rail. *AREA Bulletin* 707, Vol. 87, 1986, pp. 311-358.
24. F. S. Hewes et al. Report on Assignment 11—Investigate the Causes of Shelly Spots and Head Checks in Rail Surfaces for the Purpose of Developing Measures for Their Prevention. *Proc. AREA*, Vol. 44, 1943, pp. 597-601.
25. F. S. Hewes et al. Report on Assignment 11—Investigate the Causes of Shelly Spots and Head Checks in Rail Surfaces for the Purpose of Developing Measures for Their Prevention. *Proc. AREA*, Vol. 45, 1944, pp. 446-462.
26. S. Kumar and S. P. Singh. *A Theoretical Study of Wheel-Rail Contact Stresses and Their Tread-Crown Curvature Relationship for Heavy Axle Loads*. Technical Report 1. Association of American Railroads, Washington, D.C., 1986.
27. H. F. Moore. Progress Report of the Joint Investigation of Fisures in Railroad Rails. *Proc. AREA*, Vol. 36, 1935, pp. 1065-1074.
28. D. D. Davis, M. J. Joerms, O. Orringer, and R. K. Steele. The Economic Consequences of Rail Integrity. *Proceedings, Third International Heavy Haul Conference*, Association of American Railroads et al., Oct. 1986.

APPENDIX

PHOENIX—The Model

This appendix deals with the theoretical basis of the PHOENIX model. Assumptions made by the model as well as modeling limitations will also be discussed.

INTRODUCTION

PHOENIX is a computer simulation of rail fatigue life under various operating conditions. It takes into account such factors as rail size, wear rate, foundation modulus, and wheel size. With the current stresses calculated and those input into the model, PHOENIX predicts the initiation of internal defects within the rail head where wheel and rail contact contributes to that initiation.

PHOENIX is designed to perform parametric studies of rail fatigue behavior for diverse operating conditions. Because of the statistical nature of fatigue analysis, it is impossible to calculate absolute values for rail life, but relative comparisons of different conditions can be obtained. The model can be run on an IBM personal computer, although extensive parametric studies should be performed on a larger machine. The model is easy to use and can be customized for particular conditions without reprogramming.

BACKGROUND

PHOENIX was designed to provide a more realistic analytical description of the rail fatigue crack initiation process than has been possible with the uniaxial model, RFLAP. The uniaxial model predicts that fatigue crack initiation should occur at the running surface of the rail, whereas rail head defects such as shells and TDs from shells, vertical split heads, and compound fractures actually initiate within the head well beneath the running surface.

The uniaxial model was made to generate believable fatigue life estimates by ignoring the short life calculations near the surface and by arbitrarily selecting a depth that is typical of shell formation. This approach is fundamentally flawed, however, because the depth of shell initiation is a function of the service history of the rail and of the inherent fatigue resistance of the rail at the region of initiation.

The underlying difficulty with the uniaxial model is that it ignores the important role of contact stresses in the transverse and vertical dimensions and that it recognizes neither the existence of a three-dimensional residual stress state nor its variation with depth and position within the rail head.

The effective stress that induces plastic flow (and leads to accumulation of fatigue initiation damage) is the octahedral shear stress; this reaches a maximum well beneath the running surface. Continuing progressive plastic flow will occur at and directly below the running surface of the rail as a result of repeated wheel passages if the wheel load exceeds some critical value (approximately 900 lb/in. of wheel diameter in the absence of externally imposed surface tractions). This plastic flow generates an internal residual stress state that is highly compressive near the surface but becomes tensile at greater depths.

Typically, shells develop in the region just at the boundary between the upper, plastically deformed, work-hardened region and the lower, undeformed base material. Therefore, the fatigue crack initiation process must respond to the combined action of varying three-dimensional stresses (both contact and flexural) and the steady stresses [residual (resulting from mill processing and service exposure), thermal, and the mean of the varying stresses]. It is this response that PHOENIX seeks to describe.

THEORY

The operation of PHOENIX is described in three parts: how wear enters into the model, the computation and combination of the three stress systems (flexural, residual, and contact), and the prediction of crack initiation. Limitations and applications of PHOENIX are discussed last.

Time, Tonnage, and Wear

The progress of a PHOENIX simulation is controlled by tonnage and wear rather than by time. Time does not enter into the simulation. Because wear is not presently computed internally, the wear rate appropriate for the given load must be specified by the user. Wear units are millimeters per 100 MGT. The simulation also requires a tonnage increment, which specifies how often the wear and fatigue calculations are to be made. This is normally set to 10 MGT, but can be changed. A very high wear rate would require a smaller tonnage increment, whereas a very low wear rate (well lubricated rail) could use a longer increment. If a tonnage increment is too long, loss of accuracy may result; too short an increment will only increase simulation time.

Evaluation Points

Stress and fatigue damage are evaluated at various depths beneath the surface of the rail. In the standard configuration there are 20 points, starting at the surface and spaced 1 mm apart. These points are positioned relative to the initial rail surface (at the start of the simulation) and do not move with the current running surface. Because fatigue damage is computed only at these points, there may be some granularity in the results. If this proves to be a problem, more points may be defined (up to 40 in this implementation) or the points may be redistributed for better coverage of the depth of interest. Of course, the more points, the longer the simulation will take to run.

Residual Stress

The triaxial residual stress field is derived from data obtained experimentally from sample rails. It is internally modelled as a cubic equation. A scale factor and a bias may be applied. The bias (or offset) may be used to simulate expansion or contraction due to temperature changes. Because strain hardening is assumed to occur much faster than wear as the current running surface recedes, the entire residual stress field moves with it. It is important to note that the residual stress calculation is very empirical and is based on a small amount of data. Residual stress fields found in rails in service can be expected to vary substantially.

Contact Stress

Contact stresses are calculated using Hertzian contact, which implies the absence of surface tractions within the wheel-rail contact patch. Both the "crossed cylinder" and line contact configurations can be used. The crossed cylinder configuration is appropriate for a contact between a new wheel and new rail where little wear has occurred. The line contact configuration assumes that the rail head has become quite flat, making the contact patch very wide. Line contact is difficult to use because a poor choice of the contact width will cause substantial errors in the calculated contact stresses.

Flexural Stress

Like three-dimensional residual stress and contact stresses, three-dimensional flexural stress occurs as the wheel moves

over a position on the rail. However, unlike the contact and residual stresses, only the longitudinal component of flexural stress (for vertical bending) appears to have large enough peak values to contribute to the effective stress term, σ_{eff} . Several points should be noted about the longitudinal flexural stress:

- At the running surface of the rail, it changes from mildly tensile when the wheel is approximately 5 ft away to strongly compressive when the wheel is directly over the point in question. Thus, in the head the mean stress associated with the longitudinal flexural stress is compressive.

- In addition to the overall beam-bending stress system, there is also a local HOW bending stress system in which the bottom of the rail head can be placed in tension directly under the wheel. The tendency for the HOW system to place the bottom of the head into tension is most evident when the track is stiff.

PHOENIX flexural stress calculations are based on the beam on elastic foundation (BEF) theory. A separate BEF calculation is performed for the rail head bending on the web. The two stress calculations are then superimposed to provide the total flexural stress. The present flexural stress package considers only longitudinal stresses and does not handle lateral loads.

Effective Stress

The key to the estimation of fatigue damage under the influence of a three-dimensional stress state is the selection of a suitable damage criterion. PHOENIX utilizes the Sines criterion, which permits the calculation of an effective stress made up of both varying and steady components of principal stress. The form of the criterion is

$$\sigma_{\text{eff}} = C_1 [\sum (\Delta \sigma_{i,j}^{\text{amp}})^2]^{1/2} + C_2 \sum \sigma_i^{\text{steady}}$$

where

- i, j = principal stress; $i, j = 1 \dots 3, i \neq j$;
- $\Delta \sigma_{i,j}^{\text{amp}}$ = differences between the principal stress amplitudes;
- σ_i^{steady} = steady principal stresses, including the mean stresses of the varying stress ranges;
- C_1 = fixed constant; and
- C_2 = constant, the value of which depends on the fatigue life, which is calculated from σ_{eff} .

The term $[\sum (\Delta \sigma_{i,j}^{\text{amp}})^2]^{1/2}$ is directly related to the octahedral shear stress.

Crack Initiation and Statistical Nature of Fatigue

PHOENIX determines the actual life at each of the evaluation depths by calculating the damage fraction for each load in a histogram (spectra) of loads. The tonnage increments are repeated until the damage fraction at any one depth evaluated reaches unity. At this point in tonnage and depth, fatigue crack initiation is considered to have taken place.

The damage fraction (DF) is calculated along the lines of Miner's law:

$$DF = \sum \frac{N}{N_f}$$

where N is the number of cycles in a block of load L only, and N_f is the total number of cycles expected to cause fatigue crack initiation for a specified life percentile at the total stress state associated with (but not necessarily caused solely by) load L .

"Life percentile" refers to the fact that under the influence of fixed repetitive load (i.e., the stress history), fatigue failures do not all occur simultaneously; rather, they are spread out over a period of loading in a relatively well-behaved distribution. Thus, if one is to calculate "life," the life percentile must be specified.

In a fatigue life prediction analysis based on stress state, the value of N_f can be obtained from laboratory constant stress-life tests (S/N tests). However, a substantial number of replicate tests must be made at each stress level in order to define the life distribution from which the life percentile is taken. Normally, if relatively few laboratory specimens are tested at each stress level, the S/N plot obtained is presumed to define the 50th life percentile. Typically, PHOENIX calculations are made at 1st, 5th, 10th, and 20th percentiles, although this is user specified. The effects of work hardening of the running surface can also be included by specifying surface and interior hardnesses and a depth range over which the hardness transition occurs.

Limitations and Applications

There are problems in using any fatigue model (including PHOENIX) to make exact life predictions. First, the residual stress state within any individual rail or even group of rails is entirely unknown and cannot be predicted accurately at present from a knowledge of service history. Moreover, the actual applied stress state is not really known either; this is especially the case for the contact stress because it is highly sensitive to actual wheel and rail profiles; true Hertzian contact exists only for new wheel and rail profiles. Finally, the inherent fatigue resistance character of the rail steel can be highly variable and is unknown for any individual rail or group of rails. Small variations in stress state or material fatigue resistance can yield large variations in life.

In spite of these limitations, modeling the rail fatigue crack initiation process can be informative if for no other reason than to allow an engineering estimate of best- and worst-case conditions when some important material, track, or service condition is altered. For instance, if the cleanest (freest of non-metallic inclusions) rail steel for which S/N data are available or a 300-BHN standard carbon rail were compared with the derived overall rail life distribution (FAST tangent track conditions), significant improvement in fatigue life (2 to 2.5 times) would be expected. Also, the effect of rail wear on rail fatigue life can be gauged. Modest wear tends to prolong fatigue life and that effect is most pronounced at larger (more worn) crown radii and at longer life percentiles.

Rail Testing: Strategies for Safe and Economical Rail Quality Assurance

OSCAR ORRINGER

Current trends toward increased mainline traffic density, greater average axle load, and extension of wear life are expected to increase the rate at which metal fatigue defects form in rails. A decade of research on rail integrity has led to better understanding of how rail defects form and propagate. The research is discussed and examples are presented to show how the results can be used to provide guidelines for improving in-service inspection methods and schedules.

A decade of federal government and railroad industry research on rail integrity has led to better understanding of how rails respond to the damaging effects of the train loads they must carry. Major elements of the research now approaching completion will soon provide guidelines for better rail quality specifications and better rail-testing strategies. These guidelines will help to meet two objectives: improved rail resistance to failures originating from defects and improved targeting of in-service inspections.

Rail quality has heretofore meant tight dimensional tolerances, high static strength, and good resistance to wear. Track and mechanical departments strive to reduce their respective wear replacement costs for rail and wheels; a generation of this competition has led to increases of 35 to 50 Brinell points in wheel tread and rail head hardness and, on the rail side, development of premium steels with strengths up to 30 percent higher than the strength of standard composition rail steel.

In the same generation the transition from 50-ton to 70-ton freight cars, quickly followed by a further transition to 100-ton cars, has placed increasing demands on rails and track structure. Rail defects statistics compiled by the Sperry Rail Service (1) illustrate the effects of increased axle loads and subsequent track renewal (Figure 1). The rising defect rate from 1960 to 1970 (mainly rail-end defects in bolted-joint track) reflects both increasing distress and better flaw detection by improved rail test equipment and procedures combining ultrasonic scanning with the older magnetic induction method. During the same period several railroads also established their own fleets of highway-rail-capable vehicles carrying ultrasonic test equipment (2). The ability of these vehicles to save time en route between test zones also increased the ratio of test hours to operating hours.

By 1970 track rehabilitations had started to turn the defect rate around, and the new trend was accelerated by improvements in rail testing. The major thrust has been to replace bolted-joint rail (BJR) with continuous welded rail (CWR), an

effort that continues today at the rate of about 2,000 to 5,000 track-mi a year. Although CWR usually retains some joints to provide electrical insulation at the ends of signal blocks, these tend to be high-quality bonded joints fabricated in plants, and they number only a few per mile in contrast to the hundreds of unbonded joints per mile of BJR. Hence, it is not surprising to see that the rail defect rate has declined almost as precipitously since 1970 as it increased beforehand.

The research program that started in the mid-1970s first tended to look back to the existing problem. As the effects of track rehabilitation and improved rail testing became apparent, however, the research direction gradually shifted from the past to the future. Three current trends in railroad operations suggest the future risk potential.

First, the merger wave that began in 1980 and continued in 1987 tends to concentrate more gross tons per year on fewer miles of track, as Figure 2 shows (3). The major mainlines naturally receive proportionately more maintenance attention, and rail stock turnover is accelerated where high traffic densities have caused excessive shelling or curve wear. New track technologies (premium-alloy rail, CWR, concrete ties, etc.) are now being introduced at rates faster than the historical ones.

Second, the focus on energy conservation stimulated by the 1973 oil shock has caused the railroads to think beyond the original idea of lubricating a curve rail for wear reduction and to seriously consider lubrication as a strategy for fuel savings. It is likely that the railroads will react to the next rise in oil prices by adopting widespread lubrication to reduce the energy lost from wheel-rail friction drag. Reduced rail wear rate will be a beneficial side effect of such a policy (4), but the increase in average rail service life also brings with it the potential for an increase in the density of rail defects.

Third, loads might increase again if cars with 110- or 125-ton capacity can be designed with payload-to-tare ratios greater than those in the current freight car fleet. A transition from 100- to 125-ton cars would likely increase the maximum static axle load from 33 to 41 tons. The Transportation Test Center (TTC) will be investigating the effects of 39-ton axle loads in its next phase of testing on the high-tonnage loop of the Facility for Accelerated Service Testing (FAST). Earlier captive revenue service experience suggests that such car loads have the potential to induce rail defect formation faster than the percentage increase of wheel load would indicate (2, 5, 6).

The accelerated pace at which rail and the demands placed on it are changing leaves little time for reaction. Therefore, the research program must be relied on for basic results that track

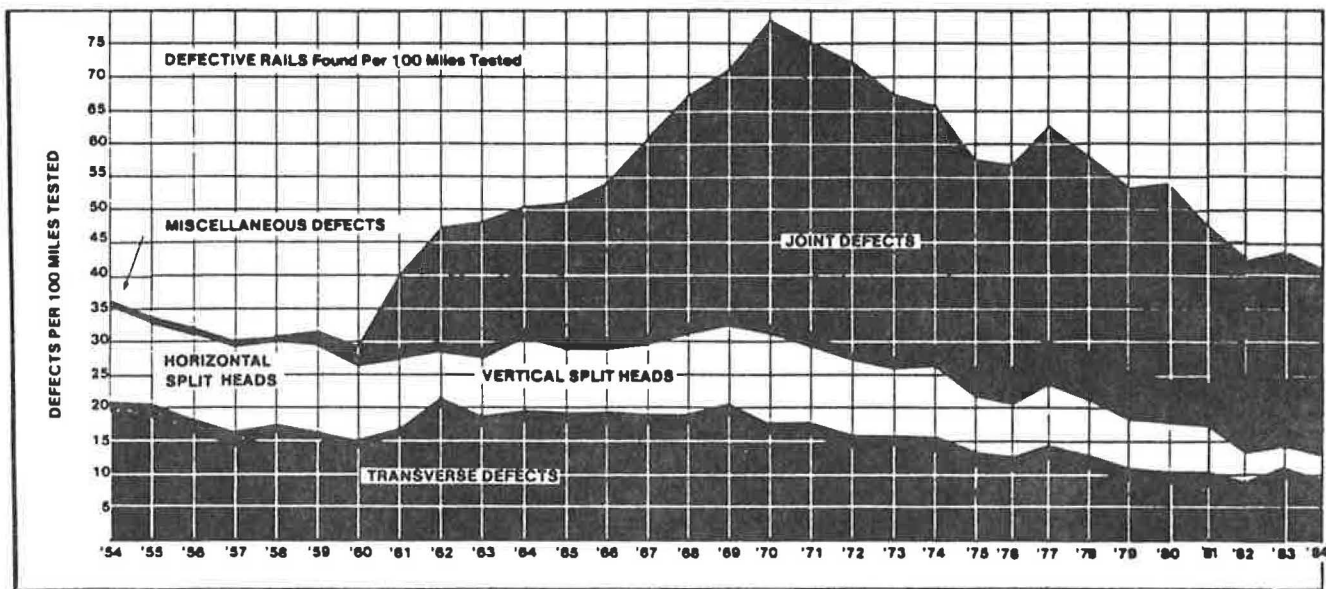


FIGURE 1 Annual density of detected rail defects (courtesy of Sperry Rail Service).

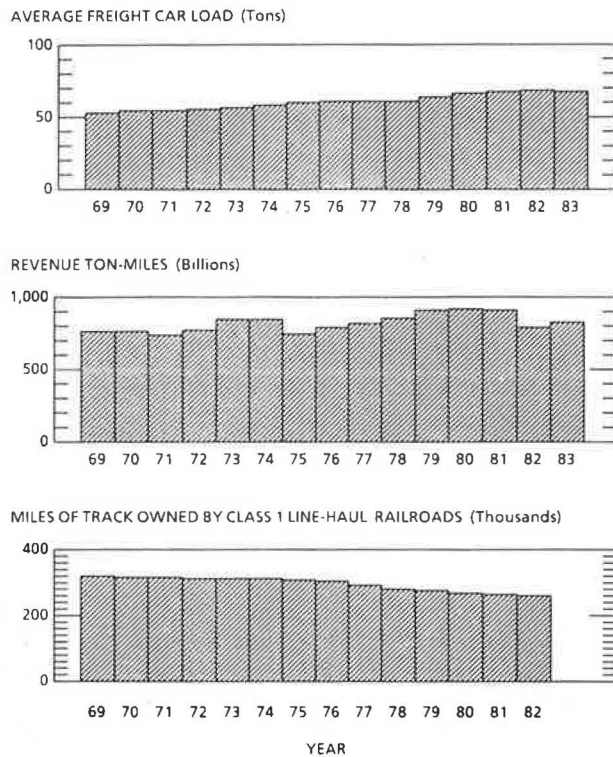


FIGURE 2 Annual statistics of railroad operations in the United States (3).

departments can translate into anticipatory engineering practices. The basic results and engineering practices have both economic and safety dimensions. This paper deals primarily with the safety question of where and how often to test rail for defects. The research program answers this question by applying knowledge of fatigue, fracture mechanics, and nondestructive inspection (NDI) technology to develop trade-offs between track quality and rail test frequency.

The most numerous rail defects are found to be those types that originate from metal fatigue. Knowledge of fatigue behavior can be used to define average rates of defect occurrence and to indicate when the rates might be expected to increase. It is impractical to apply NDI in service at frequencies that would guarantee opportunities to detect every conceivable defect, but occurrence-rate trends can provide a basis for adjusting the frequency to keep the rate at which trains are exposed to undetected defects within reasonable bounds.

Knowledge of fracture mechanics, that is, the propagation behavior of rail defects that have become growing cracks, can be used to translate familiar railroad engineering factors (train makeup, rail section, track curvature, etc.) into estimates of time available to detect defects. In practice such estimates are of most interest for the common defect types, those that should pace rail-testing schedules. Fracture mechanics can also quantify the potential benefit of improved NDI equipment, since a crack propagation model relates time available for detection of a defect to the defect size that the equipment is able to find.

DEFECT OCCURRENCE

The Federal Railroad Administration (FRA) annually publishes national summaries of accident statistics compiled from railroad reports and categorized by cause. The statistics of accidents caused by rail defects provide a guide to the relative importance of different defect types but must be supplemented by other data for proper interpretation. A study of railroad records of rail defect occurrences was undertaken for this purpose (7). The study encompassed about 25,000 detected defects and service breaks on some 8,200 track-mi owned by four railroads (Table 1).

Each railroad has its own system of record keeping for the purpose of identifying rail defects and monitoring repair and removal actions. Most of these systems closely correspond to the definitions established by the FRA for accident reporting. Those FRA cause codes that are of interest in the present case

TABLE 1 COVERAGE OF RAIL DEFECT OCCURRENCE STUDY

Territory	Years Covered	No. of Lines ^a	Total Track Miles	Density of Traffic ^b	Total Defects
Southwest BJR and CWR	1974 to 1979	6	1,005 ^c to 1,104 ^d	Average to High	2,478
Northeast Line upgraded from BJR to CWR during period covered	1976 to 1980	1	247	Average	2,000
Midwest with severe mid-continent winter climate BJR and CWR	1976 to 1981	16	6,438	Low to High	18,944
Midwest Single rail section on 80% of line	1976 to 1980	1	508	High	1,395

^a As defined by traffic division points.

^b Average means 10 to 20 million gross tons (MGT) per year; low density means 1 to 10 MGT/year; high density means 20 to 120 MGT/year.

^c For the years 1974 to 1976.

^d For the years 1977 to 1979.

(together with common industry symbols) are summarized in Table 2, which also classifies the defects by the source of the damage causing them.

Practical knowledge of two particular behavior factors is essential to the understanding of rail defect databases. First, true broken-base defects result from damage by foreign objects, for example, a nick from a misapplied spike maul, and propagate in a manner such that a half-moon-shaped piece about 4 to 8 in. long is separated from one side of the rail base. The consequent increase of base tension under train loads may later reinitiate a propagating crack and cause the rail to fail, but the distinctive half-moon separation can still be seen, and the original defect is easy to correctly classify. True broken-base defects are rare because damage by foreign objects rarely occurs. However, other types of defects are often misreported as broken bases. These mistakes are not made by track inspectors, but errors inevitably occur when others attempt to fit the inspectors' informally written descriptions into the formal definitions of the record-keeping system.

Second, true fissure defects [transverse fissures (TFs) and compound fissures (CFs)] result from the accretion of excess hydrogen into flakes that locally embrittle the rail steel and thus promote early crack nucleation. A high fissure occurrence rate early in this century led to the general adoption of the controlled cooling process around 1936, and rails manufactured thereafter generally contain too little hydrogen to form damaging flakes. Fissures can still be found occasionally in rails that have not been properly cooled, but today fissure reports more often result from misclassification of detail fractures. Rail test personnel are generally well versed in the difference between detail fractures and fissures and rely on interpretation of ultrasonic signals to classify these internal defects. Ultrasonically determined location in the rail head provides a good guideline for most such defects, which are usually small to medium-sized when found, but large defects are much less easily classified (Figure 3). Track maintenance personnel can visually examine the crack propagation surfaces of a service break, but they are not skilled fracture specialists and can easily

TABLE 2 CODES FOR REPORTING RAIL DEFECTS THAT HAVE CAUSED ACCIDENTS

Code	Symbol	Defect Type	Damage Source
130	BHC BHB	Bolt hole crack Bolt hole break	Fretting fatigue
131	BB	Broken base	F.O.D. ^a
132	DFW	Defective field weld	Fabrication
133	DPW	Defective plant weld	Fabrication
134	DF	Detail fracture	Fatigue
135	EBF	Engine burn fracture	Operations
136	HWS (O)	Head-web separation outside the joint bar area	Fatigue
137	HWS (I)	Head-web separation within the joint bar area	Fatigue
138	HSB	Horizontal split head	Fatigue
139	PIPE	Piped rail	Fabrication
141	TF CF	Transverse fissure Compound fissure	Fabrication
142	VSH	Vertical split head	Fatigue
149	---	Cause code not reported	--- ^b

^a Foreign object damage. ^b Damage sources unknown.

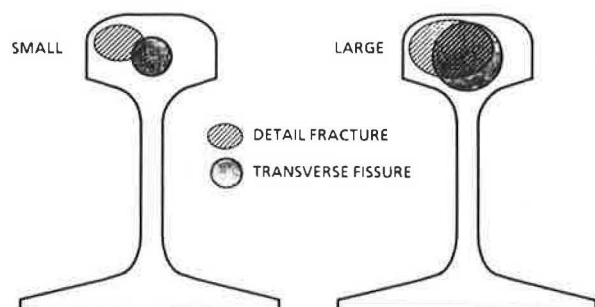


FIGURE 3 Locations of detail fracture and transverse fissure in rail section.

misclassify a detail fracture as a transverse fissure. Under these circumstances one should expect a low percentage of misclassification for detected defects, a moderate percentage for the service defects found and classified by track inspectors, and

a high percentage in the summary reports that form the national accident database.

The national accident reporting system came into being in the early 1970s, and the raw statistics of accidents caused by rail defects have been consistent from year to year. The 1975 statistics are compared with aggregates of 1978–1985 and 1983–1985 in Figure 4. The accidents in each cause code are normalized as a percentage of the total accidents for the period covered to provide a common basis for comparison. The percentage of accidents caused by bolt-hole cracks has declined, as has the density of detected rail-end defects (Figure 1). The data in Figure 4 also suggest that the percentage of accidents caused by detail fractures has increased, but no other clear relative trends appear. The absolute trend of accidents caused by rail defects has been generally downward since 1970. The total number of accidents attributed to all types of rail defects has declined from a peak of about 500 a year to a steady rate of about 250 a year at present.

A superficial assessment of Figure 4 would lead one to conclude that fissures and broken bases are the most worrisome types of rail defects, but this appearance results from the reporting artifacts mentioned earlier. Track inspectors might naturally tend to use the word "fissure" or its synonyms to refer to the fractured appearance of a rail failure at a defective weld, detail fracture, or engine burn fracture. Words such as "broken through to the base" might as easily be used to describe rail failures from bolt-hole cracks, defective welds, detail fractures, or engine burn fractures. If the raw accident data are adjusted by reassigning equal proportions of the broken-base and fissure defects to the indicated categories, the relative proportions appear as shown in Figure 5, in which the defective welds have also been grouped to simplify the picture. Defective welds, detail fractures, and engine burn fractures now appear as significant accident causes in contrast to their apparently minor roles in the raw data. The recategorization probably overemphasizes engine burn fractures relative to bolt-hole cracks, defective welds, and detail fractures.

How realistic is the recategorization? One can get some idea by constructing similar plots of detected defects and service breaks. The data in Figure 6 illustrate a typical sample taken from an aggregate of the records of two railroads (Engineering Economics Division, Association of American Railroads, unpublished data, 1985). The following four adjustments have been made to account for differences between the FRA reporting definitions and the classification system used on the railroad data. First, defective field and plant welds were reported as a single category, which is shown under the field weld cause code. Second, head-web separations within the joint bar area were lumped together with bolt-hole cracks and are included under the latter cause code. Third, piped rails were included and are shown under cause code 136 (head-web separations extending outside the joint bar area). Fourth, crushed heads, broken rails, and other transverse defects are shown under the "not reported" category (149) because

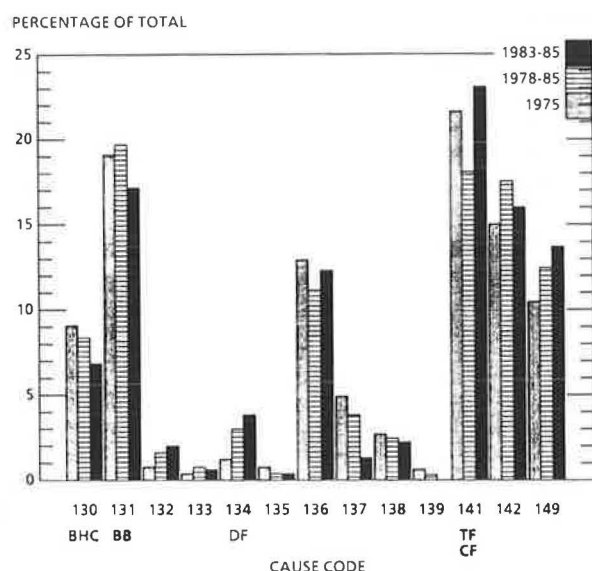


FIGURE 4 Accident causes broken down by rail defect type.

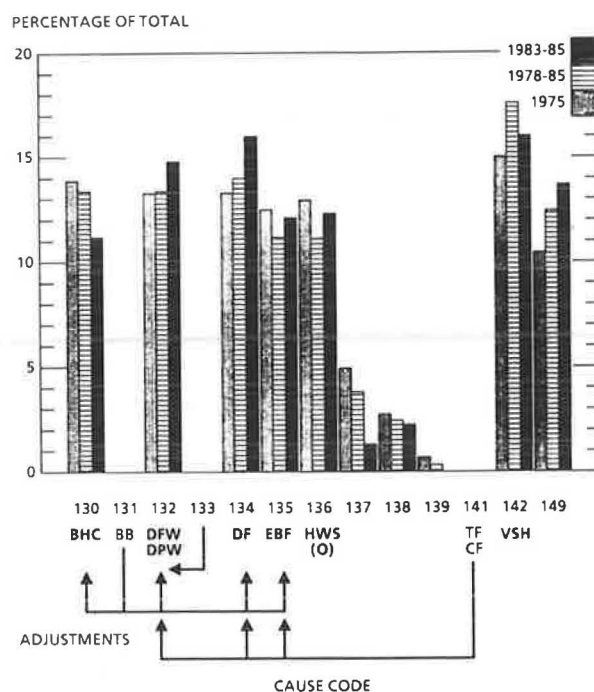


FIGURE 5 Accident statistics after adjustment for reporting artifacts.

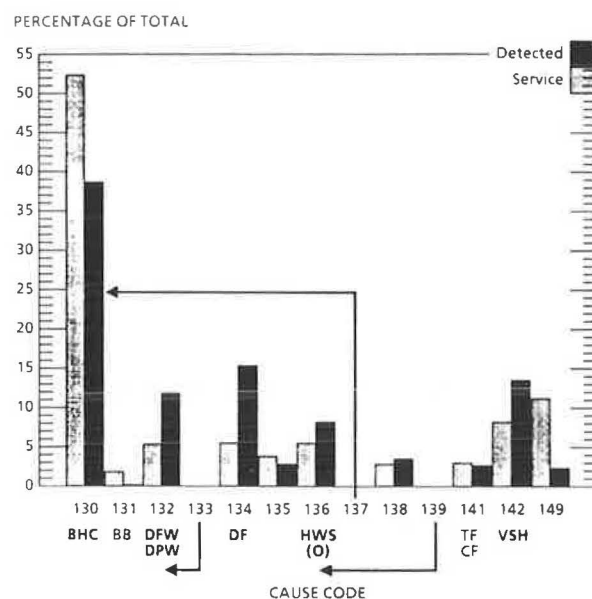


FIGURE 6 Sample of detected and service defects (1980-1983).

there are no specific cause codes for these defect types. However, those defects that the railroad classified as broken base or fissure have not been recategorized. The percentage of rail-end defects is much higher than the corresponding accident percentage, a result that probably reflects the inclusion of sidings in the sample as well as mainline track. Otherwise the sample highlights defective welds, detail fractures, head-web separations outside the joint bar area, and vertical split heads; fissures appear only as a small percentage and broken base defects have almost disappeared from the population. The

ratios of detail fractures to fissures reflect the previously mentioned difference in classification skill, and comparison of Figure 6 with Figure 4 reveals the existence of the reporting artifacts mentioned earlier. The relative proportions of accident causes are thus likely to lie somewhere between the proportions shown in Figures 5 and 6.

By what means are rail defects most often found? The Figure 6 data are replotted in Figure 7 to answer this question. For each defect type, the proportion found by rail test is shown as a percentage of the total found by testing and track inspectors. Bolt-hole cracks, defective welds, detail fractures, head-web separations outside the joint bar area, and vertical split heads thus emerge as the most common defect types, and rail testing emerges as the principal means by which most defects are found.

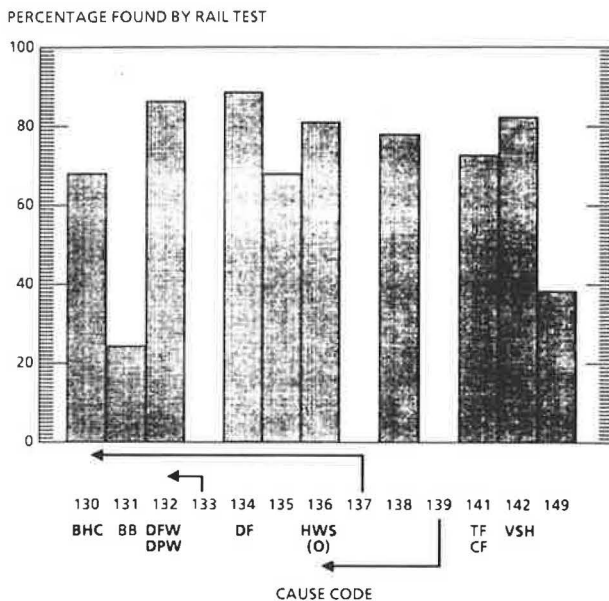


FIGURE 7 Percentage of defects found by rail test.

The defect occurrence pattern study (7) consistently revealed bolt-hole cracks, detail fractures, and vertical split heads to be the most common defect types in rail that has carried at least 100 million gross tons (MGT). The result should not be surprising, because these types of rail defect are all caused by metal fatigue. Conversely, defective welds result from imperfections in welding processes and reflect transient situations associated with CWR installation. The economic limit on rail life, as determined by scheduled replacement of worn rail, lies between 500 and 700 MGT and might be extended to 1,000 MGT by means of widespread lubrication. Thus, the major proportion of rail service life is and will continue to be spent in the fatigue crack nucleation regime, and the crack propagation behavior of the principal fatigue defect types should be taken into account when rail test schedules are established.

Compilations of defect rate histories on the TTC FAST track and a number of revenue lines have shown how exposure of trains to rail defects is related to tonnage (6). The cumulative percentage P of defective rails in a rail population is generally found to follow a Weibull probability distribution with respect to the cumulative tonnage T that the rail has carried:

$$P(T) = 1 - \exp[-(T/\beta)^\alpha] \quad (1)$$

where the exponent α is about 3 and the characteristic life β is about 2,000 MGT. Exposure (the rate of defect occurrence per million gross tons) is obtained by differentiating Equation 1:

$$dP/dT = (\alpha T^{\alpha-1}/\beta^\alpha) \exp[-(T/\beta)^\alpha] \quad (2)$$

The characteristic life is the cumulative tonnage at which 63 percent of the rail population would have developed defects, but rail is generally removed from service well before that point. In the service regime ($T \leq 1,000$ MGT), the exposure increases as tonnage accumulates. Fatigue defect occurrences generally become noticeable at about 250 MGT, when P is about 0.2 percent. Table 3 shows the increase in cumulative density and defect occurrence rate as the rail accumulates tonnage. The occurrence rates in the table are the number of new defects that would be generated in the next 20-MGT interval following the accumulated tonnage. On many revenue lines that have high traffic densities, rail tests are performed at about 20-MGT intervals.

The foregoing idealized model accurately describes exposure only when applied to short segments of track with homogeneous structural and operational characteristics. Conversely, most revenue lines contain a wide variety of rail, ballast, grade and curvature, special trackwork, and so on; are subject to varying load characteristics from the effects of train handling; and often receive rail renewals piecemeal. Exposure on a revenue line thus tends to fluctuate as particular track segments enter the fatigue regime, become problem areas, are controlled by rail test, are renewed, and relinquish the problem role to other segments.

The defect occurrence study (7) brought this behavior to light when analyses of defect density at 1-mi resolution revealed patterns of occurrence in clusters. The lengths and locations of defect cluster zones tended to remain stable over the study's several-year span. As a general rule, the results suggested that 90 percent of the rail defects in a revenue line would be located in 30 percent of the track miles, although there was wide variation from one line to another. For a few lines, 90 percent of the rail defects were concentrated in as little as 10 percent of the track miles, whereas for other lines, there was little or no concentration. The most concentrated zones were those associated with obvious construction features such as bridges, where sudden changes in track modulus could be expected to excite dynamic oscillations in passing trains. Zones reflecting fatigue of aging rail were similarly concentrated and were well defined by rail relay boundaries. On the other hand, well-maintained BJR of uniform age generally showed little or no concentration of rail defects.

The complexity of the actual behavior makes it difficult to define a simple measure of exposure to guide the adjustment of rail test schedules. Some of the measures that have been used by some railroads or proposed from the research activities are traffic density, a rising trend of defect density, a rising trend of service breaks, the ratio of service breaks to detected defects, cumulative tonnage, and exceedance of a specified number of defects per mile per test. There is no agreement on how to deal with exposure, and none is likely in view of the strong opinions of track engineers based on their own experiences.

TABLE 3 DEFECT DENSITY AND RATE VERSUS ACCUMULATED TONNAGE

Accumulated Tonnage (MGT)	250	500	750	1,000
Cumulative rail defects (percent)	0.2	1.5	5.1	11.7
Cumulative density (defects per track mile) ^a	0.5	4.1	13.6	31.9
Defect rate (defects per track mile per 20 MGT) ^a	0.1	0.5	1.1	1.8

^a Based on 273 rails per track mile.

Although control of exposure is difficult to translate into a standard, the results of the research program have suggested some general guidelines that individual railroads can follow. For example, an occasional plot of defect reports by milepost is a good way to spot cluster zones, and such zones can be given supplemental inspections or special maintenance. One railroad has applied this technique to 2,500 mi of mainline track that had previously been tested three times a year. The plot revealed some 200 mi of cluster zones, a few of which were dealt with by means of track modifications. Because the line had had a low accident rate and was already being tested three times as often as required by the current safety regulations, the railroad cut back to two complete tests a year and concentrated the third test on the critical 200 mi. The service break rate has remained stable during 2 years of the revised test schedule, a result that suggests that the new strategy saves resources without sacrificing safety.

Another example of a general guideline involves the scheduling of a fixed number of rail tests so as to increase the test frequency toward the end of the rail's useful service life instead of keeping the frequency constant. This strategy has been studied by means of a simulation that combines a defect occurrence, growth, and detection model (2) with economic analysis of the expected costs of defective rail removal and accidents caused by undetected defects (8). The economic analysis employs cost factors compiled by the Association of American Railroads (AAR) and uses a national average accident rate of the order of one accident per 200 service defects. When a preliminary version of the model was applied to a hypothetical line with a traffic density of 60 MGT per year, the lowest-cost strategy was found to be 25-MGT intervals between tests of new rail, decreasing to 10-MGT intervals toward the end of the useful service life. These results suggest that cumulative tonnage can be used to control exposure, but a wide variety of cases must be analyzed to provide a good basis for guidelines on test frequency adjustment.

CRACK PROPAGATION BEHAVIOR

Once a defect has formed in a rail, it generally becomes a propagating crack; that is, its size gradually increases under the influence of the cyclical stresses that trains impose on the rail. Sooner or later the defect will grow to a size that has some chance of being detected, but if not, it will eventually grow large enough to fracture the rail under a train. The number of stress cycles or equivalent gross tonnage required to make the

defect grow from the minimum size for detection to the incipient fracture size is referred to as the safe crack growth life. If the minimum detection and incipient fracture sizes were known with certainty, safe crack growth life would be synonymous with the safe interval for rail testing to find the given type of defect under the given conditions. In practice, however, these defect sizes are not well defined, and complete coverage of the possible conditions cannot be guaranteed; therefore, two or more rail tests must be performed within the safe crack growth life to properly control the risk of rail failure.

Table 4 gives 10 factors that affect safe crack growth life for detail fractures. Other kinds of rail defects have many of these factors in common, but each defect type generally has one or more unique factors. Because there are so many factors to consider, one must have a model of each defect type as a propagating crack in order to make life estimates for the many possible combinations of factors. Such models can be constructed from the principles of engineering fracture mechanics (9) but are necessarily idealizations of the actual rail defects. Therefore, both laboratory and field testing are also essential to establish confidence in the engineering model. Laboratory specimen testing in accordance with established standards (ASTM E-399-72) is performed for two purposes: characterization of basic material properties and assessment of memory

TABLE 4 FACTORS AFFECTING DETAIL FRACTURE PROPAGATION

Quantity	Minimum Value	Maximum Value
Track foundation modulus ^a (ksi)	1	10
Track curvature ^b (degrees)	0	8 ^c
Rail section ^c	100 RE	155 PS 32.6 ^d
Average axle load (tons)	10	38.5 ^e
Normal dynamic load factor (<i>g</i> , rms)	0.1	0.8
Dynamic load factor for wheel anomalies (<i>g</i> , peak)	1	3
Anomalous wheel density (%)	0	0.5
Rail neutral temperature ^f (°F)	60	90
Rail service temperature ^f (°F)	-40	150
Axial residual stress in rail head (ksi)	10	30

^aValues shown are for vertical modulus.

^bRadius of curvature (ft) = 5,730 ÷ degree of curvature; e.g., *R* = 5,730 ft for a 1-degree curve; *R* = 573 ft for a 10-degree curve.

^cExcludes low-density branchline track.

^dUnder current interchange rules.

^eLoaded 125-ton cars in unit train.

^fAffects CWR only.

effects. Field testing is required to confirm the validity of the idealized defect model.

The material property most important to safe life is the propagation rate (crack size increment per cycle) as a function of the current crack size and the cyclical stress amplitude. Several such investigations of rail steel have been made (10–12). The most conveniently applied life estimation models simply sum the crack-size increments corresponding to the spectrum of service stress amplitudes, without regard to the effect one stress cycle might have on the rate of crack propagation in succeeding cycles (13).

Memory phenomena can appear when materials are subjected to varying stresses; variable-amplitude (“spectrum”) stress tests are required to assess the effect for each material and service environment. For example, cracks in aluminum alloys tend to grow more slowly than one would predict under high-low sequence aircraft stress spectra (14). Recent experiments on rail steel subjected to a real sequence rail head stress spectrum simulating heavy-haul train loads have shown that crack propagation is moderately accelerated (15, 16).

Rails containing detail fractures have also been field tested in tangent sections of revenue track and the TTC FAST track (17). The unique FAST traffic pattern (running direction reversed approximately once per million gross tons) during the test formed prominent ridges on the crack propagation surfaces, providing the means for accurate definition of the flaw location and area as functions of the gross tonnage applied in the test. The rail residual stresses near one of the FAST test defects were also measured by strain gauges in a destructive sectioning technique specially developed for rail residual stress determination (18). This detail fracture thus has the least uncertainty in the description of its service environment.

The crack-size histories for the laboratory spectrum test and the FAST test defect just mentioned are plotted in Figure 8. Also shown are predictions of the crack size histories obtained from a preliminary version of the detail fracture crack propagation model. The laboratory results have been converted to equivalent defect area and tonnage and have been shifted to correctly superimpose the starting point on the FAST test data.

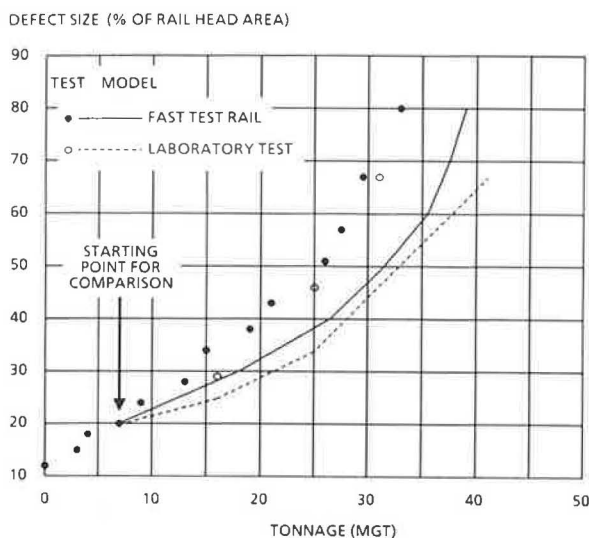


FIGURE 8 Laboratory simulation and field test results for detail fracture growth.

Comparison of the two results shows that the laboratory test was a reasonable simulation of the FAST test. Comparing the model prediction of the laboratory test with the data illustrates the moderate acceleration effect mentioned earlier. The model-to-test relation for the FAST experiment is similar to that for the laboratory experiment; that is, the actual safe crack growth life should be taken as about 80 percent of the calculated life.

Additional confidence was gained when the model was applied to the analysis of another detail fracture that had been involved in a derailment on a curve at FAST about 2 years before the tangent-track field test. Table 5 shows how the model inputs for this defect differ from those for the test defect. In Figure 9 the model prediction is compared with an estimate of the actual defect growth history. The curve of defect size versus number of wheel passages was obtained by means of post-test measurements on the crack propagation surface (4), but there is some uncertainty about what value of average axle load best represents the FAST train at the time this defect grew. Because of the unusually severe thermal and residual stresses in this rail, the defect grew rapidly to 11 percent of the rail head area, whereas the test defect grew slowly from 12 to 80 percent of the rail head area. Nevertheless, actual crack growth life is 75 to 80 percent of the calculated life in the present case, suggesting that the detail fracture model has a consistent bias.

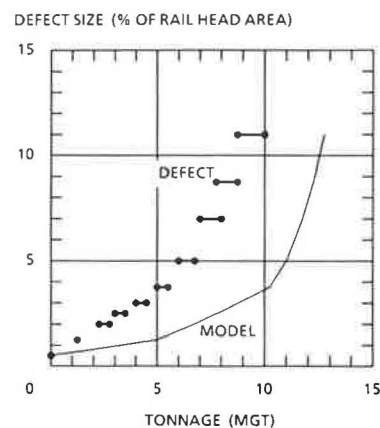


FIGURE 9 Application of model to defect involved in 1980 FAST derailment.

Tables 6 and 7 show how the model can be used to assess the sensitivity of safe crack growth life to some of the factors affecting detail fracture propagation. The FAST test is taken as the baseline, and the effect of changing a single variable is examined in each case. Table 6 shows how the safe crack growth life of the fast test detail fracture is projected to decrease as the average axle load increases, and vice versa.

The effects of three track construction features are demonstrated in Table 7. First, heavier rail sections increase safe life, but little is gained in going from 136 RE to 140 RE rail, and there is only a modest gain in going to 155 PS, the heaviest section manufactured for U.S. freight service. Second, a stiffer track foundation increases safe life. A vertical track modulus of 1 ksi represents poorly maintained wood-tie track, 2.5 ksi reflects average wood-tie track conditions, 5 ksi represents the best foundation achievable with wood-tie track or average

TABLE 5 INPUT FACTORS FOR DETAIL FRACTURES AT FAST

Quantity	Test Rail	1980 Derailment
Vertical track foundation modulus (ksi)	2.5	2.5
Track curvature (degree) ^a	0	4
Rail section	136 RE	115 RE
Average axle load (tons)	30.8	27.0 ^b 31.0 ^c
Normal dynamic load factor ("g"-rms)	0.26	0.26
Dynamic load factor for wheel anomalies ("g"-rms)	--- ^d	--- ^d
Anomalous wheel density (%)	0	0
Rail neutral temperature (°F)	95 ^e 60 ^f	60 ^g
Rail service temperature (°F)	62 ^e 26 ^f	20 ^g
Axial residual stress in the rail head (ksi)	10	30

^a Radius of curvature (ft.) = 5,730 ÷ degree of curvature.

^{b,c} Minimum and maximum estimates.

^d Not used; no large wheel anomalies in the FAST train.

^{e,f} Approximate initial and final values for the test period; monthly average mean values for service temperature.

^g Estimated for January-February period during which crack growth occurred.

properties for concrete-tie track, and 10 ksi represents the best foundation achievable with concrete-tie track. Third, track curvature decreases safe life. The curvature effect shown here is that for the high rail, which is subject to severe lateral loads from the lead wheel of each truck (19). The model predicts that safe crack growth life of the FAST test defect on a 5-degree curve would have been about half that on the tangent track.

The foregoing results are realistic because they refer to a detail fracture that grows from 12 to 80 percent of the rail head area. These sizes are consistent with current detection capability and knowledge of incipient fracture size under normal conditions. The safe crack growth life estimates should not be applied to revenue track, however, because the FAST test defect was subjected to a unique history of thermal stress,

which might have caused the day-to-day crack growth rate (and hence the safe life) to differ from the rates and safe lives associated with typical revenue-track thermal stress histories. Also, the preliminary detail fracture model still requires some refinement, and a modified version is now being developed (20). Nevertheless, the examples show that expected variations of construction and operational factors can have important effects on safe crack growth life and that track engineers might usefully consider the safe rail test interval when they assess track quality design trade-offs.

The detail fracture is currently the best understood rail defect from the viewpoint of crack propagation. Similar efforts to develop models of the bolt-hole crack and vertical split head are under way. Some factors that affect these defects but have

TABLE 6 EFFECT OF TRAIN MAKEUP ON SAFE CRACK GROWTH LIFE

Train Makeup	Average Axle Load (Tons)	Safe Crack Growth Life (MGT) ^a
Empty unit coal train: 4 locomotives; 111 cars; 3,847 trailing tons	9.9	98
Mixed revenue freight: 2 locomotives; 41 cars; 2,583 trailing tons	16.5	40
FAST test consist: 4 locomotives; 81 cars; 9,957 trailing tons	30.8	34
Loaded unit coal train: 6 locomotives; 111 cars; 15,665 trailing tons	32.6	30
Loaded 125-ton unit coal train: 6 locomotives; 101 cars; 16,950 trailing tons	38.5	25

^a Factor of 80 % for acceleration has been applied.

TABLE 7 EFFECT OF TRACK CONSTRUCTION CHARACTERISTICS ON SAFE CRACK GROWTH LIFE

Characteristic	Safe Crack Growth Life ^a (MGT)
Rail bending stiffness	
100 RE	21
115 RE	24
132 RE	36
136 RE	34 ^b
140 RE	36
155 PS	40
Track stiffness (vertical track foundation modulus, ksi)	
1.0	21
2.5	34 ^b
5.0	39
10.0	47
Track curvature (degrees)	
0	34 ^b
5	18

^aFactor of 80 percent for acceleration has been applied.

^bBaseline case.

little or no influence on detail fracture growth are rail end tolerance, train speed, and in-plane residual stress.

Rail end gap and height mismatch can have a strong influence on bolt-hole crack propagation because such conditions induce large dynamic wheel loads on the receiving rail. The dynamic load factor increases with train speed and can be

comparable with the anomalous wheel factors in Table 4 when the train speed exceeds 20 mph. In this case, however, every passing wheel imposes a large load on the rail. The effects of these variables were investigated in a recent test at the TTC, where crack growth data are now being gathered as bolt-hole cracks are detected in the FAST track. A laboratory test of a short length of rail under simulated joint loading conditions provided the basis for a bolt-hole crack propagation model (21).

In-plane (lateral and vertical) residual stresses in the rail head promote the formation and growth of vertical split head defects, just as axial residual stress promotes detail fracture growth. The residual stress measurement program has shown that the in-plane residual stresses are three to four times as large as the axial stress (18). Development of a crack propagation model for vertical split heads is just starting, and field test requirements for these defects remain to be defined.

NDI TECHNOLOGY AND SAFE INSPECTION INTERVAL

The typical interval of 20 MGT for rail tests on lines with high traffic density is based on experience with current (i.e., 1960s to 1970s) technology for rail test equipment. Railroad records of detected defects and service breaks suggest that the current NDI systems are finding about 80 to 90 percent of the rail defects (see Figure 7).

NDI research projects in the mid-1970s investigated real-time signal processing, improved display, and automatic control of sensor alignment on the rail (2). The research goals were improved flaw detection reliability and the ability to test rail at higher speed with no sacrifice of reliability.

The current detector-car fleet is generally able to perform reliable rail testing at 15 mph. Each time a defect is detected, the crew must also stop to hand-test, verify, and classify the defect, an operation that generally takes about 1 min. Trains stacked up behind detector cars cause reduced revenue throughput, whereas detector cars sitting on sidings cause available equipment hours to be lost from the rail test schedule.

The data in Table 8 show the effect of the conflict between rail testing and revenue traffic from the viewpoint of the operating department. The example is for 150 mi of single-track line on which revenue traffic is assumed to travel at 45 mph without interference. The current situation is represented by a 15-mph rail test operation that is assumed to find one defect per mile per inspection, that is, corresponding to rail with just under 750 cumulative MGT (see Table 3). Under these assumptions, the time required to get the detector car over the line is 10 hr of travel at 15 mph plus 2.5 hr of 1-min stops to verify 150 defects, for a total of 12.5 hr of track occupation at an effective speed of 12 mph. Trains traveling behind the detector car close at the rate of 33 mph (45 mph – 12 mph). The product of track occupation time and closure speed (12.5 hr \times 33 mph = 412.5 mi) is a measure of the stackup effect, because the number of trains delayed is simply the stackup length divided by the average headway. The second case in Table 8 shows that the stackup length can be reduced to less than 200 mi if an improved system capable of testing at 30 mph is postulated. In the third case a net benefit is shown even if the improved system is assumed to find more defects per mile.

Figure 10 shows schematically the difference between current and improved equipment in terms of the chance $P(X)$

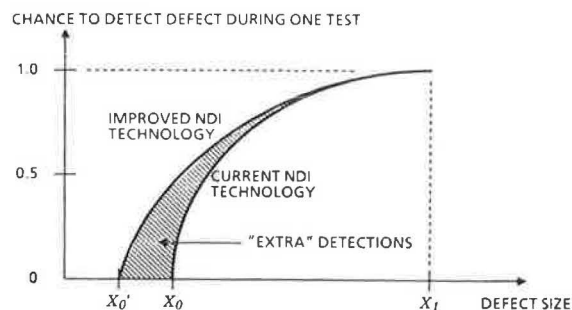


FIGURE 10 Chance of detection versus defect size.

for one rail test to detect a defect of a size represented by X . The lower limit of detection capability is represented by the size X_0 for the current technology and by a smaller size X_0' for the improved technology. In each case the chance of detection increases until the defect size reaches X_1 , for which detection is virtually certain. The shaded area between the curves represents "extra" detections by the improved equipment under the idealized assumption that there exists an infinite number of defects of all sizes. Because the actual defect population is finite, however, a detection improvement will cause only a transient rise in the detection rate as the population of smaller flaws is initially accessed. The detection rate will return to the historical level determined by the defect occurrence rate after one or two tests, a fact that has been illustrated by the inspection simulations mentioned earlier (2, 8).

Confusion of finite and infinite population effects led to the misconception that better equipment would always find more defects, and the reduced attractiveness of the benefit temporarily decreased the interest in research on rail test equipment. The interest has revived in the past 3 years, however, and an active program is again under way. The current program has also taken into account the current operational trends and some of the knowledge gained about defect behavior. The main thrust of the research at present is the investigation of electromagnetic

TABLE 8 EXAMPLE OF INTERFERENCE WITH REVENUE THROUGHPUT

Assumptions About Rail Test Operation		Hours Required to Test 150 Miles	Effective Speed (mph)	Stackup Distance (miles) ^a
Speed (mph)	Defect Density (defects/mile)			
15	1	12.5	12	412.5
30	1	7.5	20	187.5
30	2	10.0	15	300.0

^a Stackup distance = (hours required) \times (45 – effective speed).

acoustic transmission (EMAT) for getting ultrasonic signals and returns into and out of rails.

Conventional ultrasonic sensors require a continuous supply of couplant fluid to form a thin film for signal transmission between the probe and the rail surface. Heavy rail lubrication can degrade the couplant properties and signal quality. The couplant also restricts signal polarization and refracts the signal at the couplant-rail interface. Refraction limits the angle at which ultrasound can be injected into the rail without being trapped near the surface.

EMAT transducers subject the rail to a DC magnetic field together with a pulsed RF signal. These two electromagnetic components combine to generate ultrasound and receive return signals directly in the rail head; thus the refraction problem is avoided. Electromagnetic transduction between the rail and the probe also suggests that EMAT systems will tolerate heavy lubrication interference better than conventional systems. A prototype EMAT system is now beginning field evaluation tests at the TTC. The next phase of the research will likely focus on the performance of signal polarizations not available in conventional ultrasonic testing equipment, in particular axially traveling shear waves. The axial shear wave is a 90-degree beam that fills the rail head and inspects 8 to 12 in. ahead of the transducer. This type of polarization is expected to be highly effective in detecting detail fractures, engine burn fractures, and other transverse defects in the rail head.

Aside from the benefit of increased detector-car speed, better NDI also has the potential to reduce costs by increasing the safe inspection interval. A simple model of detection performance serves to demonstrate this benefit. The chance of detecting a defect of size X can be represented by the function

$$P(X) = 1 - \exp[-\lambda(X - X_0)/(X_1 - X_0)] \quad (3)$$

where X_0 and X_1 are defined in Figure 10 and λ is a scale factor. If X is interpreted as the size of a detail fracture in percentage of head area (HA) and X_0 and X_1 are taken as 5 and 75 percent HA, respectively, then $\lambda = 5$ gives about the right chance of detecting a 10 percent HA detail fracture and about the right fraction of defects detected based on experience with detail fracture populations ($P_{AV} = 0.9$; see Figure 7). Taking the average of $P(X)$ over the interval $\{X_0, X_1\}$,

$$P_{AV} = (X_1 - X_0)^{-1} \int_{X_0}^{X_1} P(X) dX$$

$$= 1 - \lambda^{-1} [1 - \exp(-\lambda)] \quad (4)$$

gives a reasonable approximation of the detection performance P_{AV} for two tests per safe crack growth interval (O. Orringer, unpublished data, 1987).

An improvement in detection technology might be manifested by either a larger scale factor λ or a smaller detectability limit X_0 . Chances are that any improvement would involve a combination of these effects. It is therefore of interest to inquire what effect a smaller detectability limit would have on rail test strategy and cost. Because Equation 4 shows that the overall detection performance on a finite population P_{AV} is independent of X_0 , it follows that safe crack

growth life and safe inspection interval can increase proportionately when X_0 decreases without increasing the risk of higher service break incidence. Early removal of defective rails would partly offset the direct savings resulting from fewer rail tests, but a first-order economic analysis suggests a potential for net savings.

An improved analysis based on current knowledge of detail fracture detectability and behavior is shown in Table 9. The basic assumptions of the analysis are full service life of 1,000 MGT, scheduled rail tests starting at 100 MGT, and NDI improvement that allows the inspection interval to be doubled from 20 to 40 MGT at the cost of removing every defective rail 20 MGT sooner than would happen under the current testing schedule. Application of the crack propagation model suggests that such a doubling could be made practical by equipment that would have the same chance to find a 5 percent HA detail fracture as the current systems have to find a 10 percent HA detail fracture (Figure 11). The analysis has been applied to 50,000 track-mi, roughly the total U.S. inventory of medium- to high-tonnage lines. Although the example is idealized, it does illustrate the way in which fracture mechanics can be used to assess the real trade-offs when the behavior and detectability of all the major defect types are better understood.

The Canadian Pacific Railroad has recently adopted a performance specification for rail testing based on average detection probabilities for finite flaw-size ranges. The CPRR specification that applies to detail fracture and other types of transverse defects in the rail head (transverse fissure, compound fissure, engine burn fracture, or defective weld) is as follows:

	Defect Size Range (%HA)			
	10-20	20-40	40-80	80-100
Required minimum detection probability	0.65	0.80	0.95	0.99

Application of the previously developed simulation methods (2, 8) and current knowledge of detail fracture propagation suggest that this part of the CPRR specification accurately reflects current rail test equipment performance (O. Orringer, unpublished data, 1987).

FABRICATION AND MAINTENANCE QUALITY CONTROL

Although periodic NDI is necessary in a world of imperfect structures, it is not a substitute for good fabrication and maintenance quality. The railroads and railroad suppliers have a long record of product improvement, and the rail integrity research program has dealt with fabrication or maintenance improvement from time to time. Examples from both sources will be cited briefly.

The adoption of controlled cooling to prevent hydrogen flake defects was mentioned earlier. Other industry improvements in rail manufacturing include vacuum treatment, hot topping, and clean steel practice. Vacuum treatment removes hydrogen and other gases from molten steel, allowing more productive rail rolling through elimination of the requirement for controlled

TABLE 9 EXAMPLE OF POTENTIAL SAVINGS FROM IMPROVED NDI TECHNOLOGY

Item	Current Technology ^a	Hypothetical Improved Technology ^b
Rail tests covering 100 to 1,000 MGT	46	23
Rail test cost: 50,000 miles @ \$70; \$M	161.0	80.5
Additional loss of serviceable rail life ^c , \$M 50,000 miles @ 32 defects per mile 20 MGT lost per defective rail @ \$1 per MGT	0.0	32.0
Life cycle cost, \$M	161.0	112.5

^a Testing at 20 MGT intervals.

^b Testing at 40 MGT intervals.

^c New technology assumed to penalize every defective rail by 20 MGT. Every defective rail assumed to require complete replacement. Number of defects based on 1,000 MGT cumulative density from Table 3.

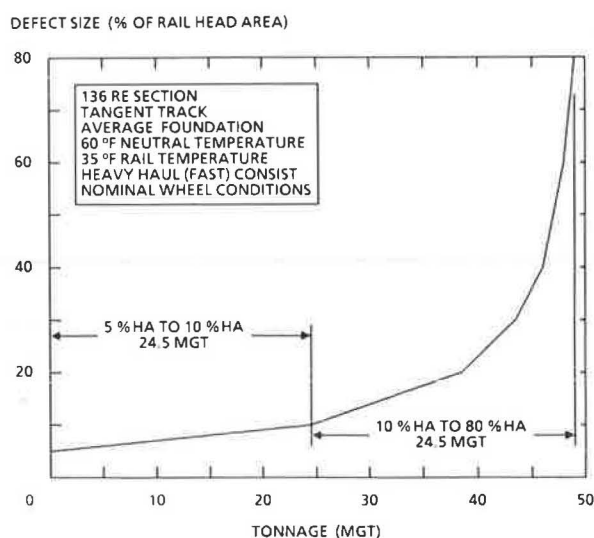


FIGURE 11 Estimated safe crack growth life for small and large defects.

cooling. Hot topping reduces ingot discard wastage and also lowers the incidence of piped rails by avoiding the formation of excessively weak dendritic seams during ingot solidification. Clean steel practice, a recent development, reduces tramp-element inclusion content and thus has the potential to improve resistance to the formation of vertical split heads.

One of the early efforts in the rail integrity research program was directed toward reduction of the high bolt-hole crack incidence that appeared in the late 1960s. Bolt-hole cracks tend

to form as a result of fretting action between the bolt shanks and the rail, a common phenomenon in mechanically fastened structures. An idea borrowed from aircraft industry practice led to the development of equipment and procedures for applying cold expansion to the bolt holes in older BJR (22). British Rail has recently improved the procedure by reaming worn bolt holes to uniform diameter before expanding and is now beginning to apply the cold expansion practice to its older BJR tracks.

Both government and industry research projects have investigated improved rail welding methods. Flash butt welds made in CWR plants generally have low defect rates because the welding process does not use foreign materials and can be accurately controlled. However, some premium alloy rails are extremely sensitive in this regard because they achieve their properties in part by delay of the austenite-pearlite transformation to produce a fine grain structure. Research on flash butt rail welds has shown that martensite formation can be avoided by delaying and extending postweld heat application, a practice that adds about 1 min per weld to the production time (4).

Attention has also been paid to field welds, most of which are made today by means of expendable kits consisting of a thermite charge and a preformed mold that fits around the rail ends. Because these kits were originally developed for joining standard composition rail, a metallurgical investigation was made into the effects of using both standard and premium kits to join premium-alloy rails or to make welds between a premium-alloy rail and a standard rail (23). The major findings from this project were that the natural air cooling of a field thermite weld is slow enough to avoid martensite formation in

all cases. However, simulated service tests at the TTC showed that these welds tended to batter because the weld metal and heat-affected zone generally had lower hardness and lower yield strength than the parent metal (4). The TTC has recently started simulated service tests of air-quenched thermite welds, which have the potential for sufficient strength to resist batter while still avoiding martensite formation. Whether the air quenching process can be controlled in the revenue track environment with sufficient accuracy to avoid martensite embrittlement is an open question.

The seamless butt weld, a derivative of the thermite field weld, has recently begun to be applied to the repair of transverse defects in the rail head. If such defects are to be locally repaired, it is generally necessary to remove 2 to 3 in. of rail length to be certain that the entire defect has been removed. Regular thermite weld kits cannot be used to rejoin the rail in such cases because they are limited to weld thicknesses of $1/2$ to $3/4$ in. The repair practices in common use have been whole rail removal in BJR and removal of a 10- to 20-ft plug from CWR. The seamless butt weld kit is a rail-end kit that has been modified to produce the weld thickness required for defect repair. Seamless butt welds are now undergoing simulated service tests on the TTC FAST track.

Despite all the effort that has gone into improvement of field thermite weld products, the process is still susceptible to the formation of internal sand pockets or lack-of-fusion defects when maintenance gangs are pressed for time or when welds must be made during severe cold weather. One good practice to compensate for these risks is to install safety straps on all field welds. Safety straps are used today mainly on lines where the perceived risk of derailment is high, for example, in the Northeast Corridor to protect high-speed passenger trains. Safety straps are essentially flexible joint bars that bulge around the weld upset and can be relied on to maintain rail alignment for one or two trains should a weld break. One useful product improvement that has not yet appeared would be insulated safety straps to provide positive assurance that a field weld failure would disrupt the track signal circuit and stop the next train.

A better long-term solution to the field weld defect problem might be found in alternative welding methods that can be more easily controlled. Several alternatives have been investigated by the former Japanese National Railways, but all require elaborate equipment on the track and have therefore had little appeal to the U.S. railroads. One promising improvement that has been the subject of some research in the United States is a consumable-guide electrosag weld developed under railroad sponsorship. The consumable guide is a prefabricated kit in the shape of the rail cross section, and the only equipment required on track is a portable generator to supply the welding current. Some of these welds have been made in the laboratory, and two have been placed in the FAST track.

The final example illustrates the unexpected side effects that can sometimes result from product improvements. The uniform reduction of rail camber by roller straightening makes widespread CWR fabrication practical, but the price paid for the improvement is residual stress left in the rail (24, 25). The residual stress magnitude generally increases as the material yield strength increases; that is, the same roller-straightening process leaves higher stresses in high-strength premium-alloy

rail than in standard composition rail. In some cases, the price paid for increased hardness and strength can be decreased resistance to fracture.

Investigation of a 1983 passenger train accident led to the conclusion that such a combination of high residual stress and low fracture resistance was a major factor contributing to the sudden rail web failure that caused the derailment (26). Similar fractures were later produced in the laboratory (R. K. Steele, AAR Research and Technical Center, unpublished data, 1984), the potential of roller-straightening stress to drive cracks was measured (27), the variation of rail steel alloy fracture resistance was characterized (28), and the web fracture instability phenomenon was recently confirmed by dynamic crack propagation analysis (29) and energy release rate calculations (F. A. McClintock and S. J. Wineman, Department of Mechanical Engineering, Massachusetts Institute of Technology, unpublished data, 1987).

The 1983 derailment was an isolated case in which abusive maintenance shortly before the passage of the train triggered the conditions for initiation of the web fracture (30). A modest product improvement in the form of a minimum specification for rail steel fracture toughness can help to reduce the risk of sudden rail failure from maintenance abuses that would normally be tolerated by rail without roller-straightening stress. The research results suggest that most rail steel alloys in use since roller straightening started would meet such a specification.

Straightening stress can also increase fatigue crack propagation rates and thereby decrease safe crack growth life. A recent case involving rapid propagation of small surface defects through the rail web thickness is believed to have been caused by straightening stress and is now the subject of a research project. Rail makers are also investigating alternative straightening processes that have the potential to produce rails with low stress as well as low camber, for example, stretch straightening (31) and combinations of roller straightening with stress-relieving heat treatment.

CONCLUDING REMARKS

The framework for rational determination of safe rail test intervals is expected to be completely in place within a few years. Future rail integrity research will likely concentrate on product improvement or effects of rail transportation system modernization.

On the product improvement side, the handling of roller-straightened rail will likely receive continued attention in the near future, and new work must be started on the subject of surface head checking. Widespread surface head checking (i.e., microcrack formation) has recently started on some heavy-haul lines and is of concern because surface microcracks can mask other safety-critical defects from detection by conventional ultrasonic testing.

On the system modernization side, the anticipated transition to 125-ton cars raises a major question about fatigue behavior. The first post-transition experience with rail that has been conditioned under 100-ton service might not provide a good guide to the behavior of new rail under 125-ton loads. Laboratory fatigue experiments suggest that a historical trend from

low to high loads tends to delay fatigue crack nucleation, not unlike the retarding effect of occasional overloads on crack propagation. Whether the useful service life of new rail under 125-ton loads will be lower than the life of preconditioned rail remains to be seen and will be one of the subjects of the next phase of experimentation on the TTC FAST track.

Although rail fabrication defects are best dealt with by means of ad hoc product improvements that increase production quality, most kinds of rail defects result from the repeated application of service loads and will always occur at rising rates as rail accumulates tonnage. In the long run, detail fractures and other defects that are the inevitable result of rolling contact will come to dominate the rail defect population as product improvements and BJR replacement continue.

Periodic testing of revenue track will always be required to control derailment risks arising from exposure of trains to rail failures. A damage tolerance philosophy based on fatigue behavior and fracture mechanics provides the unifying framework for understanding how inspection equipment improvements can be traded against test frequency requirements and how maintenance resources can be efficiently targeted on critical track sections without sacrificing operational safety. Examples of both kinds of applications have been presented and in most cases suggest that safe practices are also economical practices.

REFERENCES

1. J. W. Thomas. *Sperry Railer*, Vol. 52, No. 1, 1985, pp. 2-5.
2. O. Orringer and H. L. Cecon. Detection of Rail Defects and Prevention of Rail Fracture. In *Proceedings, 31st MFPG Symposium on Failure Prevention in Ground Transportation Systems*, National Bureau of Standards, Gaithersburg, Md., 1980.
3. *Railroad Facts*. Association of American Railroads, Washington, D.C., 1984.
4. R. K. Steele and R. P. Reiff. Rail: Its Behavior in Relationship to Total System Wear. In *Proceedings, Second International Heavy Haul Railway Conference*, Paper 82-HH-24, Association of American Railroads, Washington, D.C., 1982.
5. G. M. Magee. Rail Fractures on the Field Side of the Low Rail on Curves Under Heavy Axle Loads. Report R-546. Association of American Railroads Research and Technical Center, Chicago, Ill., 1985.
6. O. Orringer and R. K. Steele. Structural Integrity of Rail in U.S. Railroad Track. In *Proceedings, 19th National Symposium on Fracture Mechanics*, American Society for Testing and Materials, Philadelphia, Pa., 1987.
7. O. Orringer and M. W. Bush. Applying Modern Fracture Mechanics to Improve the Control of Rail Defects in Track. *American Railway Engineering Association Bulletin*, Vol. 84, 1983, pp. 19-53.
8. D. D. Davis, M. J. Joerms, O. Orringer, and R. K. Steele. The Economic Consequences of Rail Integrity. In *Proceedings, Third International Heavy Haul Railway Conference*, Association of American Railroads, Washington, D.C., 1986.
9. D. Broek. *Elementary Engineering Fracture Mechanics*. Noordhoff International Publishing Co., Leyden, Netherlands, 1974.
10. D. H. Stone and G. G. Knupp, eds. *Special Technical Publication 644: Rail-Steels: Developments, Processing, and Use*. American Society for Testing and Materials, Philadelphia, Pa., 1978.
11. R. Rungta, R. C. Rice, and R. D. Buchheit. *Post-Service Rail Defect Analysis*. Interim Report. Battelle Columbus Laboratories, Columbus, Ohio, 1982.
12. J. J. Scutti, R. M. Pelloux, and R. Fuquen-Moleno. Fatigue Behavior of a Rail Steel. *Fatigue and Fracture of Engineering Materials and Structures*, Vol. 7, 1984, pp. 121-135.
13. O. Orringer. Rapid Estimation of Spectrum Crack Growth Life Based on the Palmgren-Miner Rule. *Computers and Structures*, Vol. 19, 1984, pp. 149-153.
14. J. Schijve. Effect of Load Sequences on Crack Propagation Under Random and Program Loading. *Journal of Engineering Fracture Mechanics*, Vol. 5, 1973, pp. 269-280.
15. B. G. Journet and R. M. Pelloux. A Direct Method for Laboratory Spectrum Crack Growth Testing. *Theoretical and Applied Fracture Mechanics*, Vol. 7, 1987, pp. 19-22.
16. B. G. Journet and R. M. Pelloux. A Methodology for Studying Fatigue Crack Propagation Under Spectrum Loading—Application to Rail Steels. *Theoretical and Applied Fracture Mechanics* (forthcoming).
17. O. Orringer, J. M. Morris, and D. Y. Jeong. Detail Fracture Growth in Rails: Test Results. *Theoretical and Applied Fracture Mechanics*, Vol. 5, 1986, pp. 63-95.
18. J. J. Groom. *Determination of Residual Stresses in Rails*. Report DOT/FRA/ORD-83/05. Battelle Columbus Laboratories, Columbus, Ohio, 1983.
19. H. Weinstock. Vehicle Track Interaction Studies for Development of Track Performance Specifications. Presented at British Rail/Association of American Railroads Vehicle Track Interaction Symposium, Princeton, N.J., 1984.
20. O. Orringer, J. M. Morris, D. Y. Jeong, Y. H. Tang, and J. Gordon. *Crack Propagation Life for Detail Fractures in Rails*. Transportation Systems Center, U.S. Department of Transportation, Cambridge, Mass., in preparation.
21. R. A. Mayville, P. D. Hilton, and D. C. Pierce. *Further Studies of Fatigue Crack Initiation and Growth from Rail End Bolt Holes*. Arthur D. Little, Inc., 1984.
22. D. V. Lindh, R. Q. Taylor, and D. M. Rose. Sleeve Expansion of Bolt Holes in Railroad Rail. Report FRA/ORD-80/5. Boeing Commercial Airplane Company, Seattle, Wash., 1980.
23. L. C. Schroeder and D. R. Poirer. Structure and Properties of Thermite Welds in Premium Rails. Report DOT/FRA/ORD-85/02. Department of Metallurgical Engineering, University of Arizona, Tucson, 1985.
24. A. D. Konyukhov, V. A. Reikart, and V. N. Kaportsev. Comparison of Two Methods for Assessing Residual Stresses in Rails. *Zavodskaya Laboratoriya*, Vol. 39, 1973, pp. 87-89.
25. V. V. Lempitskiy and D. S. Kazarnovskiy. Improving the Service Life and Reliability of Railroad Rails. *Russian Metallurgy*, Vol. 1, 1973, pp. 111-117.
26. O. Orringer and P. Tong. Investigation of Catastrophic Fracture of a Premium-Alloy Railroad Rail. In *Fracture Problems in the Transportation Industry* (P. Tong and O. Orringer, eds.), American Society of Civil Engineers, New York, 1985.
27. R. C. Rice. *Measurement of Rail Web Fracture Sensitivity*. Interim Report. Battelle Columbus Laboratories, Columbus, Ohio, 1985.
28. D. J. Jones and R. C. Rice. *Determination of K_{IC} Fracture Toughness for Alloy Rail Steel*. Final Report. Battelle Columbus Laboratories, Columbus, Ohio, 1985.
29. M. F. Kannien, R. J. Dexter, and J. W. Cardinal. *Determination of Dynamic Toughness Properties of Rail Steels*. Final Report. Southwest Research Institute, San Antonio, Tex., forthcoming.
30. *Railroad Accident Report—Derailment of Amtrak Train No. 21 (The Eagle) on the Missouri Pacific Railroad, Woodlawn, Texas, November 12, 1983*. National Transportation Safety Board, U.S. Department of Transportation, 1985.
31. R. Y. Deroche et al. Stress Releasing and Straightening of Rail by Stretching. *Proceedings, Second International Heavy Haul Railway Conference*, Paper 82-HH-17. Association of American Railroads, Washington, D.C., 1982.

Production Processes To Yield Superior Rail Steel

W. H. HODGSON AND R. R. PRESTON

Today is a time of great technological change in rail production. Improvements have been noted in basic rail oxide, sulfide, and hydrogen controls, as well as surface inspection techniques and the use of lasers and computers for rail flatness, straightness, and geometry. Improvements in microstructure control and its effect on wear are discussed along with some of the latest developments in both off- and on-line continuous mill hardening. Finally, the overall package of such improved rail offered over a hardness range of 300 to 400 Brinell Hardness Number (BHN) gives the user a wide range of choices. It is suggested that this freedom of choice will be characteristic of rail in the next decade.

Finished rail must give a satisfactory life over a suitably long period. Wear resistance can now be built in, but before full wear performance can be achieved the rail must be capable of limiting local stress raisers connected with microinclusions, microhydrogen, surface defects, surface flatness, and geometry.

The production of basic rail to the required standard of consistency will be reviewed and the processes capable of promoting the desired wear properties will be considered in this paper.

BASIC RAIL

Raw Material and Bloom Production

For consistent results it is better to begin with standard raw material. For that reason liquid iron from a modern blast furnace is the ideal starting material. This iron can be pre-treated before basic oxygen steelmaking. In 250-tonne vessels, the iron is blown to 0.1 percent carbon steel in around 40 min. Gas stirring and the addition of low aluminum bring the ladle almost up to rail steel chemistry. Vacuum degassing and further trimming stations allow final chemical control, so that 98 percent of rail steel can be produced within a range of 0.05 percent carbon and 0.10 percent manganese. No aluminum is added directly, which ensures steel free from angular, brittle aluminous stringers.

The degassed and trimmed steel, temperature controlled to $\pm 10^\circ\text{C}$, is then continuously cast under fully tubed and submerged conditions. Sequence lots of around 2,000 tonnes are typical. These batches are placed into 2,000-tonne insulated boxes while still at 600°C . With a cooling rate of less than 1°C per hour, the blooms are given a second hydrogen treatment

British Steel Corporation, Mass Bay, Workington, Cumbria CA14 5AE, England.

for a period of 3 to 5 days. Blooms are removed and are available for rolling to rail without any need for surface correction.

Internal Discontinuities

At this early stage decisions have already been made that preset oxide inclusion type, sulfide amount and distribution, and hydrogen preflake presence.

Oxide

To date, British Steel Corporation (BSC) has developed a special low-aluminum process in which no direct additions of aluminum are allowed. Figures 1 and 2 show the oxide levels obtained. In this process, the main choice is oxide type—either aluminum silicate or manganese silicate (Figure 3). Whichever oxide is used, the level must be minimal.

Sulfide

Sulfide has a generally positive effect in helping to reduce hydrogen problems but a negative one on toughness and wear. A balance has to be found. BSC uses a typical sulfur range of 0.01 to 0.015 percent at the moment, but development work is continuing at BSC Swinden Laboratories.

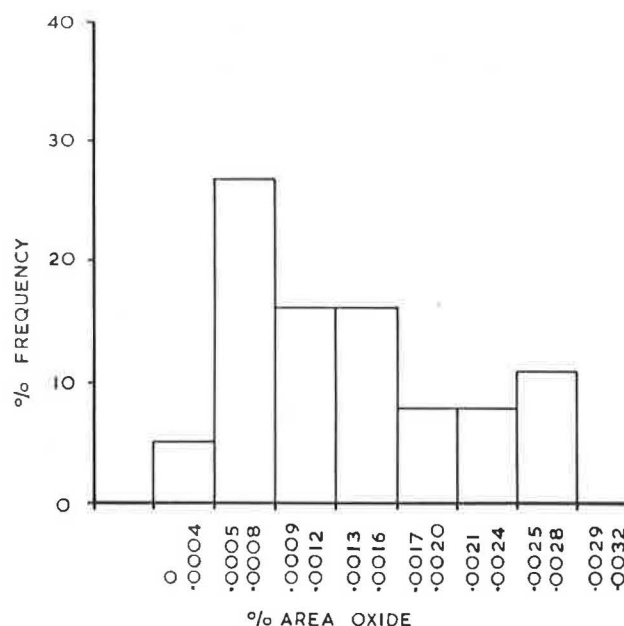


FIGURE 1 Distribution of percent area oxide in rail head.

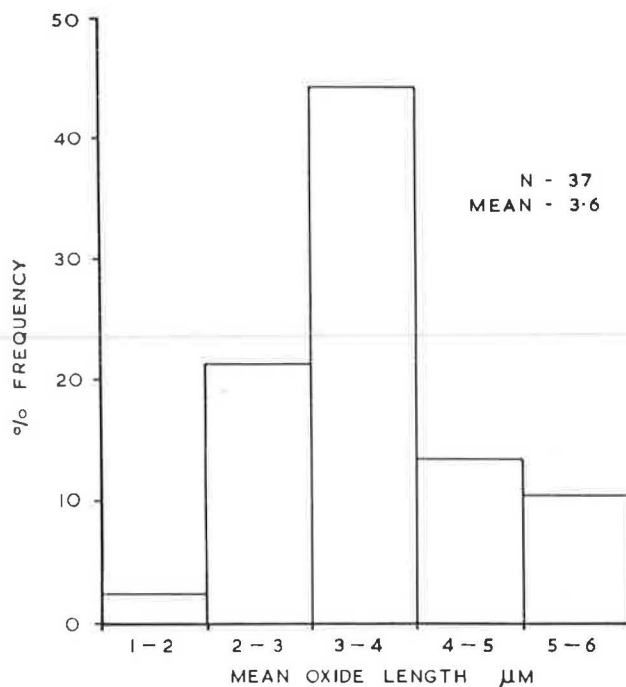


FIGURE 2 Distribution of mean oxide length in rail head.

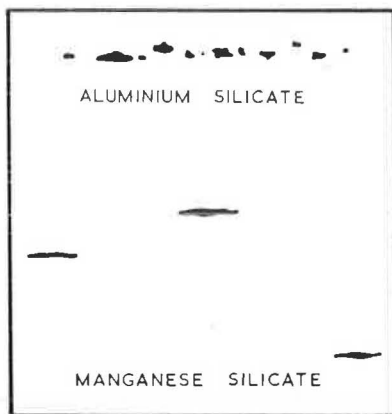


FIGURE 3 Oxide inclusion types.

Hydrogen

The decisions regarding hydrogen are difficult. Assuming that a manufacturer avoids the actual production of detectable flakes, it takes from 3 to 15 years for microflakes to develop by fatigue into measurable defects. The testing span is therefore extremely long, and, which is still worse, actual hydrogen tests are not exact. Figure 4 is a graph showing hydrogen requirements typical in the rail industry. The lower dashed line shows where hydrogen damage—not flakes—has been observed under laboratory test conditions. In view of this and while research is continuing, BSC uses a double hydrogen treatment, that is, full vacuum degassing and full bloom cooling. The average hydrogen in the finished rail is around 0.5 ppm.

RAIL PRODUCTION

Blooms are reheated and rolled into rail. At this stage there are two main options that produce the correct wear resistance. These will be discussed later.

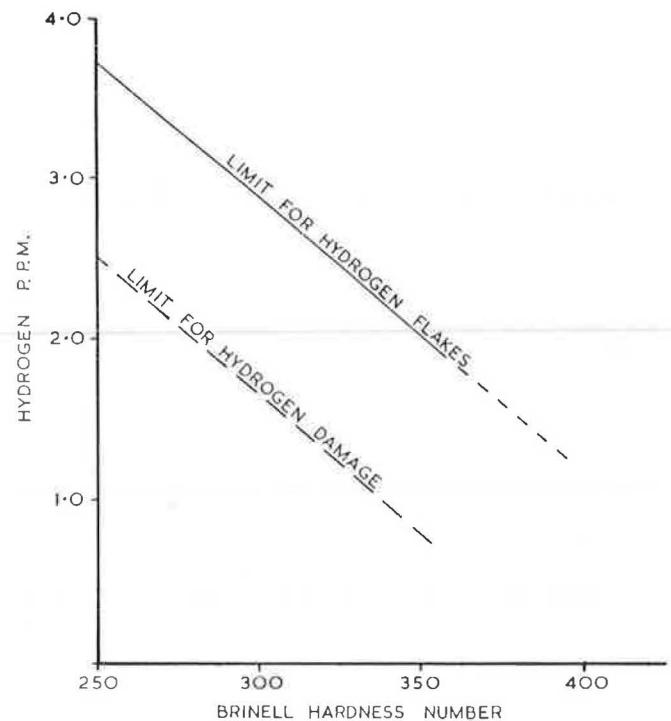


FIGURE 4 Hydrogen requirements typical in rail industry.

Rails are produced in multiple lengths to improve straightness control. A single plane roller straightening machine straightens the rails. Immediately after leaving the machine, the rails are checked for inclusions, surface defects, and surface flatness. Equipment is being installed to check straightness and section geometry.

Inclusion Testing

All rails are checked for microinclusions by a 16-probe ultrasonic machine (Figure 5). The number of rails rejected is

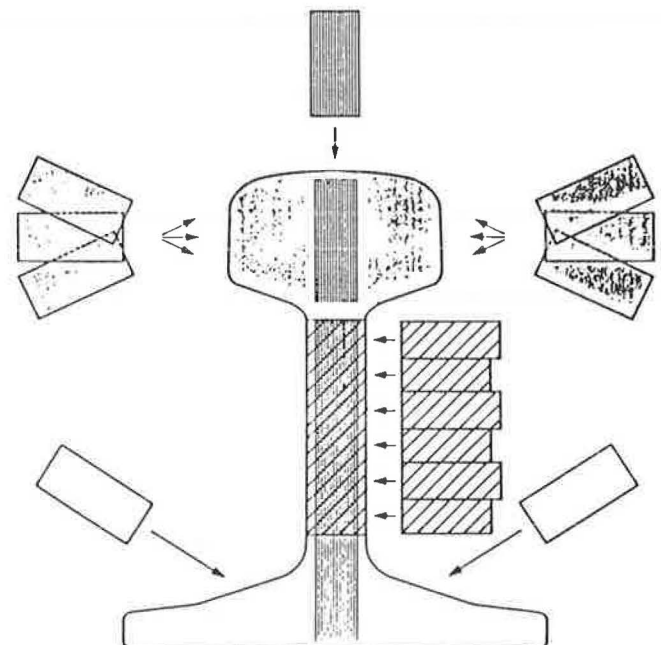


FIGURE 5 Ultrasonic testing.

negligible, which should be a comfort to travelers. Background inclusions are so small that ultrasonic machines are now of little use. Consequently, although it is only 2 years old and one of the best available, this latest machine has come at a time when steelmaking advances have almost eliminated the need for it.

Surface Quality Assessment

Mirror-assisted visual inspection under ideal light conditions has been used for many years, but rail standards are now such that mirror inspection is less acceptable, for two main reasons:

1. Less than 0.25 percent of rails contain any form of steelmaking defect. It is therefore difficult for an operator to maintain the concentration required to find 1 defective rail in 400, particularly because for any individual operator the ratio is 1 rail in 2,400.
2. Modern railmaking requires such defects that are present to be measured for manufacturing control purposes.

BSC has developed fully automatic eddy current inspection for the foot of the rail, and during 1987 newly developed rail-head testing will be installed. The basis of the system is the measurement of magnetic eddy currents set up in the rail surface by a coil carrying an alternating current. For defect-free steel the back effect of the coil is constant. If a surface defect is present, this change in eddy current pattern can be picked up either by the original or by a separate coil. The current system uses six probes spinning at 2,000 rpm, giving a sweep every 5 mm. Figure 6 shows a schematic view.

Running Surface Flatness Measurement

Rail surface waveforms introduced during manufacture have a significant effect on the stress pattern and hence life of rail and associated equipment, and in some instances on structure some distance away from the track. Although every effort is made to control these, the sources are many. Accurate measurement is therefore one way of obtaining feedback for greater control.

In May 1986 BSC introduced a laser system for measuring rail running surface flatness. The system uses six laser units, which are calibrated against a straightedge so that datum

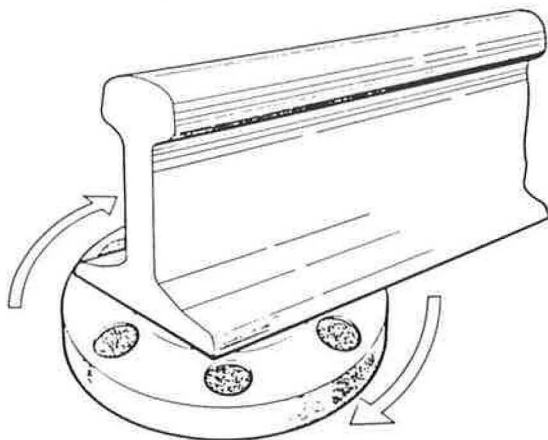


FIGURE 6 Eddy current testing.

positions are established within the controlling computer software.

At each measurement interval the two outer probes are used to establish the current position of the straightedge in space. The central four lasers measure the relative position of the rail surface, and this information is stored for subsequent wavelength and amplitude analysis. Characteristic wavelengths and maximum amplitudes are displayed in tabular and graphical form. Figure 7 shows the laser system and Figure 8, a typical waveform printout.

Rail Straightness Measurement

Straightness measurement is a simplified form of surface flatness measurement but taken over a long wave. Three laser units in both the vertical and horizontal planes are used. The two outer lasers define the straightedge, and the central laser measures the deviation from straightness. The equipment is being installed at the exit from the straightener machine and should give almost instant feedback to the straightener's mathematical model. Unfortunately, straightness adjustment, although motor driven, will still be manual for some time to come.

As an aside on rail straightness, rails with a good crown profile for wheel guidance in track move through the roller straightening machines more readily and finish as straighter rails than do more poorly designed rails. The 132-lb American rail performs well in this respect.

Rail Section Measurement

Lasers are being installed to measure principal dimensions and twist. It is not anticipated that this equipment will improve the rail, but it will give customers more peace of mind.

RAIL WEAR PROPERTIES

Other things being equal, the best wear resistance is given by rails that have 100 percent fine pearlite structure and high hardness. Wider pearlite spacings or any alternative microstructure gives increased wear. Figure 9 shows true fine lamellar pearlite and Figure 10 shows degenerate pearlite, both originally photographed at $\times 6,250$. Both structures look fully acceptable under a light microscope at $\times 500$.

The one known exception to the pearlite rule is austenitic manganese rail, which gives very good service in certain types of wear situation only.

Figure 11 shows laboratory results that support site trials carried out by BSC.

Historically BSC has manufactured rails that range in hardness from 240 to 340 Brinnell Hardness Number (BHN) by a combination of controlled fan cooling during head transformation only in the mill and the addition of alloying elements such as chromium. Up to around 340 BHN the technique was successful, but above 330 BHN, there was a weld cost penalty. On increasing hardness over the range 340 to 400 BHN using alloy systems, it became extremely difficult to avoid the presence of degenerate forms of pearlite and even some traces of bainite. Consequently, although the hardness increased, the wear performance did not improve to the expected degree. For

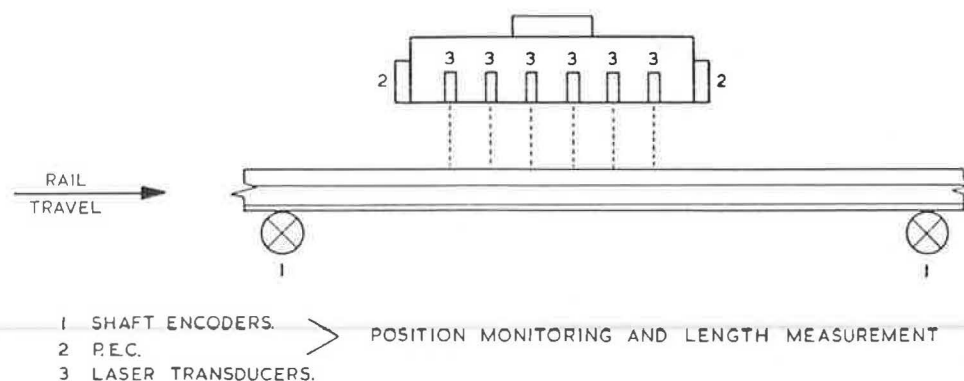


FIGURE 7 Rail surface flatness measurement.

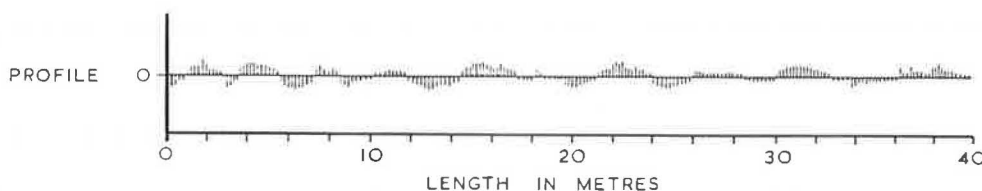


FIGURE 8 Rail surface flatness profile.



FIGURE 9 Fine lamellar pearlite structure ($\times 4,745$).

these harder and more wear-resistant rails, BSC had the long-term aim of using on-line mill heat treatment, but in the short term turned to the more immediately available off-line head hardening type plant. The resulting pearlites follow (Figure 11), at least to the 425 BHN tested.

Off-line treatment was expensive, and even while the equipment was being installed, BSC was cooperating with the Centre de Recherches Métallurgiques (CRM) in Liège, Belgium, and Métallurgique et Minière de Rodange-Athus (MMRA) in the development of the new on-line process. The two processes are briefly described here.

Off-Line Head Hardening

Rails are passed through a four-inductor heating unit that penetrates deep into the head of the rail. The rail surface reaches

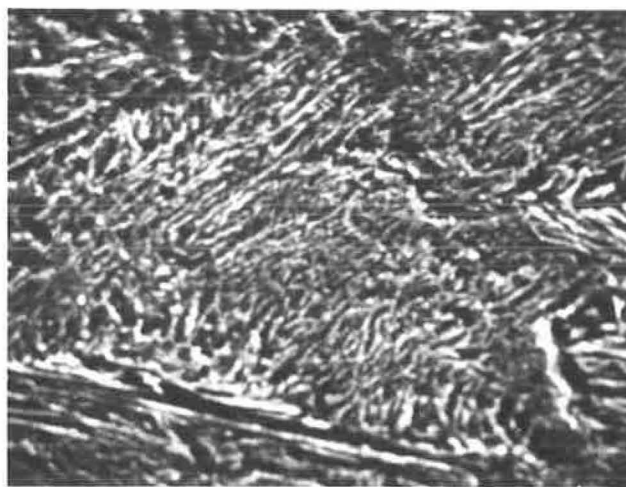


FIGURE 10 Lamellar and degenerate pearlite ($\times 4,550$).

1000° to 1050°C at around 20 mm/sec. After a free air soak period the rail is pre-cooled with air to transformation temperature. The major part of the transformation then takes place in still air.

The hardness profile for a 132-lb carbon rail shows that, although produced off line, this is very much a deep-hardened rail. A relatively flat hardness profile is produced, so that the underlying rail is hard enough to support the wearing top surface. The base rail in this instance would have a hardness of 290 BHN. All manufacturing parameters are fixed at the start of a contract and are not altered for any reason. Computer control is therefore unnecessary. The machine performance is continuously recorded on a multipoint system, and the charts can be read once a day to confirm that all rails are treated within specifications. Obviously all normal mechanical and hardness tests are also carried out.

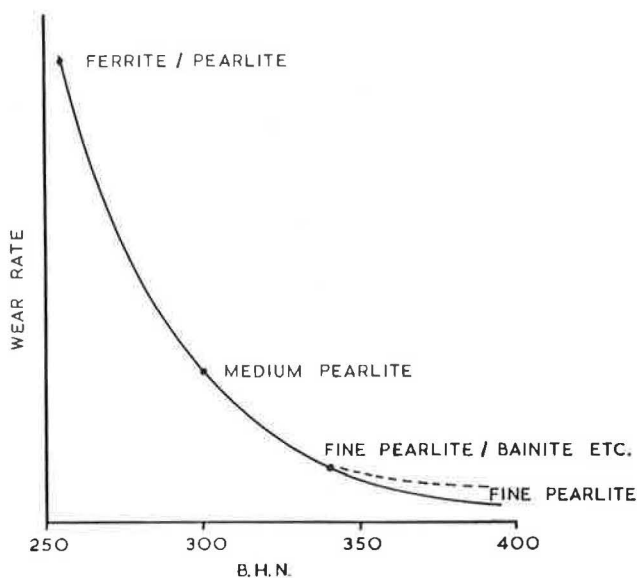


FIGURE 11 Laboratory wear tests.

Mill Hardening

The idea for the plant was developed by CRM and the pilot plant was installed at MMRA. The full 130-tonne/hr production unit was installed by BSC and began operating in September 1987.

CRM had been heavily involved in on-line cooling of lower-carbon steels for over 20 years, and the development to higher-carbon and rail steels was a logical outcome of their work. Their first actual trial runs of on-line treated rails were carried out at MMRA in 1982. By 1984 the feasibility of the process had been fully demonstrated. The current pilot plant was completed in September 1985, and this equipment has successfully worked through a test program of over 14,000 tonnes of rail.

The general layout of the plant at MMRA is shown in Figure 12, and Figure 13 shows the process control system.

The plant at BSC is similar but with a size difference of $\times 2.5$. The sequence of events is as follows: The hot rail passing from the finishing stands at 1000°C is placed head up. The rail then passes under temperature monitors that supply the temperature profile along the rail length to the computer. The rail passes through a cooling train (54 m long at BSC) in which rollers maintain both drive and straightness of the rail and water sprays all surfaces continuously as required over the length of the cooling train. The outgoing rail leaves the cooling area at a dull red heat, and the main transformation to pearlite structure takes place in still air. The straight rail is turned on its side and passes down the cooling banks for finishing in the normal manner.

Needless to say, the whole process is fully computer controlled. In fact, the plant at MMRA at 65 tonnes/hr and that at BSC at 130 tonnes/hr do not require any operators.

A wide range of sections, including asymmetric shapes, have been successfully produced at MMRA, and extensive testing has been carried out by BSC, MMRA, and CRM.

The process is very controllable and a hardness range of 300 to 400 BHN can be encompassed. Figure 14 shows a typical hardness pattern for a 132-lb rail.

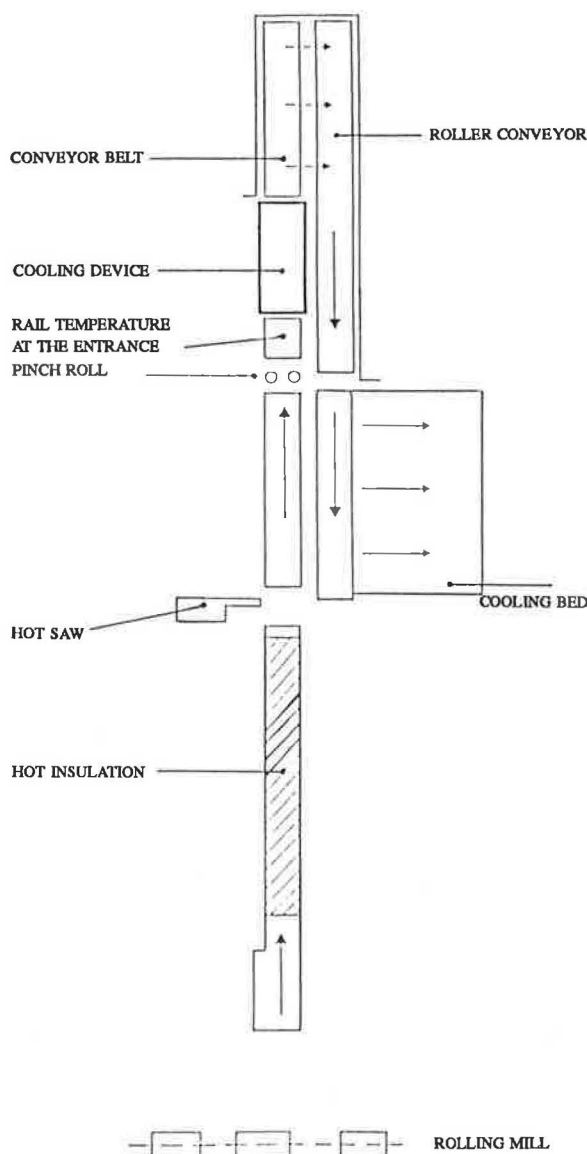


FIGURE 12 Layout of heat treatment facilities.

This rail also has the desirable flat hardness profile of great depth, and as with the BSC off-line treatment, the still-air transformation eliminates the possibility of a sharp hardness cut-off or transition zone.

Full mechanical testing and metallography have been carried out, and when conditions are met, wear results appear as those in Figure 11.

Full-section fatigue tests have also been carried out at BSC's Swinden Laboratories. Here results were found to be dependent on steelmaking and rolling techniques rather than treatment or strength. However, continuing work on push-pull fatigue testing in the transverse direction indicates that sulfur may have an effect on fatigue.

SUMMARY

BSC rail development has been aimed at producing a basic rail that is clean and hydrogen and defect free to the extent that modern technology will allow. Such rail can be heat treated on

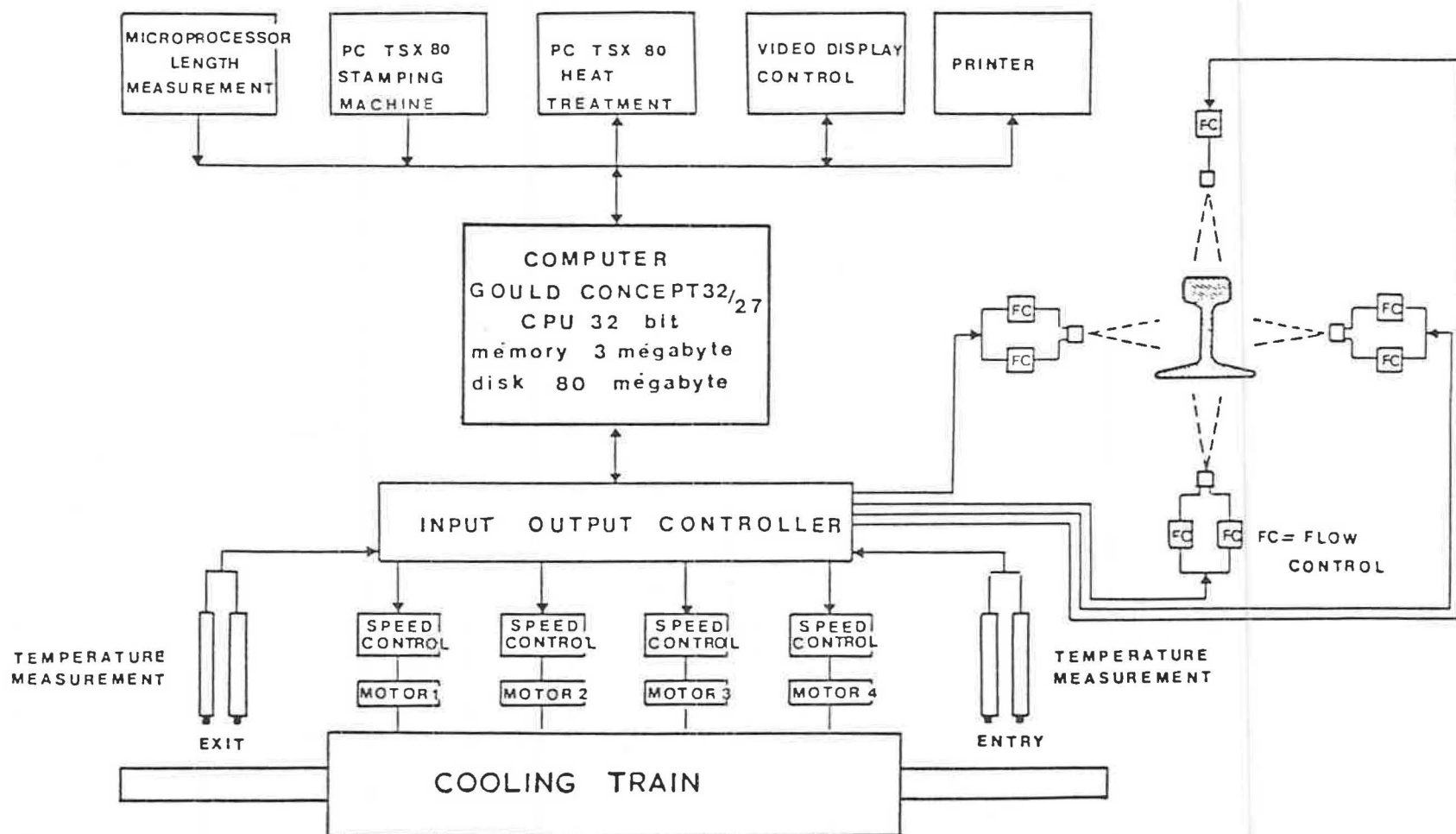


FIGURE 13 Process control system for mill hardening.

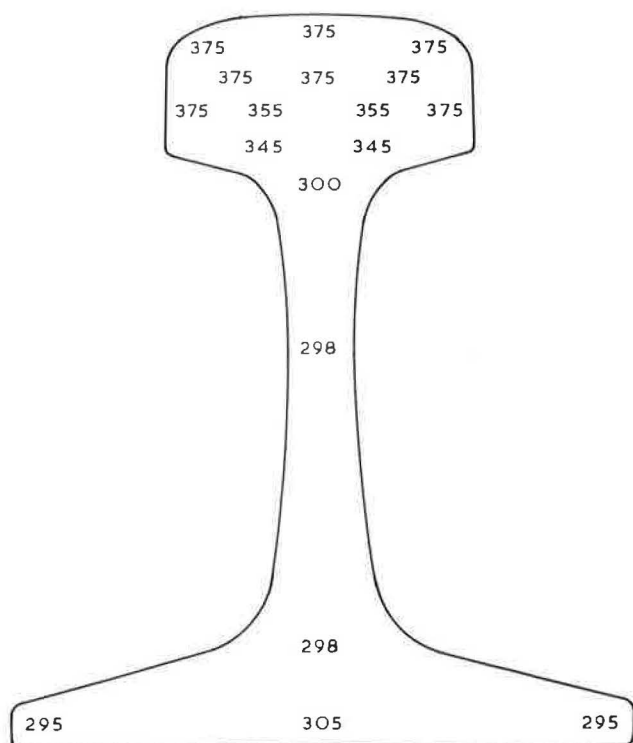


FIGURE 14 Brinell hardness pattern for 132-lb rail.

or off line to give hardness values in a continuous band from 300 to 400 BHN. This new technological package offers the railroads a complete break from the previous restrictive steps involved in the chemistry-controlled process. Rail can be produced anywhere in the 300- to 400-BHN band and can therefore give the user the benefit of the correct wear resistance for his particular system on tangent shallow curves, severe curves, and million-gross-tonne-per-year traffic, and satisfy his views on rail grinding. This can bring about a fine balance between surface fatigue and wear rate.

The majority of these improvements have come about without pro rata increases in cost relative to the improvements obtained, which is generally possible when the improvements are brought about by manufacturer push rather than market pull. The overall package should therefore be a very cost-effective offer to railroads and sets a pattern for the next decade.

ACKNOWLEDGMENTS

The authors wish to thank their many colleagues within both BSC and the railroad industry for their contribution to these developments. Thanks are particularly due to friends at MMRA and CRM for the joint development work on the mill-hardening project.

Manufacture and Properties of Deep Head Hardened Rail

H. YOSHITAKE, Y. MAKINO, K. SUGINO, H. KAGEYAMA, T. SUZUKI,
K. FUKUDA, AND T. MIYATA

Slack-quenched rails made by Nippon Steel have made an important contribution to reducing the maintenance cost of railroads. Recently, the number of companies that use heavy lubrication and grinding of rail heads to improve rail life has been increasing. Thus, depending on the conditions under which the track will be used, rails with various types of hardness and a much deeper hardened layer are in great demand. To satisfy this demand, Nippon Steel has developed a new heat-treated rail called the deep head hardened (DHH) rail, which can be produced by in-line direct heat treatment with a special cooling system designed by Nippon Steel. Features of DHH rail are as follows: (a) various grade types of hardness, (b) a deep and uniformly hardened layer in the rail head, and (c) high weldability. The construction of these rails has been completed and tested. The new rail will be available late in 1987.

Because of increases in train speed and freight car capacity aimed at improved efficiency, rails are subject to severer conditions than ever. The tonnage of trains has increased markedly, and the axle load and tangential force or impact force applied to the rails by the wheels have become exceedingly great.

Recognizing the increasingly severe service conditions for rails, in 1976 Nippon Steel developed a new head hardened (NHH) rail that is continuously slack-quenched by air after being subjected to induction heating (1, 2). In 1979 the company developed NS-II rail (Super rail), the purpose of which was to prevent the welded joints from softening (3).

In a test conducted at the Facility for Accelerated Service Testing (FAST) (4, 5), these rails proved to have excellent wear resistance. As a result, they have been widely used in the United States, Canada, Australia, Brazil, and other countries, in which their use has contributed to a saving in track maintenance costs.

In recent years railways have been making the following technical changes:

1. Development and practical use of lubrication technology aimed at improved fuel efficiency in train operation and prolonged rail service life (6),
2. Implementation of rail head grinding to secure the optimum rail top profile while eliminating rail surface damage and matching between rails and wheels (7), and

3. Use of 125-ton or heavier freight cars rather than the 100-ton cars introduced in the 1970s.

These changes made necessary the development of rails based on an entirely new concept. The manufacture and properties of deep head hardened (DHH) rail, developed by Nippon Steel in response to the foregoing technical changes, are described in this paper.

OBJECTIVES OF DEVELOPING NEW RAILS

In developing new rails, Nippon Steel gave the recent changes in rail applications careful consideration and set the following objectives.

1. To develop rails of different strengths (hardnesses) for different uses: The use of lubrication reduces rail wear and causes fatigue layers to accumulate on the rail surface, which can cause damage to the rail surface. For this reason, it is necessary to use a rail that is slightly less hard than conventional high-strength rails. On the other hand, with the increase in freight car tonnage, medium-strength (H_B 285–320) rails have come to be used in tangent and gently curved tracks. Thus, rails of different hardnesses are necessary to meet diverse service conditions.

2. To increase hardened layer thickness: Rail head grinding requires that the rail interior have the same wear resistance as the rail surface. This means that the hardened layer should be made as thick as possible.

3. To improve weldability: Improving rail weldability is an important point to facilitate welding work and cut welding cost.

4. To secure homogeneous rails: In order to ensure a high level of rail safety under increasingly severe conditions, it is important to produce rails that are homogeneous throughout.

The off-line heat treatment process based on high-frequency induction heating currently employed at Nippon Steel cannot be applied to the manufacture of rails that meet the above-mentioned requirements without significant slowdown of hardening speed and marked deterioration in production efficiency. In addition, with this process, it is extremely difficult to obtain hardened layers of the desired thickness. In view of this, a direct heat-treatment process was developed to produce such rails.

DIRECT HEAT-TREATMENT TECHNOLOGY

Selection of Coolant

Various cooling media were studied and subjected to laboratory tests. The test results are shown in Table 1. It was found that salt, air, and mist might be feasible as cooling media for the direct heat treatment. These three media were thus subjected to detailed laboratory tests. In addition, the media were used in a heat-treatment test on rails immediately after rolling.

Test Results

Salt

A salt bath capable of accommodating 4-m rails was fabricated, and a heat-treatment test was conducted on rails immediately after rolling. The test results obtained with standard carbon steel rails are shown in Figure 1.

By maintaining the salt bath temperature at 400°C, it is possible to produce rails whose strength is comparable with that of NHH rails. In order to produce medium-strength (H_B 285–320) rails, it is necessary to raise the salt bath temperature

to 500°C or higher, which poses the problem of salt evaporation. In addition, immersion of the rails causes the salt bath temperature to rise. Therefore, a large-scale heat removal system is needed if a salt bath is to be employed on an industrial scale.

Mist

A testing facility capable of treating 39-ft rails was built, and a heat-treatment test was conducted on rails immediately after rolling. The test results obtained with standard carbon steel rails are shown in Figure 2.

The test results indicate that it is possible to produce medium-strength and high-strength rails comparable with NHH rails. However, the influence of surface properties, especially scale, was found to be so great that the cooling rate varied throughout the length of the rail. In addition, local bainitic or martensitic structure makes it extremely difficult to secure uniform quality.

Because one of the primary objectives was to produce rails that were homogeneous throughout, mist, which causes

TABLE 1 SELECTION OF COOLANT FOR STANDARD CARBON STEEL RAIL

Grade Cooling media	High strength rail ($H_B \approx 370$)	Medium strength rail ($H_B \approx 300$)	Estima- tion
Boiling water (98°C)	<ul style="list-style-type: none"> Insufficient cooling capacity Martensitic or bainitic structure 	<ul style="list-style-type: none"> Martensitic or bainitic structure 	No good
Hot water (60~70°C)	<ul style="list-style-type: none"> Martensitic or bainitic structure 	<ul style="list-style-type: none"> Martensitic or bainitic structure 	No good
Quenching oil (100~180°C)	<ul style="list-style-type: none"> Martensitic or bainitic structure 	<ul style="list-style-type: none"> Martensitic or bainitic structure 	No good
Salt.	(Good)	<ul style="list-style-type: none"> Salt evaporation High cost 	Adoptable
Air	<ul style="list-style-type: none"> Insufficient cooling capacity 	(Good)	Adoptable
Mist	<ul style="list-style-type: none"> Local bainitic structure 	<ul style="list-style-type: none"> Local bainitic structure 	Adoptable

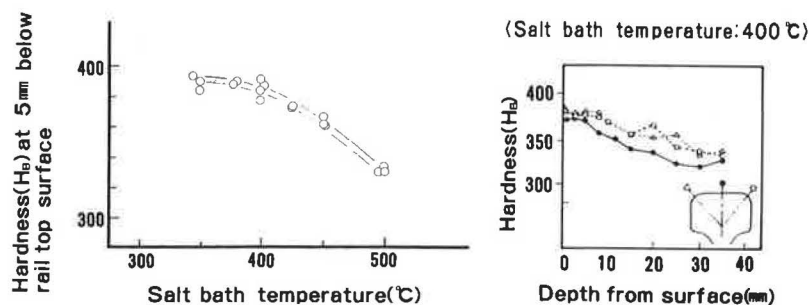


FIGURE 1 Hardness of rail (test using salt bath).

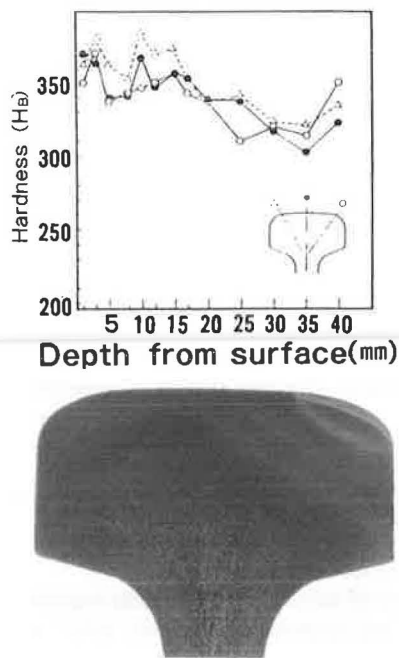


FIGURE 2 Hardness (top) and macrostructure (bottom) of rail (test using mist).

substantial variation in rail quality, was judged extremely difficult to use as a cooling medium.

An example of the variation in cooling with mist is shown in Figure 3.

Air

The test using air was conducted on rails immediately after rolling at a testing facility capable of treating 39-ft rails. The test results, obtained with standard carbon steel rails (Figure 4), indicate that rail quality is homogeneous throughout and that rails of different hardnesses can be produced by varying the air pressure. However, it is difficult to produce rails comparable in strength with NHH rails.

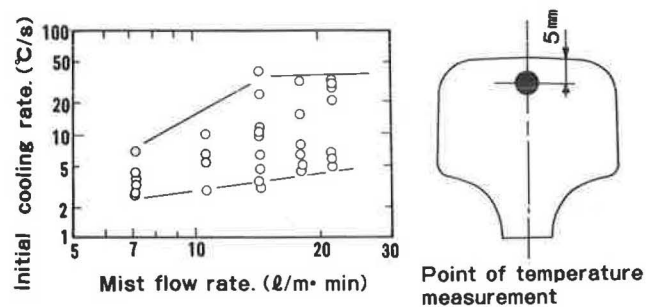


FIGURE 3 Variation of cooling rate in mist cooling.

Test results obtained with alloy steel rails (which have the same composition as Super rails) are shown in Figure 5. By adding elements such as chromium and silicon, it is possible to manufacture high-strength rails comparable with NHH rails.

Use of Air for Direct Heat Treatment

On the basis of the test results, it was decided to employ air quenching for the direct heat treatment. As the test results indicate, direct heat treatment with air quenching produces rails that are homogeneous throughout, and facilitates heat treatment of alloy steel. The drawback with this process is that, because air cannot cool the rails at the required rate, it is extremely difficult to manufacture high-strength ($H_B \div 370$) rails of standard carbon steel on an industrial scale. Though this problem may be solved by raising the air pressure, it is difficult to apply this method in industrial production.

Eventually it was decided to manufacture high-strength rails by adding very small amounts of alloying elements. Figure 6 shows initial cooling rate versus rail head surface hardness for three types of steel. The cooling rate can be controlled by regulating the air pressure with nozzles designed on the basis of the test results.

PROPERTIES OF DHH RAIL

The principal properties of rails manufactured by direct heat treatment using air quenching are described below.

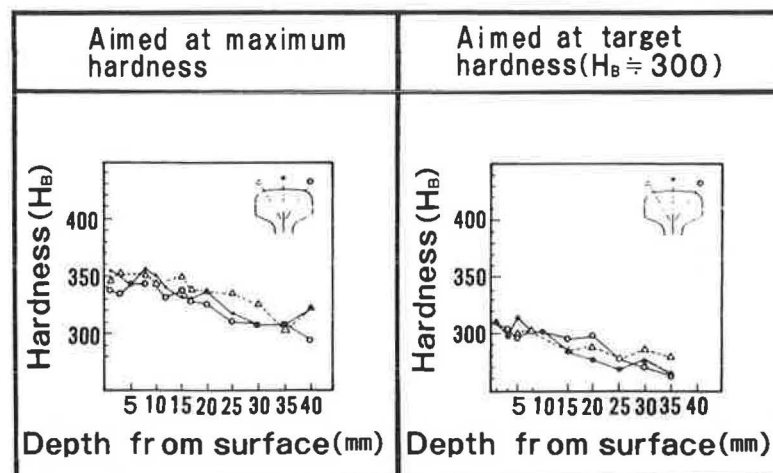


FIGURE 4 Hardness of standard carbon rail (test using air).

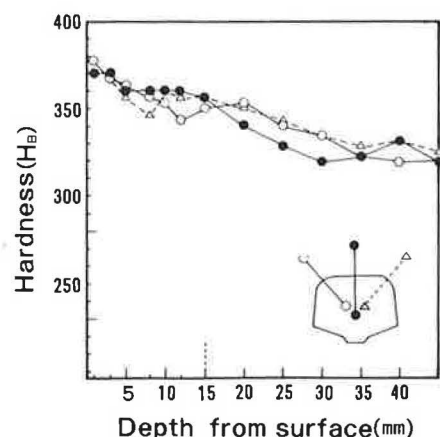


FIGURE 5 Hardness of alloy steel rail (test using air).

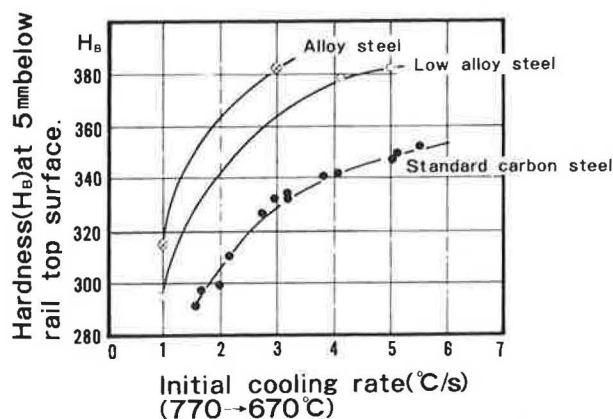


FIGURE 6 Relation between hardness and initial cooling rate.

Rails manufactured by this process are called deep head hardened rails.

Mechanical Properties

The mechanical properties of DHH rail in comparison with those of NHH rail are shown in Table 2. The strength of DHH rail measured at a point near the surface is almost the same as that of conventional NHH rail, but at a point further inside, it is higher than that of NHH rail.

Hardness and Structure

Figure 7 shows the section hardness distribution and macrostructure of direct heat-treated rails manufactured with an aimed hardness of H_B 370 compared with conventional NHH rail. It can be seen that the two types of rail have nearly the same surface hardness, but that the DHH rail has hardened deeper than the NHH rail. The DHH rail shows a uniform macrostructure pattern, whereas the NHH rail shows a softened layer caused by reheating.

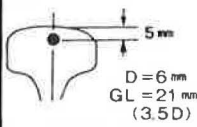
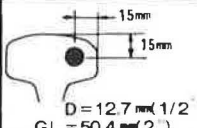
Figure 8 shows the microstructure of both types of rail. Like NHH rail, DHH rail has a fine pearlitic structure.

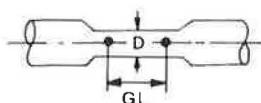
Figure 9 shows the hardness distribution over the entire section of DHH rail. The rail head shows a good hardness distribution.

Wear Resistance

Figure 10 shows the results of a wear test using test pieces taken from the head surface layers of various types of rail. In the case of rails that have a pearlitic structure, harder rails generally show better wear resistance. This suggests that DHH rail can retain the wear resistance of its surface layer even

TABLE 2 MECHANICAL PROPERTIES OF DHH 370 RAIL COMPARED WITH NHH RAIL

Item Sampling position	DHH 370 rail				NHH rail			
	0.2% Proof stress (Mpa)	Tensile strength (Mpa)	Elongation (%)	Reduction of area (%)	0.2% Proof stress (Mpa)	Tensile strength (Mpa)	Elongation (%)	Reduction of area (%)
	863	1,294	15	34	843	1,304	15	35
	834	1,275	12	29	745	1,157	10	25



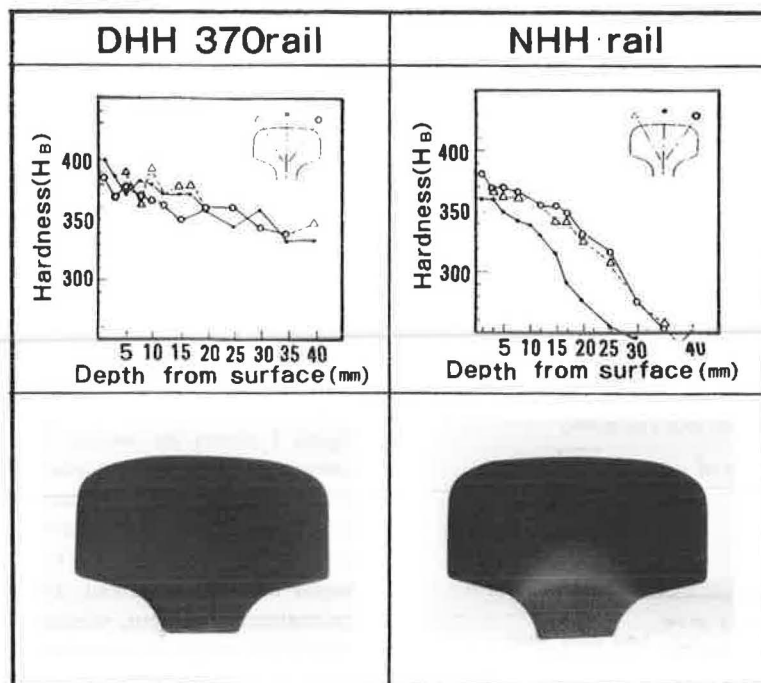


FIGURE 7 Hardness (top) and macrostructure (bottom) of DHH 370 rail compared with NHH rail.

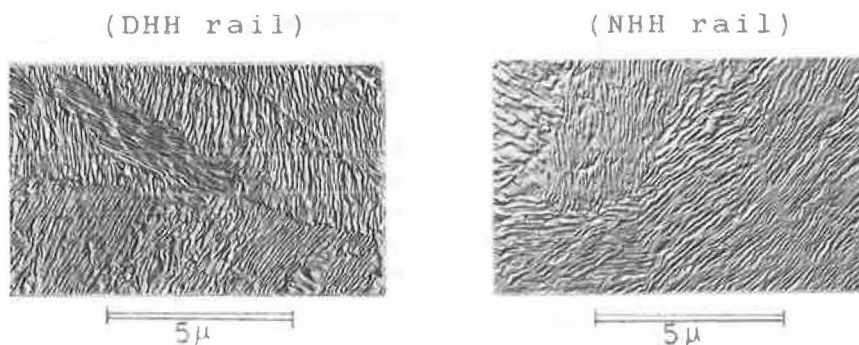


FIGURE 8 Microstructure of DHH rail compared with NHH rail.

when the head surface is ground; the wear resistance of its surface layer is almost the same as that of NHH rail.

Rolling Contact Fatigue Characteristics

Figure 11 shows the results of a rolling contact fatigue test conducted on DHH and NHH rail. The test was conducted on rail that was oil lubricated to prevent wear. The DHH 370 rail showed excellent resistance to damage compared with that of conventional NHH rail. DHH 340 rail also showed good resistance to damage.

Residual Stress

Figure 12 shows the residual stress in DHH and NHH rails. In the direct heat-treatment process, the amount of rail bending can be minimized by controlling the air blow. Hence the reduction through roller straightening can also be minimized. This makes it possible to reduce the surface residual stress in the rail top to near zero.

Weldability

Figure 13 shows the hardness distribution of DHH rails subjected to flash-butt welding. Compared with conventional NHH rail, in DHH rail the hardness of welded sections is subject to less deterioration, which suggests that no heat treatment is needed after welding.

DHH rail that is manufactured by adding a small amount of alloying elements and by controlling the rate of air quenching offers excellent weldability, as shown in Figure 13, thanks to the favorable effect of the alloying elements.

MANUFACTURE OF DHH RAIL

On the basis of the results found during development, Nippon Steel started construction of production equipment at the beginning of 1986. The equipment was completed at the end of May.

Each rail is rolled to 150 m, cut to specified lengths, and immediately subjected to direct heat treatment. It has become

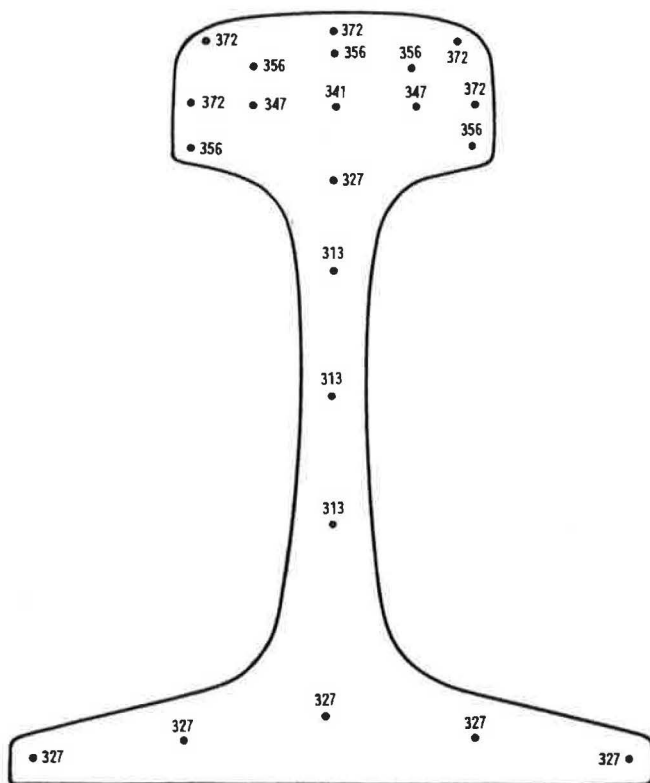


FIGURE 9 Hardness distribution on transverse section of DHH 370.

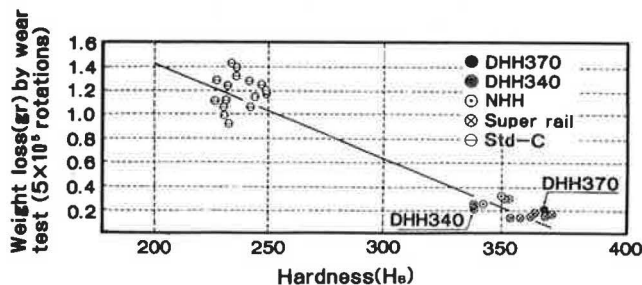


FIGURE 10 Relation between weight loss by wear test and rail hardness.

possible to produce large volumes of high-strength rails; formerly, production was limited by the capacity for off-line heat treatment.

The production equipment features a fully automatic rail conveyor system and an automatically controlled cooling system; hence it can stably produce high-strength rails.

Testing of the equipment and an in-depth quality examination of rails produced by the equipment was completed in 1987, and Nippon Steel has started shipment of high-strength rails manufactured by this equipment. Nippon Steel plans to market three types of rails—DHH 340 ($H_B \div 340$), DHH 370 ($H_B \div 370$), and DHH 370S ($H_B \div 370$)—to be produced by this equipment. All three types can be applied, depending on track conditions and the use of suitable lubrication. Continued research and development for further improvement of rail quality is expected.

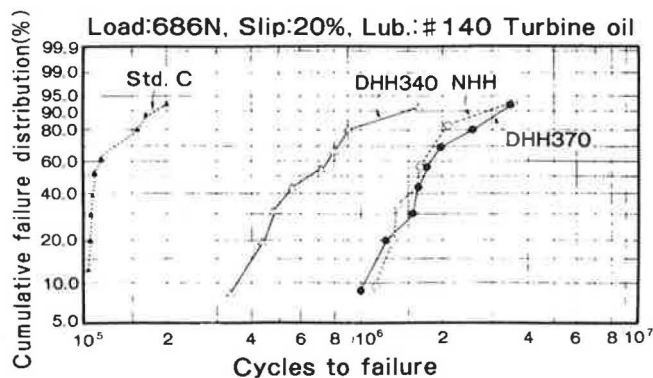


FIGURE 11 Rolling contact fatigue characteristics of various rails.

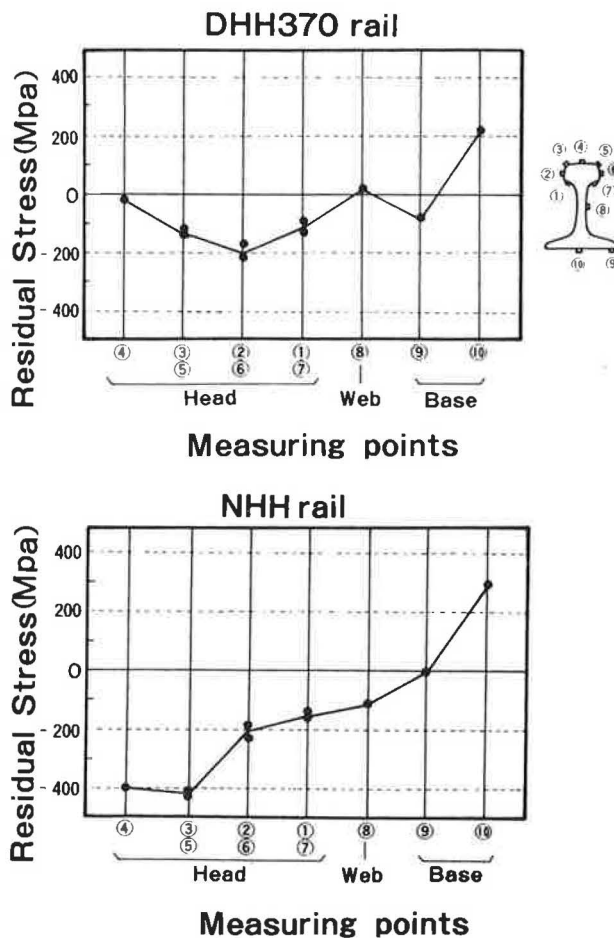


FIGURE 12 Typical residual stress on rail surface.

CONCLUSION

Nippon Steel has developed new heat-treated rails called DHH rail, the features of which are as follows:

1. Various grade types of strength and hardness,
2. A deep and uniformly hardened layer in the rail head,
3. High weldability, and
4. Uniform quality throughout the entire length.

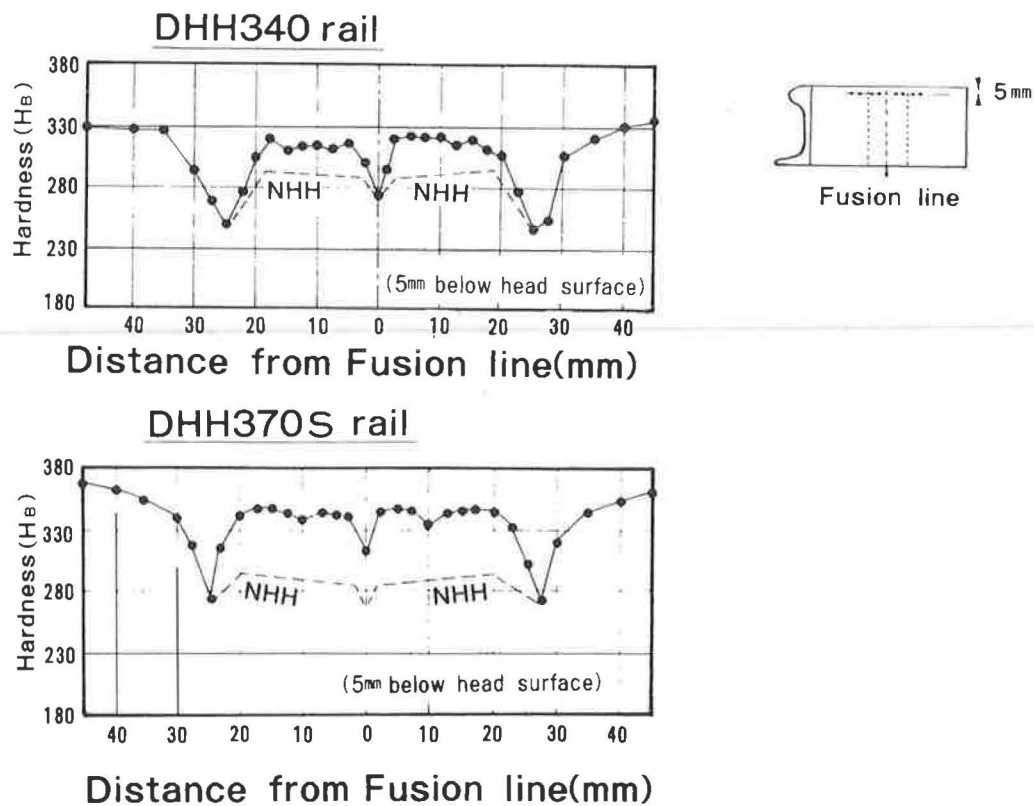


FIGURE 13 Weldability—flash-butt welding (welder k355).

Nippon Steel has completed the production equipment and started commercial shipment of DHH rail.

REFERENCES

1. H. Masumoto, K. Sugino, and H. Hayashida. Development of Wear Resistant and Anti-Shelling High Strength Rails in Japan. Presented at Heavy Haul Railway Conference, Perth, Australia, 1978.
2. H. Masumoto, S. Sugino, M. Hattori, and T. Terada. Production and Properties of High-Serviceability Rail. In *Transportation Research Record 838*, TRB, National Research Council, Washington, D.C., 1982, pp. 2-7.
3. K. Sugino, H. Kageyama, and H. Masumoto. Development of Weldable High-Strength Steel Rails. Presented at Second International Heavy Haul Railway Conference, Colorado Springs, 1982.
4. J. R. Lundgren. FAST Results: Selected Highlights. Presented at 80th Annual Technical Conference, American Railway Engineering Association, Chicago, 1981.
5. R. K. Steele and R. P. Reiff. Rail: Its Behavior and Relationship to Total System Wear. Presented at Second International Heavy Haul Railway Conference, Colorado Springs, 1982.
6. R. P. Reiff. Rail-Wheel Lubrication: A Strategy for Improving Wear and Energy Efficiency. Presented at Third International Heavy Haul Railway Conference, Vancouver, B.C., 1986.
7. D. A. Stewart. CN Rail's Experience with Profile Grinding of Premium Rail. *AREA Bulletin* 702, pp. 306-325.
8. C. Wesselmann. . . But What's It Doing to The Track? *Modern Railroads*, Mar. 1986, pp. 39-40.

In Situ Rail Head Rectification on British Railways

P. LEECH

The economic climate that led to the development of a system of in situ rail head rectification by planing, the history of its development, and the equipment used are described. Included are comments on how rail planing forms an integral part of the overall strategy adopted by British Railways for the maintenance of rail head geometry.

Ever-increasing economic pressures demand that the use of track components be optimized. On heavy curves it had been the practice to transpose or turn rails when a side on the high rail had reached unacceptable levels. Little attention was paid to the low rail. With the widespread use of continuously welded rail, turning was no longer an option, but transposition of rails was. As line speeds increased it was soon discovered that transposed rails gave an unacceptably poor ride because of bogie instability.

The "new" high rail clearly exhibited a flattened crown radius and often displayed mushrooming; this was caused when slow-speed traffic transferred a significant proportion of its weight to the low rail before transposition. Mushrooming or lipping can also lead to the formation of stress cracks, which ultimately cause failure of the rail.

The attractiveness of reusing rails rather than purchasing new ones led British Railways to develop a process by which to reprofile the head of rails in situ and gain, as it were, a second life for them. This permitted rails to be transposed on the same site or to be relocated on another route, that is, to cascade from a primary to a secondary line where speeds might still be high (in excess of 75 mph) but axle loads and gross tonnage lower.

Locating a reprofiling machine in a depot was an alternative, but it would have incurred substantially higher rail transport and handling costs.

DEVELOPMENT HISTORY

The British Railways network is made up of some 20,000 route km. Because of the legacy of a piecemeal construction history and many geographical features (which presented railway construction pioneers with barriers that tested their ingenuity), much of this network is on curves.

With one notable exception, namely, the London-to-Bristol route, all the main routes have their fair share of significant curves, and, in order to cut overall trip times and remain

competitive with other transport modes, railway engineers designed these curves to the tightest possible standards.

British Railways is a mixed-traffic network. It attempts to cater to the widest possible range of traffic including, at one extreme, high-speed passenger trains going up to 200 km/hr and, on the other, short-wheelbase freight wagons with a maximum speed of 45 km/hr. The maximum permitted axle load is 25 tonnes with a speed limit of 96 km/hr, but freightliners (bogie container-carrying wagons) with a maximum axle load of 22 tonnes are permitted to go 120 km/hr.

Therefore for all main lines curve design is a difficult compromise, but inevitably both high and low rails will experience substantial forces that cause side wear and flattening and mushrooming.

It was realized that on curves where rails had been transposed, the flattened head crown radius was producing an unacceptably poor ride. This led to prohibition of rail transposition on all but the slowest-running lines.

The result was the generation of rails that were ultimately worn to unacceptable limits. If reprofiled, they could have been reused, because they still contained a substantial amount of metal, but without such a process, these rails were fit only for scrap, a waste of a potential asset.

In 1978 Plasser and Theurer offered a machine that reprofiled the back edge of the low rail to facilitate transposing (Figure 1). It was designed to treat a maximum of 50 percent of the head width, and the cutting sequence was as follows: first cut—one cutter at 45 degrees; second cut—two cutters, one at 15 degrees and the other at 75 degrees; third cut—a clean-up profiler.



FIGURE 1 General view of production machine.

Trials began in 1979, and it was soon realized that it would be beneficial to adjust the cutters. The new arrangement was as follows: first cut—one cutter at 45 degrees; second cut—two cutters, at 30 degrees and 60 degrees; third cut—gauge corner radius profiler.

The profiles thus achieved were disappointing, giving an equivalent conicity of between 0.3 and 0.45. The target was set at 0.213, which was achieved by a worn wheel set of a Mark II passenger coach relative to the standard British Railways 113A flat-bottomed rail.

This machine was able to plane at 55 to 60 m/min, and the life of each cutting tool was 1.3 to 1.5 km. The cutting tools were designed for easy changing and adjustment, and the operators soon learned that the cutters became very hot during planing. The swarf generated was also red hot, and clearly, even when it had cooled sufficiently to be handled, it was unpleasant material to load and dispose of. If left on the ballast, it presented a major hazard to track maintenance staff and any electrical equipment. A trolley equipped with four magnets was soon added to the planing machine to handle this problem (Figure 2).

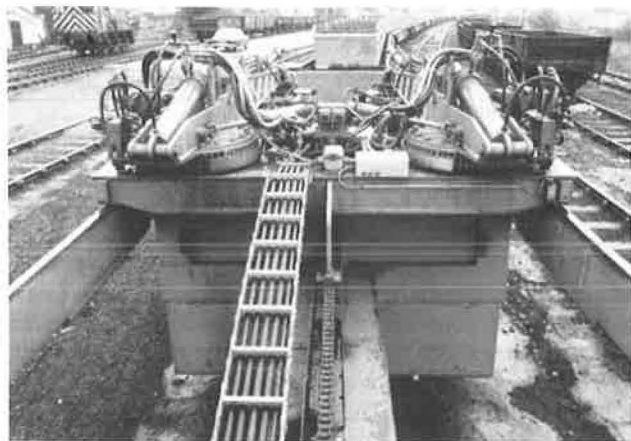


FIGURE 2 Earlier swarf collector.

New trials in 1980 involved planing the whole head in 8 and 10 passes. The results this time achieved an equivalent conicity of better than 0.213, even though the cutters had been set for a rail inclined at 1 in 40 rather than the British Railways standard of 1 in 20. It is interesting to note that at this site the rails were also corrugated and that the planing successfully removed all trace of the corrugations.

Further developments involving various ideas for swarf collection followed, because the magnet arrangement was slow and less than effective (Figure 3). Great care had to be exercised near signal equipment to avoid damage leading to signal failure. A vacuum cleaner was considered but rejected. A continuous magnetic loading system was preferred, and amendments to facilitate discharge of swarf from the collection hopper followed (Figure 4).

As experience was accumulated, other problems came to light. Some welds caused the cutting tools to shatter because of the sudden change in hardness.

The program of trials continued in 1981 using the following cutting sequence:

1. Middle of rail shoulder,
2. 45 degree chamfer on gauge corner,
3. Deeper cut than in step 2,
4. 25 and 67 degrees on gauge corner,
5. Just inboard from cut 1,
6. Just inboard from cut 5,
7. Center of rail head, and
8. Radius cutter on gauge corner.

The results showed that if the planing sequence is interrupted and trains are permitted to run over the rails at an intermediate stage, no temporary speed restriction is required.



FIGURE 3 Loading swarf.



FIGURE 4 Later type of swarf collector.

The success of this extended development sequence led to the placing of an order for four machines in 1982. The major difference from the prototype concerned the swarf collector. A twin rotating magnetic-drawn system plus conveyors replaced the four magnets supported by jibs. A ballast profile plate was also adopted to avoid the swarf's being trapped by uneven ballast.

Since 1984 these machines have formed an important part of the British Railways rail rectification regime; their prime purpose is to reprofile lipped and mushroomed rails so that they can be transposed or relocated (Figures 5 and 6). Corrugation removal is not the primary function of these machines, although they will successfully eliminate head defects



FIGURE 5 General view of reprofiled rail.



FIGURE 6 Reprofiled rail with gage.

of that type. British Railways employs four Speno grinding machines for the removal of corrugations and recently has begun some reprofiling with the latest grinding machine. This, however, is to improve the quality of ride over those rails that are not to be removed from the track.

MACHINE SPECIFICATION

The Plasser rail planing machine (PPM-100) is based on the standard 07 chassis. It is a self-propelled unit capable of running at a sustained speed of 80 km/hr up gradients of 1 in 500. It can negotiate a curve of 80-m radius and can work on track curved to 100-m radius.

It is designed for British Railways standard gauge (1432 mm) and is able to reprofile both rails simultaneously. The operating speed is up to 60 m/min and it is able to cut sections up to 25 mm². The cutting heads are controlled hydraulically and are guided by a series of rollers (Figure 7).

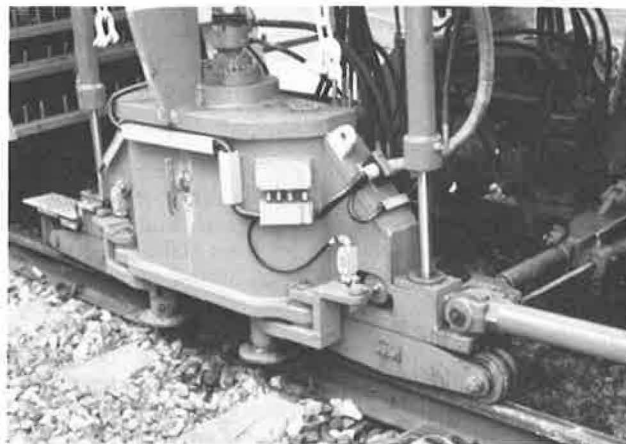


FIGURE 7 Cutting head in working position.



FIGURE 8 Cutting tools.

The unit is designed to be operated by a crew of two. The cutting process is observed using a TV monitor.

The cutters are of the chip breaker variety to reduce the risk of producing long lengths of swarf (Figure 8). The operator can change the cutters without having to stand on the "six foot" side, that is, risking being foul of an open track.

Technical and Financial Appraisal of a Contemporary Repair Technique for Rails and Crossings

R. S. JOHNSON

Maintenance welding on British Railways (BR) track is confined to two areas—crossings are repaired to fix the batter and cracking caused by passing traffic (these repairs outperform the original crossing material), and plain line is repaired to fix the damage caused by wheelslip and to remove rolling contact fatigue (“squat”) defects. These two types of repair operate in different stress environments; crossings are mainly subject to impact and plastic deformation, whereas plain line is subject to rolling contact fatigue and wear. Maintenance repair of rails within BR was until recently carried out almost exclusively with manual metal arc (MMA) welding using 3.2- or 4-mm diameter electrodes and small portable site welding alternators capable of producing welding currents up to 250 A. Welder training and repair procedures have been developed and improved over the years; however, these techniques are governed by the weldability of the base material and the limitations of the MMA process. Therefore, further development of the present system for improved productivity and quality is limited. Semiautomatic welding procedures using flux-cored wires have been demonstrated in industry to offer great economic and technical benefits over MMA arc welding, and the application of the concept to the maintenance repair of track components has been the subject of an extensive laboratory and field assessment, the results of which are presented in this paper.

Maintenance welding on British Railways (BR) track is confined to two areas. Crossings are repaired to fix the batter and cracking caused by passing traffic; these repairs outperform the original crossing material. Plain line is repaired to fix the damage caused by wheelslip and to remove rolling contact fatigue (RCF), or “squat,” defects. These two types of repair operate in different stress environments; crossings are mainly subject to impact and plastic deformation, whereas plain line is subject to RCF and wear.

Maintenance repair of rails within BR was until recently carried out almost exclusively with manual metal arc (MMA) welding using 3.2- or 4-mm diameter electrodes and small portable site welding alternators capable of producing welding currents up to 250 A.

Welder training and repair procedures have been developed and improved over the years; however, these techniques are governed by the weldability of the base material and the limitations of the MMA process. Therefore, further develop-

ment of the present system for improved productivity and quality is limited.

Semiautomatic welding procedures using flux-cored wires have been demonstrated in industry to offer great economic and technical benefits over MMA welding, and the application of the concept to the maintenance repair of track components has been the subject of an extensive laboratory and field assessment, the results of which are presented in this paper.

MMA WELDING

Weld repairs to the permanent way can be broken down into two main categories: (a) maintenance and repair of crossings, and (b) repair of plain line surface defects.

Repair of Crossings

The repair of crossings can be broken down into two distinct types.

Maintenance repair involves the removal of deformed and defective material, which results from the impact loading of passing traffic, and its replacement with sound material (Figure 1). This type of repair is carried out in track, generally before the amount of wear on the crossing exceeds 6 mm in depth. Both the wing rails and the crossing nose (frog) are treated at the same time and in the same manner.

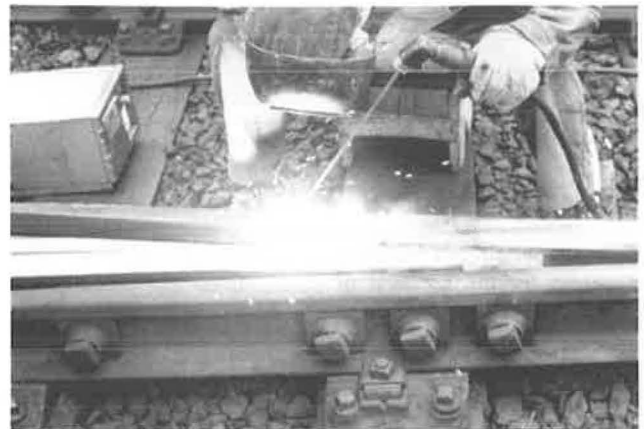


FIGURE 1 Crossing nose undergoing maintenance welding.

Structural repairs to crossings are usually executed out of track and can involve large weld repairs to fatigue cracks or fabrication defects anywhere within the body of the crossing (Figure 2). The objective of both types of crossing repair is to enhance the life of the crossing at minimal cost. Whereas most maintenance welding can be undertaken with the crossing in situ, larger repairs necessitate the removal of the unit before its repair, either at lineside or in a workshop.



FIGURE 2 Crossing nose requiring repair welding.

Repair of Plain Line

The adoption of MMA welding for the rectification of surface damage and defects in plain line is relatively recent and was stimulated by the widespread use of continuous welded rail with its attendant high cost of rail replacement.

Initially repairs were restricted to inherent rail defects (rolling defects) or wheelburns (Figure 3). However, the identification of large numbers of RCF defects (Figure 4) in the mid-1970s (1) enhanced the cost-effectiveness of repairs by welding as an option to rail replacement. Procedures have been developed for the repair of plain-line defects, either with or without possession of the line, to remove cracked or defective material and restore a smooth-running surface with sound, defect-free weld metal.

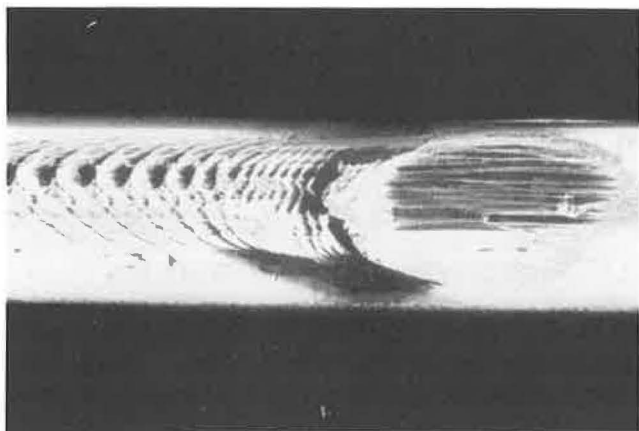


FIGURE 3 Typical wheelburn.

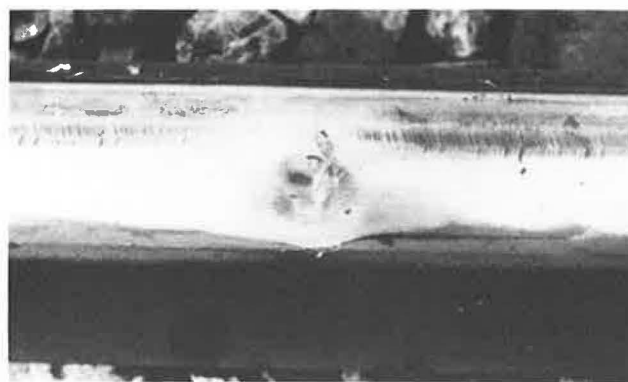


FIGURE 4 Rolling contact fatigue ("squat") defect.

Weld Metal Considerations

The stress environments encountered in these two types of repair are quite different. Crossings are mainly subject to impact loading from the transfer of the axle load from the wing rail to the crossing nose, or vice versa: Plain line is subject to cyclic dynamic loading from the smooth passage of the wheel along the rail. The properties required of any weld metal for these repairs would appear to be quite different, but this is not necessarily the case. For crossings, resistance to impact is of prime importance; other properties required are resistance to fatigue crack initiation and growth and a degree of ductility. A hard, tough weld metal is therefore required. Plain line repairs need to be very resistant to fatigue crack initiation and growth and should wear at approximately the same rate as the rail steel. A hard and tough high-integrity weld metal is required.

In 1967 (2) an assessment of electrodes was completed by BR to determine their suitability for maintenance of crossings. The results of this work, based on weld integrity and hardness, showed that "low alloy," hydrogen-controlled electrodes (2 $\frac{1}{4}$ percent Cr/1 percent Mo) or "stainless" rutile electrodes (18 percent Cr/8 percent Ni/3 percent Mo) produced deposits suitable for surfacing BS 11 normal quality steel (see Table 1). Electrodes of these two broad types were adopted by BR for welding crossings (3), and several electrodes of each type were subsequently approved (Table 2).

Following the adoption of these electrode types, a number of reports were received as to the performance of the repairs. Some reports indicated that the stainless electrode exhibited poor resistance to batter, whereas other reports revealed that although the low-alloy types were more resistant to deformation, problems were encountered with cracking, either as a result of inadequate preheat (4) or as a result of weld defects (5) (see Figures 5 and 6).

In 1970 a project was undertaken by the BR Research Division to investigate further the choice of welding procedure (including preheating requirements) and the most suitable electrode for the repair of worn crossing components. This work culminated in the recommendation that the minimum preheat temperature for normal quality rail steel be 350°C (6) and the finding that the most crack-resistant electrodes were Philips kV3L and Murex Duroid 11. The properties of these two electrodes are given in Table 3. It was also recommended that semiautomatic welding methods be investigated (6).

TABLE 1 RAIL COMPOSITION AND CRITICAL COOLING DATA

	CARBON WT%	MANGANESE WT %	SILICON WT %	CHROMIUM WT %	SULPHUR WT %	PHOSPHORUS WT %	C.E.*	COOLING DATA FOR FULLY PEARLITIC TRANSFORMATION T 800-400 COOLING (SEC) RATE (°C/S)	
BS 11 (1978) NORMAL QUALITY	0.50	0.95	0.05	-			0.61	40	10.0
	0.60	1.25	0.35	-	0.05	0.05	0.81		
BS 11 (1978) GRADE A	0.65	0.80	0.05	-			0.73	35	11.4
	0.78	1.30	0.35	-	0.05	0.05	0.97		
BS 11 (1978) GRADE B	0.50	1.30	0.05	-			0.72	590	0.67
	0.70	1.70	0.50	-	0.05	0.05	0.98		
BSC 110 kg mm ⁻² CHROMIUM	0.68	0.80	-	0.95			1.06	1200	0.33
	0.78	1.20	0.50	1.25	0.04	0.03	1.27		
NORMAL AUSTENITIC MANGANESE STEEL	1.0	11.0	-						
	1.25	-	1.0	-	0.06	0.07	-		
LOW CARBON AUSTENITIC MANGANESE STEEL	0.7	12.0	-	-			-		
	0.9	16.0	0.4	-	0.05	0.05	-		

$$* CE = C + \frac{Mn}{6} + \frac{Cr + Mo + V}{5} + \frac{Ni + Cu}{15}$$

TABLE 2 ORIGINAL APPROVED LIST OF MMA ELECTRODES

Electrode	Manufacturer	Type of deposit
kV3	Philips	2-1/4% Cr/1% Mo
Ferron 42	B.O.C.	2-1/4% Cr/1% Mo
Suprex B	Murex	2-1/4% Cr/1% Mo
Duroid 11	B.O.C.	18% Cr/8% Ni/3% Mo
Armex 2	Murex	18% Cr/8% Ni/3% Mo
Manganese Nickel	Murex (Hymet)	0.7% C/11% Mn/4% Ni*

* Used as a work hardening capping layer on cast manganese crossings only.

Although the foregoing investigation was aimed primarily at the repair of crossings, the repair of wheelburns was also being studied (7). MMA, oxyacetylene, and aluminothermic processes were considered. However, the MMA welding was found to be the most practical, and, as in the work on crossings, the Philips kV3L electrode was found to be the most suitable for the repair of wheelburns.

FLUX-CORED SEMIAUTOMATIC WELDING

Background

By the early 1970s it was recognized that the use of a continuous wire "semiautomatic" welding process might be of benefit to the civil engineer, both in terms of productivity and deposit quality.

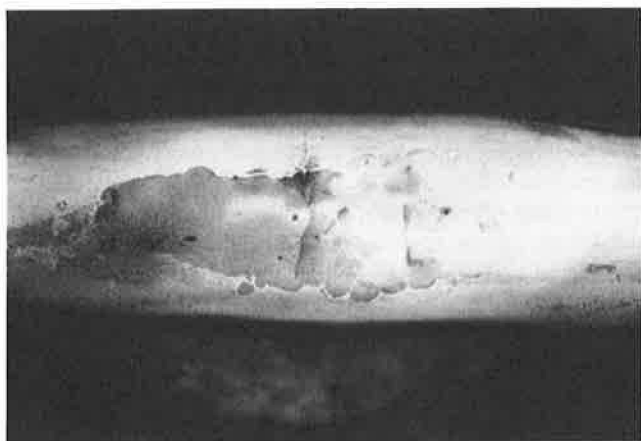


FIGURE 5 MMA repair of cracked plain line.

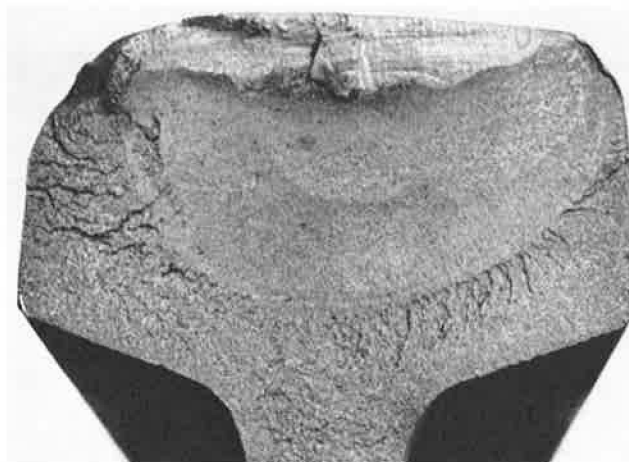


FIGURE 6 MMA repair of fractured rail.

TABLE 3 CHARACTERISTICS OF CURRENT APPROVED MMA ELECTRODES

TYPE	"Low Alloy"	"Stainless"
APPROVED PRODUCT	Philips kV 3L	Murex Armoid 1 *
electrode : dia. (mm) length (mm) coating type AWS Class	3.2, 4.0 350 Basic (low hydrogen) BS2493 - 2 Cr Mo B E 9015 B 3L	300 Rutile BS2926 - 20-9-3 -
Welding - O.C.V. AC/DC tgp. current (a)	80 DC+ or AC 4 mm:- 115-165	80 DCT or AC 3.2 mm:- 110-130
Typical Composition (wt %) C Si Mn S P Cr Ni Mo	.07 0.4 0.9 .014 .018 2.5 - 1.0	.06 .90 2.03 .013 .033 20 8.2 3.2
U.T.S. (N/mm ⁻²) Y.P. (N.mm ⁻²) % Elong Hardness (Hv 30)	810 - 903 602 - 765 21 - 31 310 - 320	670 - 760 450 - 540 31 - 48 235 - 290
Microstructure	Fine Bainite	Austenitic + 25% Ferrite

* Murex Armoid 1 is the current alternative to Murex Duroid 11, which is no longer available.

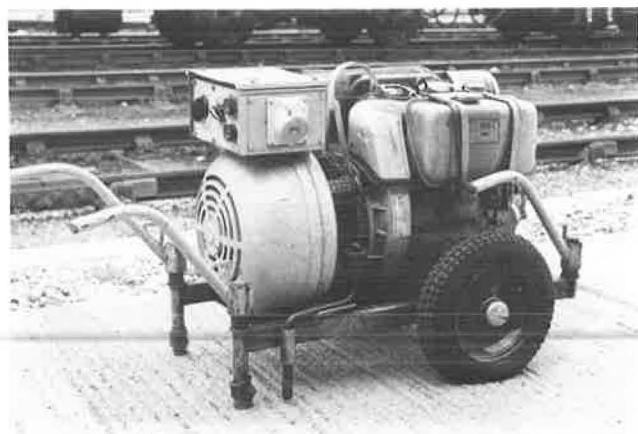


FIGURE 7 Hayter "Mighty Midget" 250a AC welding machine.

An analysis of typical maintenance repairs to crossings demonstrated that only 25 percent of the welder's time on site was actually spent welding (see Appendix A). The remaining time was consumed by ancillary operations, some of which were peculiar to the MMA process (electrode drying and changing, slag removal, etc.). In addition, a large number of repairs subsequently failed as a result of welding defects such as lack of fusion or porosity.

Semiautomatic welding in industry has proved to offer great economic and technical benefits over MMA welding (in addition to the improved weld quality), primarily as a result of higher deposition rates and greater heat input. The concept, therefore, if applied to track repairs, could both increase the speed of repairs, thus releasing staff for more repairs,

and reduce the number of subsequent failures. A further potential benefit was the possibility of repairing rail steels not repairable with MMA as a result of the greater heat input.

A preliminary appraisal of a number of products was carried out between 1968 and 1973. However, the consumables were off-the-shelf products deposited using conventional heavy-duty plant, and the appraisal drew attention to their limitations for use on site. This was primarily because of the need for additional shielding gas (CO_2) and heavy, high-current (350 to 400 A) welding machines because of the large-diameter (3 to 4 mm) wires then available (8).

From this initial review of products, requirements were formulated for a suitable process for site deposition of a wear-resisting surface on rails. The basic criteria were as follows:

1. The process should use self-shielding consumables to avoid the need to supply and transport gas bottles, and
2. The process should operate satisfactorily from existing portable MMA welding power sources.

Both aspects required considerable development, and although they are obviously interrelated, for the purpose of this paper they will be examined separately.

Equipment Development

The most common type of MMA welding machine used by BR is the Hayter 250a AC "Mighty Midget" alternator, of which approximately 400 are currently in service. The majority are diesel powered (Figure 7). The unit operates nominally at 427 Hz, and the output is rated as 250 A maximum at 60 percent duty cycle. Machine tests have shown that the

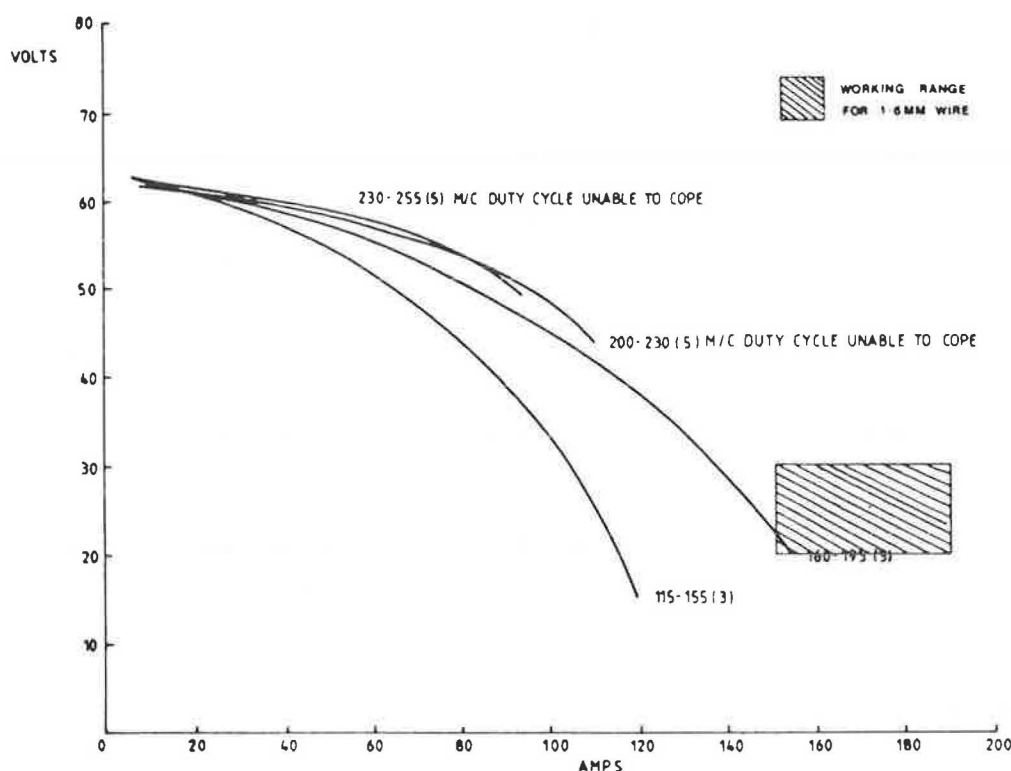


FIGURE 8 Current-voltage relationship for the "Mighty Midget" operating on ac.

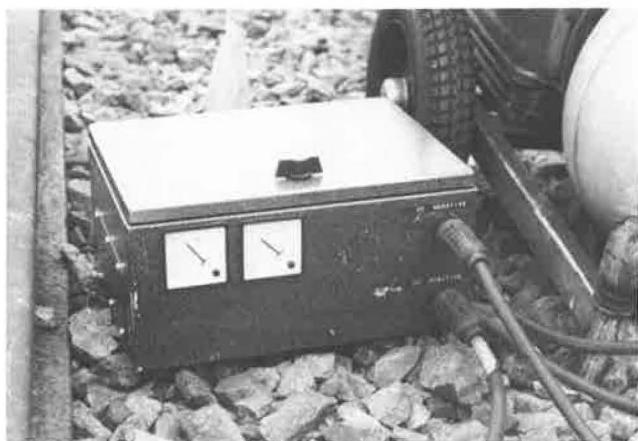


FIGURE 9 Example of an ac-dc rectifier.

maximum current at 100 percent duty cycle, which would be required for a continuous wire process, can be as low as 160 A, particularly if deterioration of the equipment is taken into consideration. In common with other MMA welding plant, the curve of machine output has a "drooping" characteristic, effectively producing constant current over the normal working range (see Figure 8).

Most commercially available wire feed systems operate off "flat" characteristic or constant voltage power supplies, using the welding current to drive the feed rolls. It was necessary, therefore, to develop a wire feed unit that would operate from the MMA supply and be lightweight yet robust in design. Welding Alloys Ltd. was developing a prototype machine, and one unit, designated the WASA 70, was purchased for research.

Initial welding trials were centered around commercially available "low alloy" hard facing flux-cored wires 1.6 mm in diameter (9; W. A. Mosley, private communication, July 1980; 10). Most of these were subsequently found to be unsatisfactory (see the next section). In addition to poor weld quality, it was found that when the portable ac supply was used, only a small amount of weld metal could be deposited before the duty cycle of the source was exceeded, and the power supply was cut. Attempts to reduce the wire to 1.2 mm in diameter to reduce the required welding current resulted in a variable weld quality due to variations in the density of the flux fill. Attention therefore was turned to the power supply. Trials with a dc mains transformer gave no such problems; additional benefits were a more stable arc, enhanced deposition characteristics, and increased arc energy (i.e., heat input). The attachment of an external rectifier or "converter" (Figure 9) to the output of the ac power supply was found to increase the output of the unit such that the duty cycle of the machine was no longer being exceeded (see Figure 10). It also produced the improved welding characteristics noted for the dc mains supply (W. A. Mosley, private communication, Oct. 1980).

The WASA 70, operating from a rectified ac supply, was subsequently used for the first site trials with the process, and certain modifications became desirable for the production model, which have subsequently been incorporated into an improved unit, the WASA 90 (Figures 11 and 12).

Rectified three-phase ac welding machines have also been investigated and are now recommended as the preferred and more economical alternative to the purchase of new ac plant with a separate rectifier. An example of one such unit is shown in Figure 13; its output is shown in Figure 14.

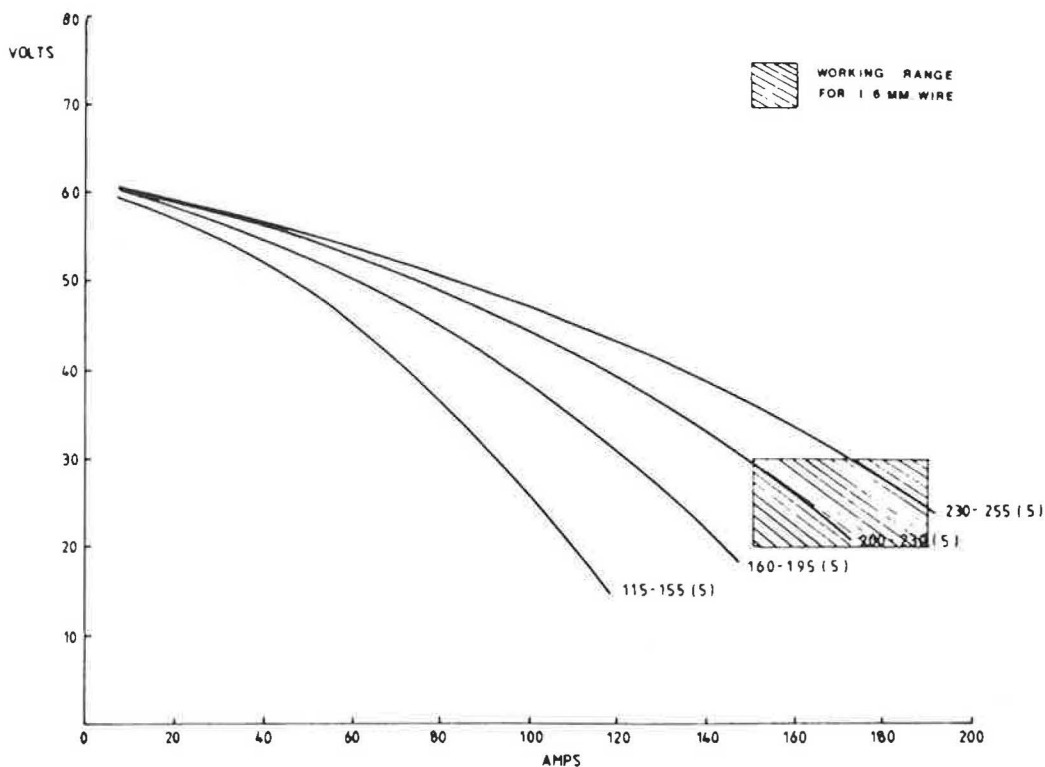


FIGURE 10 Current-voltage relationship for "Mighty Midget" and rectifier.

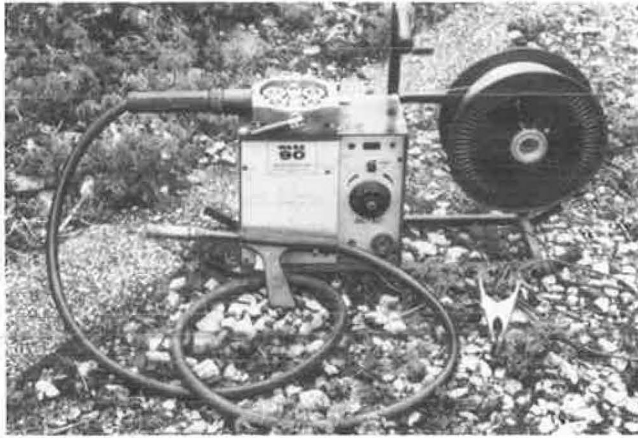


FIGURE 11 Welding Alloys WSHA 90 wire feed unit.

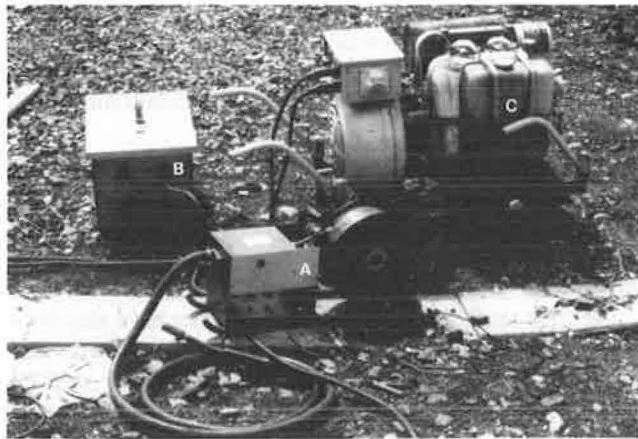


FIGURE 12 Equipment arrangement consisting of (A) welding torch, (B) converter, and (C) ac welding machine.

Development of Wire for Repair Welding

Initial Work

The basic requirements of any deposit on rails are high integrity (freedom from defects), resistance to deformation and wear, and resistance to fatigue cracking, with good welding characteristics.

Initial trials with commercially available consumables proved unsatisfactory. The main problems were as follows:

1. Defects occurred in the weld metal—porosity and slag were trapped because of premature freezing of the deposit as a result of the low current available for depositing large-diameter wires (>1.6 mm) (9).
2. Conventional hard-facing consumables, typically containing high C, Si, and Mn levels, resulted in excessively hard and brittle deposits (W. A. Mosley, private communication, July 1980).
3. Consumables containing titanium (added as a deoxidant) resulted in retention of large titanium carbonitride inclusions in the weld metal (10), which impaired the fatigue properties.
4. Deposits that were sound, defect free, and metallurgically acceptable were usually too soft compared with



FIGURE 13 Petbow Arc Centre 200 dc welding machine.

MMA deposits (W. A. Mosley, private communication, Oct. 1980).

From the experience gained through this work, the requirements of candidate wires became more evident.

Wires had to be limited to 1.6-mm diameter or less and dc current was necessary to obtain adequate welding characteristics from site plant, and to increase the duty-cycle capacity of the equipment. A “stringer” bead welding technique tended to increase defect levels (W. A. Mosley, private communication, Oct. 1980). Therefore a weave technique was proposed. The use of deoxidants such as titanium was to be avoided, as were high carbon and manganese levels. Preheat could be reduced to 250°C for normal-quality rail steel as a result of the higher heat input of the process (W. A. Mosley, private communication, July 1980).

Evaluation Program

To handle the number of products that were expected to be submitted for assessment, the evaluation program used simple, low-cost procedures for initial sorting, following by more sophisticated tests on selected wires.

The program evolved around two deposition arrangements, with the candidate wire being deposited on mild steel plate for “undiluted” weld metal analysis and on prepared lengths of BS 11 normal-quality rail steel for diluted weld metal analysis. The tests used and their order are given in Table 4 (test specimen weldments are shown in Figure 15).

A number of possible consumables have been assessed; one of the most successful is a CR/Mn wire submitted in August 1983. The wire was initially supplied as a single 13-kg reel; however, additional reels were made available following the satisfactory preliminary assessment (11).

Laboratory Assessment of Cr/Mn Flux-Cored Wire

Before any test samples were prepared, “exploratory” weld deposits were produced to determine the welding parameters. All welds were made using rectified ac, a 25-mm weave, and a run length of approximately 90 mm. All the welds on normal-quality rail were deposited using 250°C preheat.

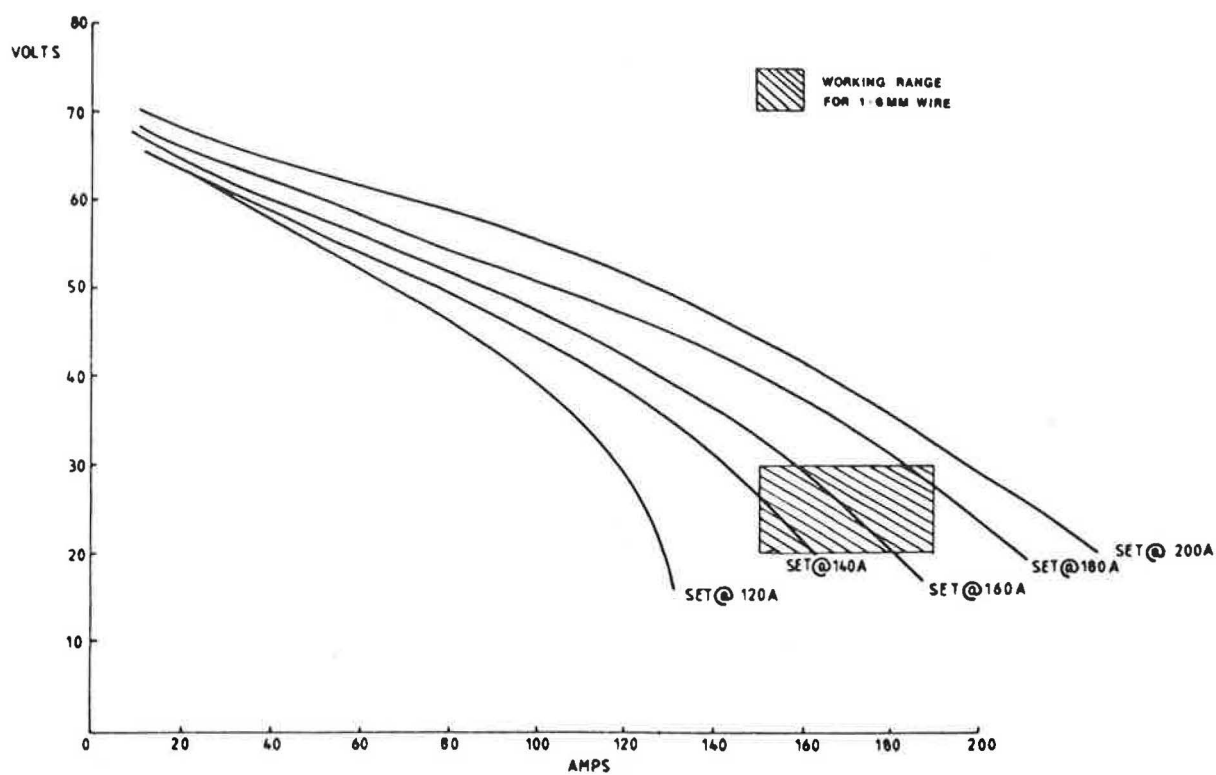


FIGURE 14 Current-voltage relationship for Pethow Arc Centre 200.

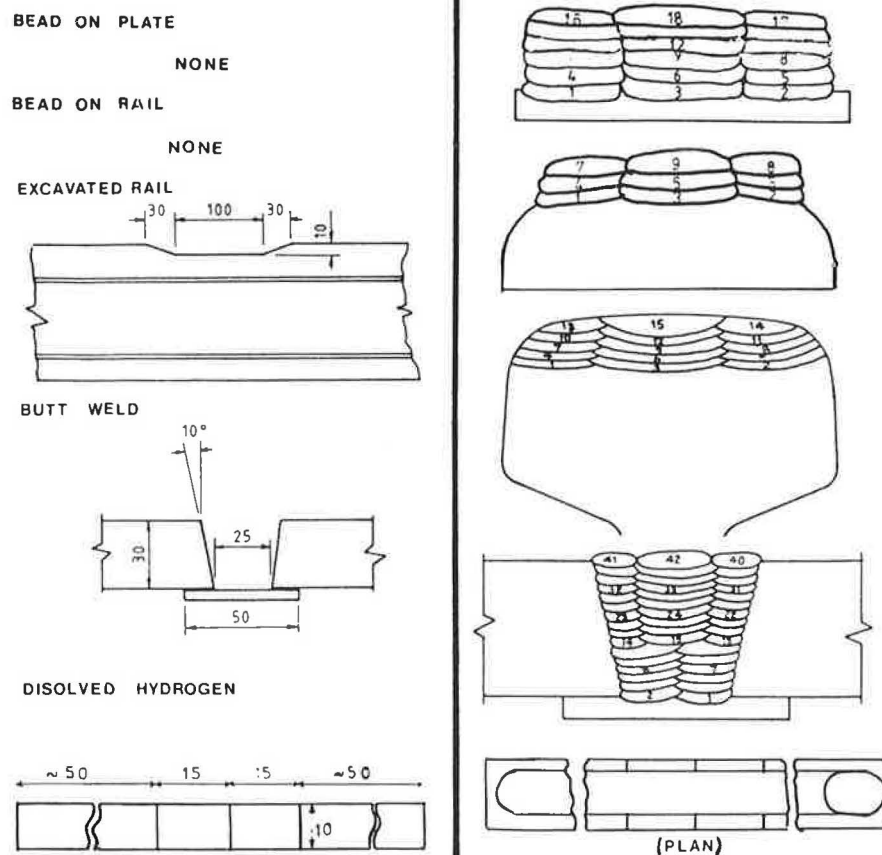


FIGURE 15 Preparation (*left*) and welding sequence (*right*) for test samples.

TABLE 4 TESTS USED TO EVALUATE WIRES

Test Piece	Applicable Test Program
Bead on MS plate (six-layer pad)	Radiography Chemical analysis Metallography Hardness
Bead on rail (three-layer pad)	Metallography Chemical analysis Hardness
Excavated rail	Fatigue test Metallography
Butt-welded M/S plate	Tensile test Toughness (Charpy V notch) Deformation (flow under impact)
Bead on plate	Diffusible hydrogen

The results of these exploratory tests are summarized in Tables 5–8, and the fatigue data are shown in Figure 16 with comparative data for MMA welds.

Metallographic examination of the weld metal in the undiluted form revealed a coarse dendritic structure (Figure 17) with a very low level of nonmetallic inclusions and no visible porosity. The microstructure of the weld metal consisted of coarse bainite and ferrite (Figure 18). The heat-affected zone in normal-quality rail steel (250°C preheat) showed no evidence of any brittle transformation products.

To assess their relative resistance to deformation, specimens of weld metal were tested in a “flow under impact” machine developed by the Research Division. An impact force produced by a compressed air cylinder was applied to 12.5-mm diameter cylindrical specimens of undiluted weld metal. The plastic deformation of the specimen after successive blows

was measured and recorded as a percentage of the original length (the smaller the value, the greater the resistance to deformation). The results for 1,000 impacts for the weld metal and comparative data for rail steels are plotted against impact stress in Figure 19.

Diffusible hydrogen determinations were carried out using the technique specified in BS 639 (12). Test samples were produced from the wire in the “as received” condition and exposed to the atmosphere without the protective container for 72 hr. The measured diffusible hydrogen content of the Cr/Mn wire and comparable data from low-hydrogen electrodes (13) are given in Table 9.

Field Trials with Cr/Mn Wire

Following the laboratory tests, a tentative specification for the wire was agreed on with the manufacturer, and a small batch of wire was purchased for field trials in the London Midland Region. Eighteen wheelburns were repaired, and subsequent nondestructive testing (NDT) examination using magnetic particle and eddy current techniques showed the deposits to be defect free. During 1985 a series of wheelburn repairs was carried out using another batch of Cr/Mn wire, but subsequent NDT examination showed that of the 26 repairs installed, 11 were found to contain transverse cracks (see Figure 20). An additional installation consisting of 36 repairs was found to contain 21 cracked deposits.

An examination of the sites showed that the cracks occurred some time after welding (when the deposit was cold), whether the repair had been exposed to traffic or not. Cracked deposits were found in both continuous welded rail and bolted track and in relatively new as well as in old rail.

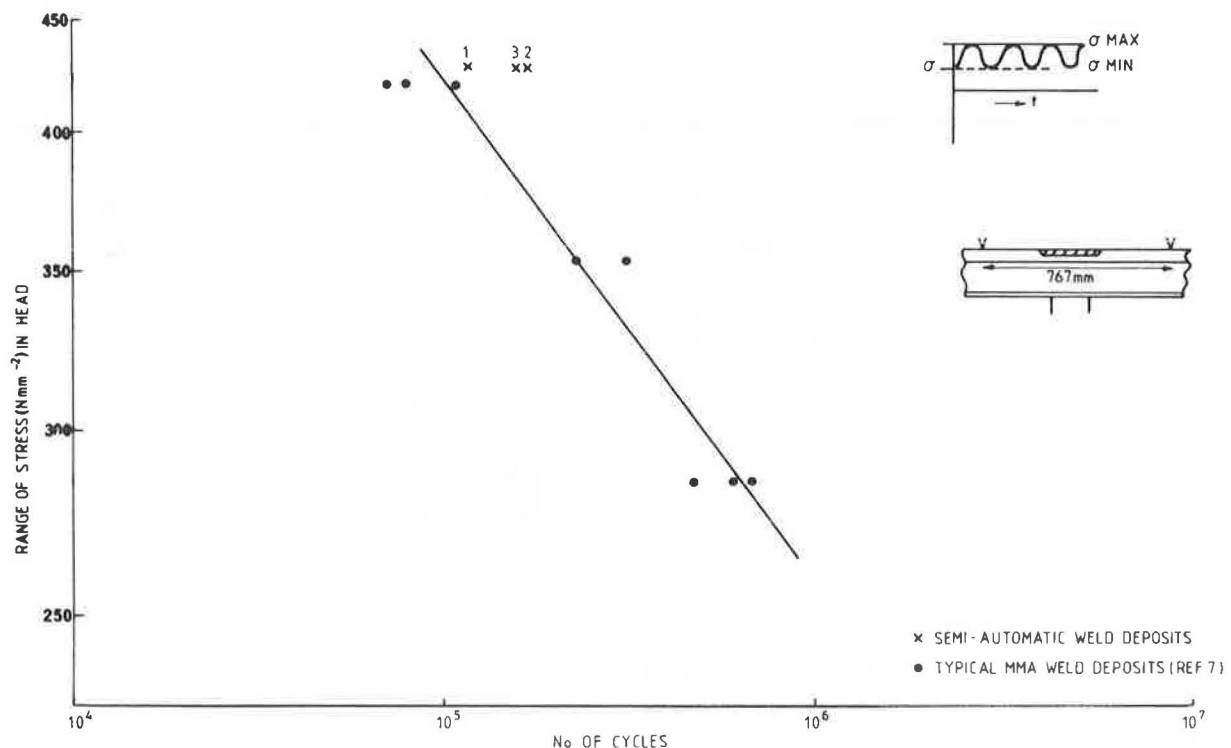


FIGURE 16 Fatigue test results for semiautomatic repairs compared with MMA repairs.

TABLE 5 CHEMICAL COMPOSITION AND HARDNESS OF CR/MN WIRE

	Batch No./Date Received				Provisional Specification ^d	
	BR-EXP/11-83 ^a	41205 ^b /3-85		EXPTL-MOD 2 ^c /10-85	Min ^e	Max ^e
		Undiluted	Diluted			
Composition (wt %)						
C	0.27	0.31	0.30	0.25	0.2	0.25
Si	0.16	0.13	0.13	0.15		0.5
Mn	1.83	2.2	2.11	1.86	1.7	1.9
Ni	0.07	0.09	0.08	0.05		
Cr	1.18	1.48	1.44	1.23	1.00	1.20
Mo	0.14	0.17	0.15	0.01		0.20
Al	2.7	2.9	2.69	1.4	1.3	1.5
Mean hardness (Hv 30)	310-350	365	—	319	300	350

^aUndiluted. Weight, 13 kg; diameter, 1.6 mm; welding current, 160-190 A; welding voltage, 23-27 V.

^bBatch resulting in defective repairs. Weight, 13 kg; diameter, 1.6 mm.

^cExperimental "low alloy" reel for crack-free deposit. Undiluted. Weight, 13 kg; diameter, 1.6 mm.

^dWeight, 13 kg; diameter, 1.6 ± 0.05 mm; welding current, 170-190 A; welding voltage, 22-24 V.

^eUndiluted weld metal.

TABLE 6 FATIGUE TEST RESULTS ON WELDED RAIL

Test Piece	Stress Range (N/mm ²)	Endurance (cycles)	Failure
1	430	112,000	Surface grinding
2	430	103,000	Isolated gas pore
3	430	158,000	Small crater crack

NOTE: Rail tested with rail head in tension.

TABLE 7 HOUNSFIELD TENSILE TEST RESULTS

Material	Yield Stress (N/mm ²)	Ultimate Tensile Stress (N/mm ²)	Elongation (%)
Corewire CS41 (mean)	623	870	14
MMA (kV3)	673	860	25
BS 11 (normal quality) rail	—	830	14

TABLE 8 CHARPY V-NOTCH IMPACT TEST RESULTS

Material	Test Temperature (°C)	Mean Impact (J)
Corewire CS41	-15	12
	0	12
	23	18
MMA (kV3)	-15	35
	0	58
	23	81
BS 11 (normal quality) rail	Ambient	5 (typical)

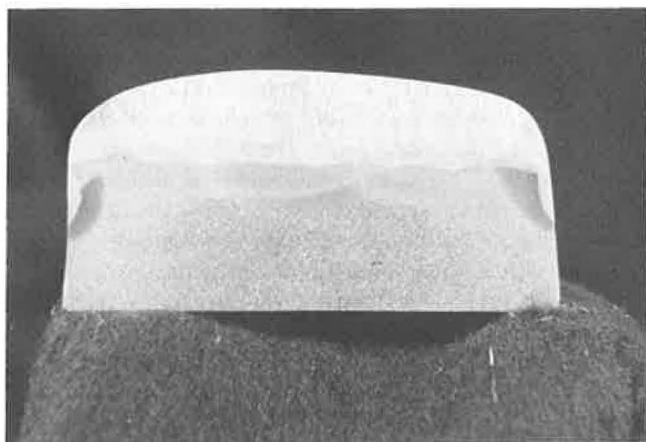


FIGURE 17 Transverse section through fatigue test specimen.



FIGURE 18 Photomicrograph of undiluted Cr/Mn weld metal.

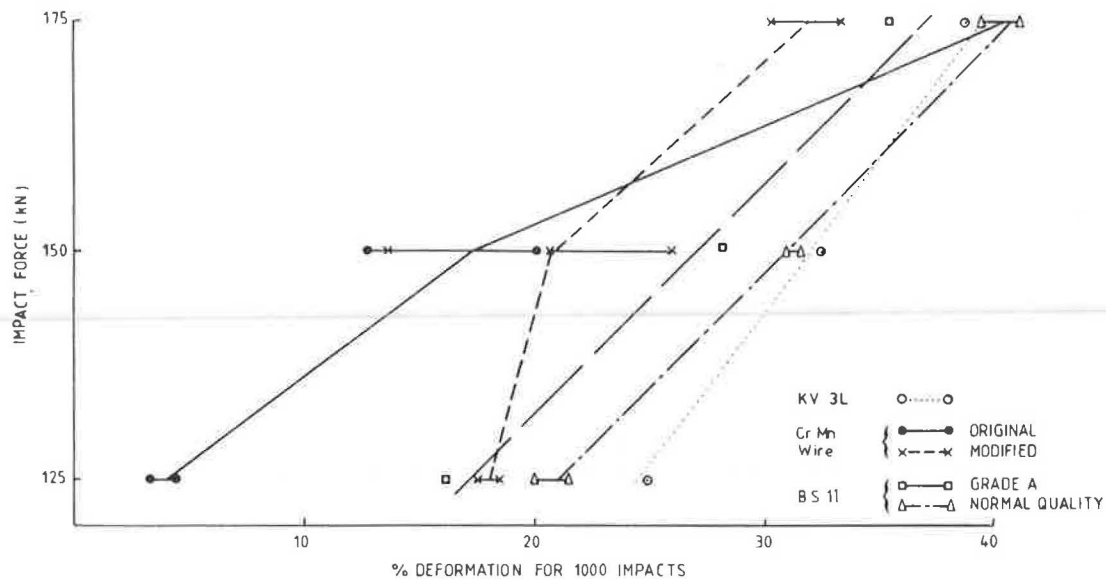


FIGURE 19 Deformation test results for semiautomatic flux-cored weld metals.

Attempts to reproduce the cracking in the laboratory have been unsuccessful, even using a range of stress environments on the test samples before, during, and after welding. As of 1987, laboratory simulation of the cracking mechanism still had not been accomplished, but cracking had been reproduced in a site trial on the Research Division test track

TABLE 9 DIFFUSIBLE HYDROGEN DETERMINATION

Consumable	Diffusible Hydrogen (m/100 g of weld metal)		
	As Received	Exposed ^a	Dried for 1 Hr at 300°C
Cr/Mn wire	5.08	4.07	—
Philips kV3L	5.74	8.40	4.76
Bohler Fox CM2K	3.9	2.64	1.99
KS1 kV 111	4.73	5.09	1.98
Oerlikon Chromaly 21	4.8	8.28	7.66

NOTE: All results are the mean of four samples.

^aExposed to atmosphere for 72 hr.

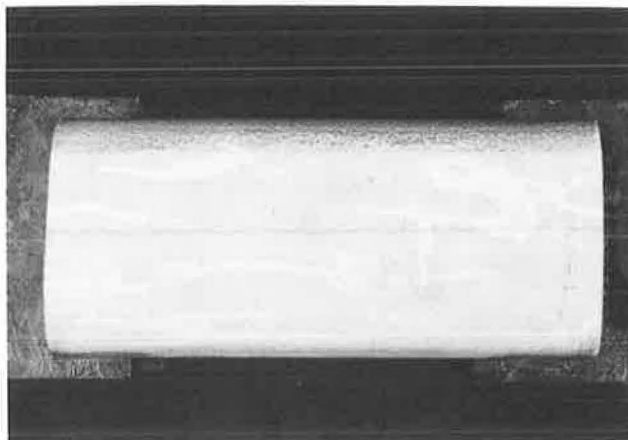


FIGURE 20 Transverse cracks in a repair on the Derby-Birmingham route.

using the batch of wire that had previously been used for the defective repairs (Batch 41205). In all cases the repairs were found to be crack free immediately after deposition, whereas 24 hr later the cracks were found to have formed, which indicated a cold (hydrogen) cracking mechanism.

Following removal of the defective rail from track, a number of the cracked deposits were broken open for scanning electron microscopy, which confirmed that the cracks were of a delayed, "cold" type. Optical microscopy of sections prepared through the cracked deposits showed that the weld metal exhibited a coarse, acicular structure consisting of high carbon bainite and martensite with a band of martensite adjacent to the fusion line (see Figure 21). It was concluded that the cracking was caused by hydrogen in the weld metal aggravated by a microstructure with inherently low levels of ductility and toughness.

The conventional solutions to the hydrogen cracking problem were considered:

1. *Use lower hydrogen levels in consumables:* The diffusible hydrogen levels were already considered to be effectively in the low-hydrogen range, and a further reduction, particularly if the likely site and storage conditions were taken into account, was thought to be impractical.

2. *Use higher preheat levels to reduce weld and heat-affected-zone (HAZ) hardnesses:* The 250°C preheat used for the process was based on metallurgical assessment of the HAZ. An increase in preheat was possible but would affect the cost benefits attributed to the process (see Appendix A).

3. *Use weld metal of lower hardenability and higher toughness:* Examination of the defective repairs showed that the weld metal was considerably harder and more brittle than the laboratory work had revealed. Subsequent chemical analysis showed that the weld metal did not comply with the agreed composition range (see Table 5, Batch 41205). Of particular note were the high aluminum and manganese levels.

Following discussion with the manufacturer, two reels of wire with lower carbon, manganese, chromium, and aluminum



FIGURE 21 Photomicrograph of transverse cracks associated with a brittle martensitic weld metal.

levels were supplied, and a further site trial on the research test track was arranged to evaluate weld metal chemistry and preheat.

The work showed that increasing preheat temperatures from 250° to 350°C (the level currently used for MMA repairs) had

no significant effect on the incidence of cracking. However, using the lower-alloy consumable (see Table 5), crack-free welds were produced, confirming the susceptibility of more highly alloyed weld metals to the problem of cracking.

The "modified" wire was subsequently subjected to the full laboratory assessment, apart from the diffusible hydrogen determination and fatigue tests. The results are summarized in Table 10 with comparative data from the original experimental batch. The results of the deformation tests are included in Figure 19. It can be seen that the modified weld metal was still more resistant to deformation than the parent rail steel and the equivalent MMA repair weld metal.

A formal specification was prepared limiting the composition of the wire (Table 5), and a batch of 21 reels was ordered. Sample reels were used to produce test pads for chemical analysis. The results are shown in Figure 22. The data show that half the batch exceeded the agreed range; consequently all reels above number 11 were rejected.

As of 1987, site trials with the revised-specification Cr/Mn wire have been mainly crack free. Of the 130 repairs being monitored, only 3 have been found to be cracked, one of which was a repair of a previously cracked deposit. The Western Region has had extensive numbers of repairs using both "high specification" and "revised" batches of wire and has reported no problems. A random sample of 100 repairs on the highrail was examined by the Research Division, and only one showed any evidence of cracking.

Manufacturers of wire have been contacted for possible consumables. The most promising to date is a 1.6-mm Cr/Mn/Ni wire that has been used on Swiss National Railways with apparent success (14, 15).

Cr/Mn/Ni Flux-Cored Wire

The wire used on Swiss National Railways is 2.4 mm in diameter and is used with portable dc welding machines of

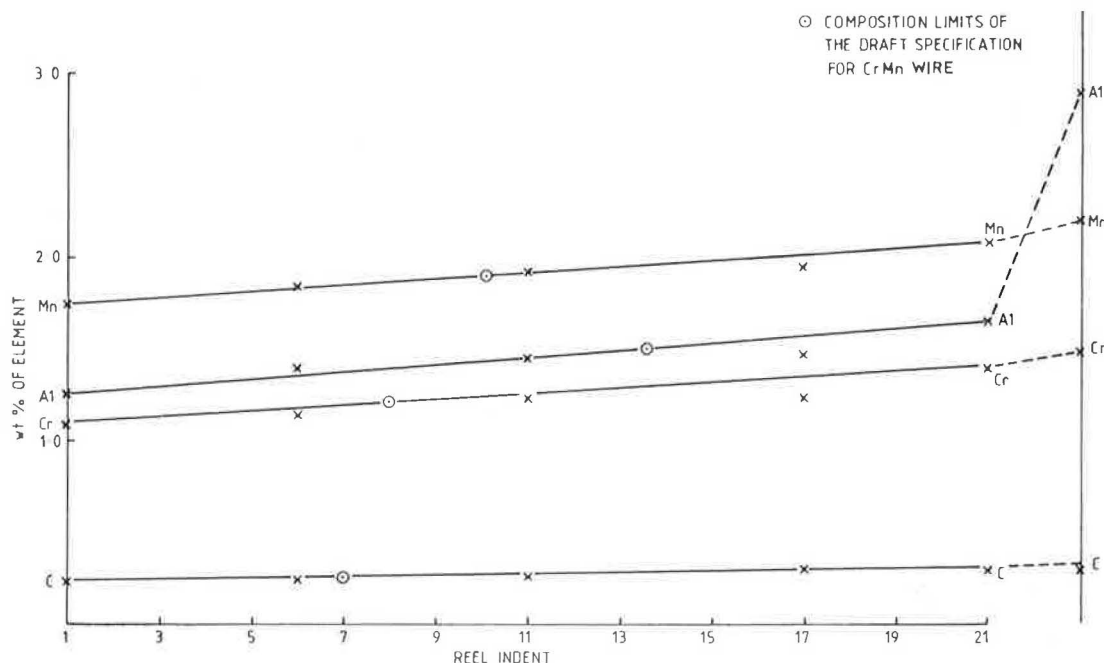


FIGURE 22 Variation in weld metal composition through a batch of Cr/Mn wire (21 reels).

TABLE 10 TEST DATA FOR CR/MN AND CR/MN/NI FLUX-CORED WIRES

	MODIFIED Cr/Mn	Cr/Mn/Ni	ORIGINAL Cr/Mn (BR-EXP)
Undiluted Weld Composition (wt%)			
C	0.25	0.15	0.27
Si	0.15	0.27	0.16
Mn	1.86	1.12	1.83
S	0.003	0.004	-
P	0.13	0.021	-
Ni	0.05	2.31	0.07
Cr	1.23	0.81	1.18
Mo	0.01	0.48	0.14
Al	1.4	1.52	2.7
U.T.S (N/mm)	1000	1001	870
Y.P. (N/mm)	682	737	623
% ELONG	11	14.0	25
Hardness (Hv30) (mean)	<u>311-328</u> 319	<u>298-321</u> 308	<u>310-340</u> 315
Impact (Joules)			
-15°C	8	8.2	12.0
0°C	10	10.5	12.0
+23°C	12.6	14.5	18.0
+50°C	15.6	20.1	-
Deformation (%) for 1000 impacts			
Impact Force (kN)			
125	17.5 - 18.5	1.9	3.5 - 4.2
150	15 - 26	32	12.5 - 20
175	31.5 - 33	35	37.5 - 38.5

300-A capacity (220 A dc at 100 percent duty cycle). Samples of the wire were subsequently drawn down to 1.6 mm-diameter for laboratory assessment using the evaluation program described earlier. The results of the laboratory work are given in Table 10. The microstructure of the undiluted weld metal was found to be similar to the MMA weld metal produced using kV3L electrodes (see Figure 23).

Following the laboratory work, an extensive site trial of the wire was carried out in the London Midland Region, where more than 40 repairs of wheelburns have been installed. To date, none of these repairs has shown any evidence of cracking.

COST BENEFITS

As previously stated, semiautomatic welding using continuous wire has been demonstrated to be a high-productivity process compared with MMA welding. During the early stages of development, the Research Division undertook a cost analysis for possible application.

Repairs to Wheelburns

An initial laboratory assessment of the relative costs of the two options for the repair of wheelburns was achieved by welding prepared excavations in a length of normal-quality rail (see Figure 24). The comparison demonstrated that the track occupation time could be halved using semiautomatic welding, and the direct cost (i.e., materials and labor) was also reduced.

A more extensive cost analysis for plain line repairs was undertaken for the London Midland Region (see Appendix A). It can be seen that the main time saving is achieved by the increased size of the individual weld beads. Overall a time saving of 149 min (59 percent) was achieved by using the semiautomatic welding process, and the unit cost of deposited weld metal was almost halved.

Maintenance Welding of Crossings

The potential cost savings for welding crossings are more difficult to derive. The cost analysis shown in Appendix A

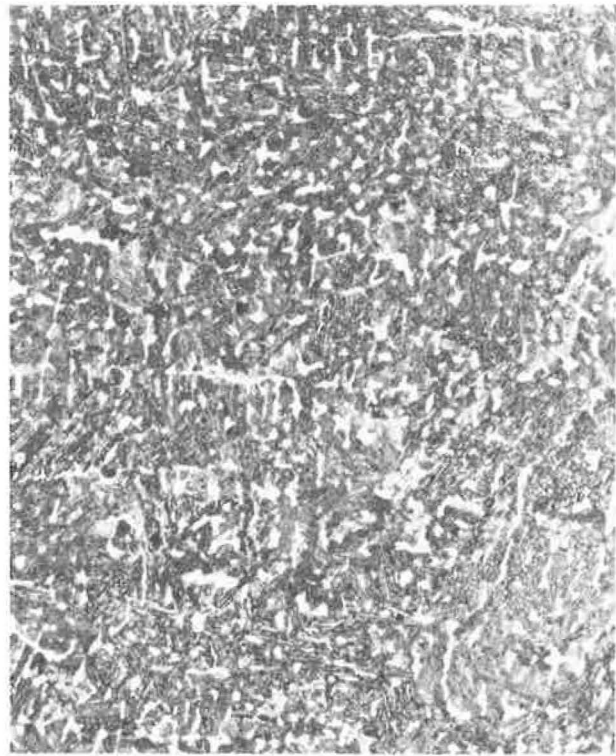
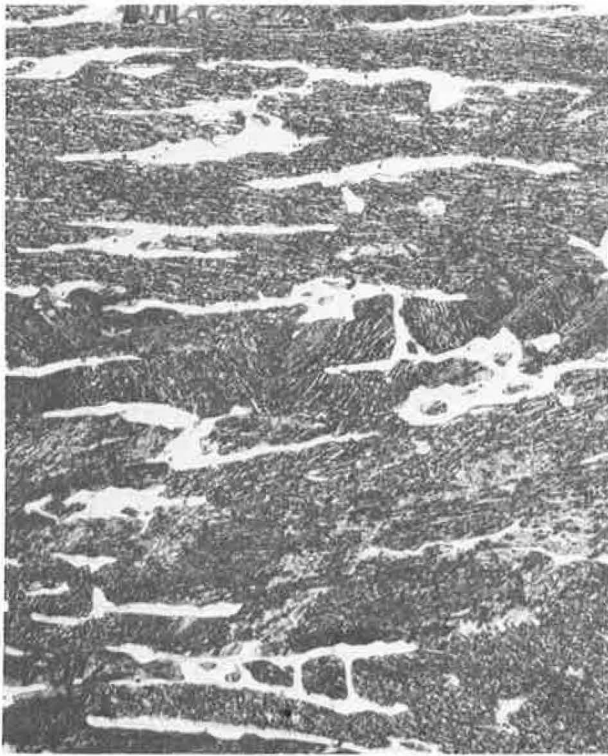
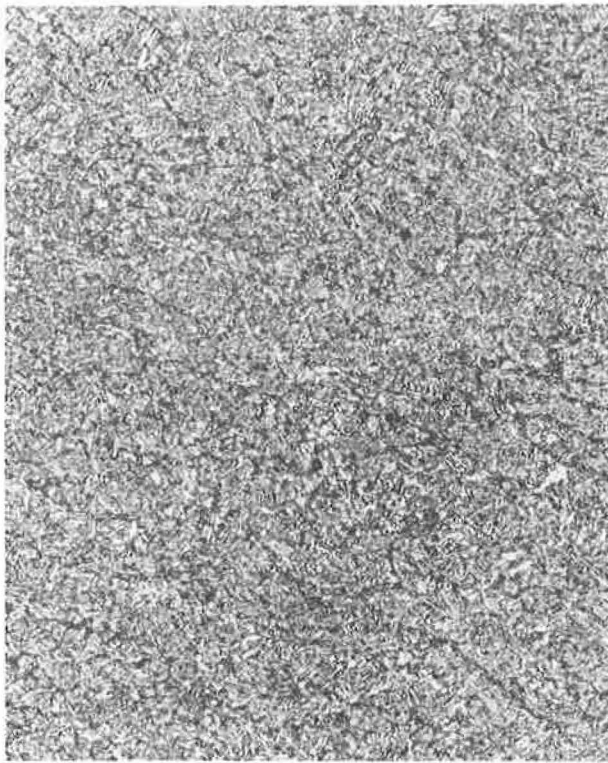


FIGURE 23 Photomicrographs of undiluted MMA and flux-cored wire weld metals ($\times 149$). *Top left:* Phillips kV3L; *top right:* Cr/Mn/Ni wire; *lower left:* original Cr/Mn wire; *lower right:* modified Cr/Mn wire.

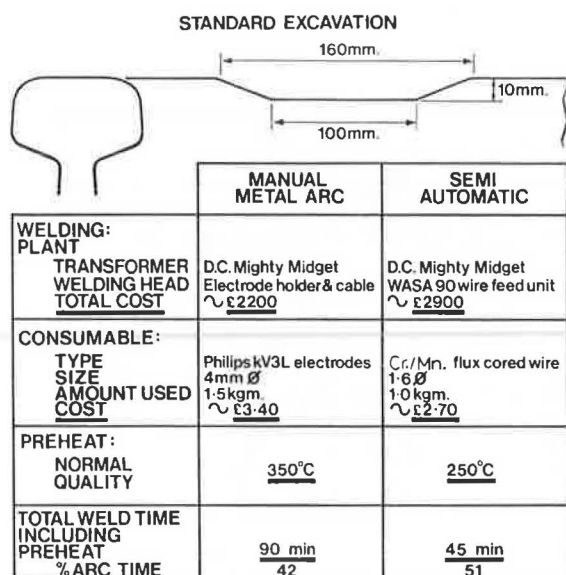


FIGURE 24 Comparison of MMA and semiautomatic repair to simulated wheelburn excavation.

demonstrates that a typical MMA repair would take approximately two shifts if both the nose and wings were to be repaired. A comparable semiautomatic repair should be accommodated within one shift.

The number of crossings in track in September 1984 was as follows:

Track Category	Track Miles	S & C Miles	Crossings	Crossings per Mile
A	2,220	79	2,370	1.07
B	6,339	264	7,920	1.25
C	8,559	330	9,900	1.16
D	4,001	397	11,910	2.98
			32,100	

Assume that the frequency of weld repair of these crossings is as follows:

Line Category	Months Between Repairs
A	9
B	12
C	18
D	None

The total number of repairs required per annum is calculated as follows:

Category A: $2,370 \times 12/9 = 3,160$;
 Category B: $7,920 \times 12/12 = 7,920$;
 Category C: $9,900 \times 12/18 = 6,600$;
 Total = 17,680 repairs/annum.

Thus the use of semiautomatic welding in place of MMA welding for the build-up repair of crossings could result in the following saving:

$17,680 \times (\text{MMA cost} - \text{semiautomatic cost}) = 17,680 \times (£305 - £162.50)$ (see Appendix A) = £2.5 million per annum.

As explained in Appendix A, the repair of a crossing using MMA welding can take two working shifts as opposed to one when the semiautomatic process is used. Therefore, assuming that the commitment to crossing repair is not increased, approximately 17,500 working periods will be released for plain line repairs without a change in the current maintenance budget.

Investment

The saving could only be achieved if investment were made in the purchase of the new equipment. It is proposed that approximately 240 welders be trained for semiautomatic welding, and on the basis of the current commitment to the welding of crossings (both maintenance welding and repair welding) approximately 24,000 welds may be required per annum, equivalent to approximately 120/day. Therefore the final investment in welding sets could be between £130 and £250 (including spare units). The British Railways Board has undertaken to purchase 120 sets, with either ac/dc converters or dc welding machines. The remaining sets are to be funded out of the regional investment budget.

Assuming an initial purchase of 130 units, two options are available (based on 1983 prices):

- 130 wire feed units at £750/unit = £97,500 + 130 ac/dc converters at £250/unit = £32,500 + spares (£1,000) = £131,000.
- 130 dc power supplies at £1,250/unit = £162,500 + 130 wire feed units at £750/unit = £97,500 + spares (£3,000) = £263,000.

Based on a 5-year writeoff period and the current crossing repair commitment, the nondiscounted cost/repair per option is as follows:

Option 1:

$$\frac{131,000}{24,000 \times 5} = £1.1/\text{repair}$$

Option 2:

$$\frac{263,000}{24,000 \times 5} = £2.2/\text{repair}.$$

In practice the cost/repair amount should be much less, because a greater number of repairs per annum should be expected.

CONCLUDING COMMENTS

It can be seen that equipment development is now almost complete, equipment specifications having been formulated. Current work is centered around the development of wires and procedures to further reduce the possibility of delayed cracking.

The most significant element in the wire is thought to be aluminum, which is introduced as the primary deoxidant. It is

known to have a deleterious effect on toughness because of the formation of aluminum-based inclusions, but it appears that a reduction in aluminum does not, in itself, result in an improvement in toughness (see Table 10). Indeed, ductility and toughness are reduced, whereas the strength is increased. This is probably due to the reduction in the volume fraction of delta ferrite in the weld metal. Most wire manufacturers recommend a minimum aluminum level of approximately 1.5 percent, below which the weldability deteriorates and weld metal contamination with oxygen and nitrogen starts to occur. Any change in the aluminum content affects the recovery of other reactive elements (Cr, Mn, C). Hence this interactive effect of aluminum has to be taken into account when modifications to the wire are considered. The current BR specification limits the aluminum level to between 1.3 and 1.5 percent.

An added complication is that the cracking problem is only prevalent in single- or double-layer deposits, when the weld metal is highly diluted with the parent material. This condition is commonly generated when shallow defects such as wheelburns are repaired. The Cr/Mn-based wires now have a specification that is thought to be the minimum alloy level for acceptable hardness. However, the cracking problem still occurs, albeit at a much reduced level. Current development is based on the use of Cr/Mo/Ni wires, which, although having similar strength and hardness to the Cr/Mn types, show a slight improvement in toughness.

As explained earlier, resistance to deformation is a major requirement of weld metals for repairing crossings. Consequently a simple flow-under-impact machine has been developed to enable the comparison of different materials. The test has one deficiency: with large deformations there is a tendency for bulk collapse or "bulging" of the specimen, for example, against surface flow. Therefore an experiment is being undertaken to investigate lower-impact forces (resulting in less deformation). In addition, crossings repaired with either Cr/Mn or Cr/Mo/Ni deposits (with MMA repairs as a control) are being monitored in service to assess the deformation of the repair.

Should the trials show that the "crack-resistant" weld metals are too soft, consideration will be given to reverting to the original formulations and amending the preheat procedure to reduce the hardenability of the deposit.

A large number of semiautomatic wheelburn repairs are now being monitored in track by the Research Division to assess their susceptibility to cracking and their wear resistance. Several brands of wire are being studied. The weld metals containing nickel appear to be the most crack resistant and also display a finer-grained acicular bainitic microstructure with less delta ferrite than the plain Cr/Mn types. Laboratory trials are about to start with a Cr/Mo/Ni wire that has an undiluted hardness of 330 to 350 Hv and an aluminum content less than 1.2 percent. If the trials are successful, this wire will be considered for use on wear-resisting rails (including 110 kg/mm² Cr grade).

ACKNOWLEDGMENTS

The author wishes to acknowledge the assistance of his colleagues, particularly W. A. Mosley and J. T. Davison, for their assistance in the preparation of this paper and the Directors of

Civil Engineering and Research for their permission to publish this paper.

REFERENCES

1. P. Clayton et al. Surface Damage of Rails. Presented at the Rail Technology Seminar, Nottingham, England, 1987.
2. *Hard Surfacing of Crossings*. BR Research Division Report SM 208. British Railways Board, London, England, April 1967.
3. *BR Research Division Report MM/19*. British Railways Board, London, England, Feb. 1971.
4. *BR Research Division Reports R68/46, R69/97, and R 7072*. British Railways Board, London, England, Sept. 1965, Nov. 1969, April 1970.
5. *BR Research Division Reports R7/37, R72/J, and R73/6*. British Railways Board, London, England, May 1971, Feb. 1972, Feb. 1973.
6. D. Ward. *Evaluation of Welding Electrodes for Resurfacing Worn Rails and Crossings*. BR Research Division Report TN FM69. British Railways Board, London, England, July 1975.
7. D. Ward. *Repair of Wheelburnt Rails by Welding*. Research Division Report TN FM74. British Railways Board, London, England, March 1977.
8. *BR Research Division Reports R68/28 and R69/28*. British Railways Board, London, England, June 1968, March 1969.
9. G. Durbin. *Evaluation of the "Teromatic" Process for Building Up Worn Rail and Crossing Components*. BR Research Division Report TM MET38. British Railways Board, London, England, May 1979.
10. T. L. Brooks. *Evaluation of Eutectic A3110 Wire*. BR Research Division Report TM MET74. British Railways Board, London, England, Dec. 1980.
11. J. T. Davison. *Evaluation of Corewire Ltd. CS41 Self-Shielding Flux-Cored Wire for the Weld Repair of Rail and Crossing Components*. BR Research Division Report TM MF102. British Railways Board, London, England, May 1985.
12. BS 639 *Covered Electrodes for the Manual Metal Arc Welding of Carbon Manganese Steels*. BS 639. British Standards Institution, Linford Wood, Milton Keynes, England, 1976.
13. W. A. Mosley. *Comparison of 2.1/4 Cr/1 Mo MMA Electrodes for the Repair of BS 11 Normal Quality Rail*. BR Research Division Report (to be published).
14. P. Lazco. *Use of Flux-Cored Wires for Repair Welding*. Mt. Newman Mining Co. Pty Ltd., May 1985.
15. *Provisional Guidelines 227 41* (appendix concerning welding work in the track). Civil Engineering Department, Swiss Federal Railways, Berne, Switzerland, April 1962.

APPENDIX A

Analysis of Costs Comparing Conventional MMA with Semiautomatic Repair Techniques

REPAIR OF PLAIN LINE DEFECTS

A limited site trial has been performed with the semiautomatic process to enable a comparison to be drawn with the MMA process. The trial took place at Didcot West Curve (Western Region), where a large number of isolated wheelburns were present. Two similarly sized defects were excavated by grinding to give similarly shaped and sized preparations 550 mm long, 45 mm wide, and 5 mm deep. The whole operation was

TABLE 11 COMPARATIVE TIMES FOR WHEELBURN REPAIRS

Characteristic	Welding Process	
	Manual Metal Arc	Semiautomatic
Type of electrode/wire	Dymal-2 coated electrode	Corewire CS41BR flux-cored wire
Diameter of electrode/wire (mm)	4.0	1.6
No. of weld layers	2	1
No. of weld runs		
First layer	15	5
Second layer	6	
Preheat temperature (°C)	350	250
Repair time (min)		
First layer		
Electrode drying	60	
Preparation	23	17
Preheating	15	6
Preheating	24	6
Welding	35	25
Grinding	5	18
Dye penetrant testing	30	30
Second layer		
Preparation	0	
Preheating	14	
Preheating	4	
Welding	14	
Grinding	20	
Dye penetrant testing	30	
Total (hr/min)	4/11	1/42

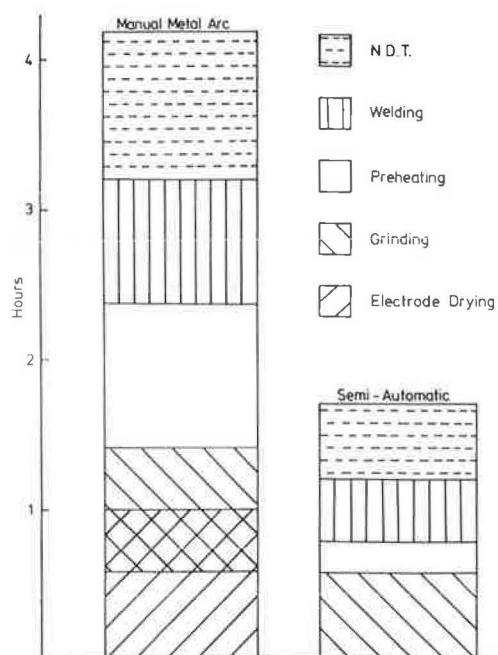


FIGURE 25 Comparison of times for wheelburn repairs.

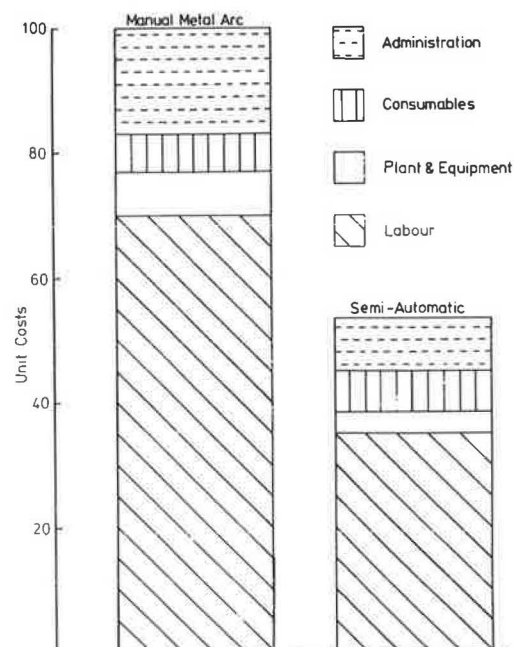


FIGURE 26 Comparison of costs for track repairs per unit volume of deposited weld metal.

timed, and a breakdown is given in Table 11. The times are also presented as a bar chart (Figure 25) and converted to costs per unit volume of weld metal (Figure 26). This conversion is based on the information presented in the next section of this appendix.

REPAIR OF CROSSINGS

The maintenance welding of crossings takes place during weekdays; welders work four 7.5-hr shifts. The 10-hr weekend shift is normally reserved for new installations.

The following times for the MMA maintenance welding of crossings have been estimated to fit in with a 7.5-hr shift. The times are based on discussions with a number of CCE welding teams and observations of MMA repairs being carried out on site and in the laboratory.

1. Traveling to site and unloading equipment, 1.5 hr;
2. Drying electrodes, 1 hr;
3. Grind crossing, 0.25 hr;
4. NDT crossing, 0.25 hr;
5. Preheating and interrun heating, 0.5 hr;
6. Welding, 2.25 hr;
7. NDT crossing, 0.25 hr;
8. Final grinding, 0.5 hr; and
9. Loading equipment and traveling to base, 1.5 hr.

Total time is 8 hr. In practice, operations 3 and 4 are carried out during operation 2, thus saving 0.5 hr and making the total time 7.5 hr.

Semiautomatic welding can save 0.5 hr by eliminating operation 2 and 0.25 hr by reducing the temperature to be attained and maintained in operation 5. Thus, the time saved can be used in operation 6, extending it to 3 hr.

The total amount of weld metal that can be deposited in one shift can be calculated as shown in Table 12.

TABLE 12 CALCULATION OF AMOUNT OF WELD METAL DEPOSITED IN ONE SHIFT

Item	Welding Process	
	Manual Metal Arc	Semiautomatic
Welding time in 7.5-hr shift (hr)	2.25	3
Arcing time		
Percent of welding time (measured in laboratory trials)	40	50
Hours	1	1.5
Deposition rate ^a (kg/hr)	1	2.35
Total amount of weld metal deposited in one shift ^b (kg)	1	3.5

^aWelding Institute Standard Data.

^bArcing time in hours times deposition rate.

Assuming that a typical repair of a 1 in 9.1/4 crossing requires 1 kg of weld metal depositing on the crossing nose and 1 kg on the wing rails,

1. With MMA welding only the crossing nose can be repaired in one shift. Two shifts are required to repair the whole crossing.

2. With semiautomatic welding both the crossing nose and the wing rails can be repaired in one shift.

ESTIMATED COSTS

Using a 1981 cost breakdown by the BR Department of Civil Engineering Welding Assistant, the costs shown in Table 13 were estimated for the repair of one crossing unit. A saving of £142.50 per repair is therefore evident.

TABLE 13 COSTS FOR REPAIR OF ONE CROSSING UNIT

Item	Welding Process	
	Manual Metal Arc	Semiautomatic
Labor		
Welders (2) at £37.50 per day	150	75
Look-out at £27.50 per day	50	27.50
	205	102.50
Plant and equipment at £10 per day	20	10
Consumables (electrodes, diesel, fuel-gas, etc.)	30	25
Incidentals (supervision, assistance, administration, etc.) at £25 per day	50	25
	305	162.50

NOTE: Costs are given in 1981 pounds.

APPENDIX B

General Specification for Semiautomatic Wire Feed Units

1. To feed 1.2-, 1.6-, and 2.0-mm diameter flux-cored wires for welding at a current range of 150 to 250 A.

2. To operate from open circuit and welding voltages of drooping characteristic welding sets on both fully rectified alternating and direct current. Typical voltages are open circuit, 70 to 120 V; welding, 20 to 30 V.

3. To carry a 300-mm o.d. wire spool.

4. To weigh less than 20 kg without wire spool.

5. To be supplied complete with a minimum 3-m-long hose and air-cooled welding torch.

6. To be supplied with wire inch controls at both the wire feed unit and welding torch.

7. To have wire feed speed control independent of the welding current.

8. To be supplied complete with protective covers to prevent entry of moisture.

Examination of Methods To Achieve Rail Lubrication

DOUGLAS B. THARP

A description is presented of the methods to apply a lubricant to rail to reduce train resistance, wheel flange wear, and rail wear. The advantages and disadvantages of application methods are discussed, as well as the characteristics of an ideal lubricant.

Applying some form of lubricant to improve the frictional characteristics of steel on steel has been popular since the invention of steel itself. Often this lubricant was applied as much for protection from corrosion as for reduction of friction between sliding surfaces. As a matter of interest, the use of journal bearings in the railroad industry inadvertently provided lubrication to the rail in the form of leakage from the journal box. The buildup of oil from this leakage became so much of a problem that laboratories of various railroads conducted elaborate experiments to determine the most practical method to remove the excess oil and grease from the rails and minimize resultant wheel slippage. The subsequent widespread use of roller bearings eliminated the dripping lubricant. Technology proved the old adage, "ignore a problem and eventually it will go away." Ironically, a great deal of time and effort is now being expended to put grease back on the rail to save energy and wheel and rail wear.

As wheel loadings increased because of heavier and improved car designs, it was not long until it became evident that the rail heads in curves wore much more rapidly. An obvious solution was to turn the high rail of the curve or to exchange the high rail for the low rail. Another obvious solution was to increase the hardness (and wear resistance) by using premium steels in curves. An eventual solution was to apply lubricant to the track to minimize the friction in curves where the forces were the greatest. The application of oil or grease for this purpose was the only benefit that the railroads considered.

Almost by accident, in 1983 the Transportation Test Center (TTC) discovered that trains operating over lubricated sections of track consistently used less fuel than when operating over unlubricated sections of track. An estimate of 30 percent savings literally staggered industry officials at a time when the cost of fuel was escalating rapidly and a great deal of effort was being used to save 1 to 2 percent on the efficiency of a locomotive engine or compressor. Even though terms like "skepticism" and "real world" permeated the discussions of those directly involved, the facts could not be ignored. As a result, a locomotive-mounted lubricating system was born and has since risen in popularity on U.S. railroads. Consolidated

Rail Corporation (Conrail) was one of the first railroads to recognize the tremendous energy-saving potential of this technology and subsequently conduct an extensive series of tests.

LUBRICATION METHODS

Initially, the main purpose of rail lubrication was to reduce severe cases of wheel flange wear and to protect highly curved track from extreme rail gage wear on the high rail. The first major undertaking to solve this severe wear problem was to install "curve oilers" along the wayside. The frequency of this equipment installation was based largely on the number of degrees of central angle in a particular set of curves. One railroad uses "curve units" (each unit is equivalent to 1 ft of a 1-degree curve) as the criteria for locating their lubricators. The strategically placed wayside oilers produced the desired effect of reducing rail wear, but additional problems developed. The large number of individual locations of wayside lubricators required replenishment of lubricant on a periodic, but often different schedule because of variations in application rates. Often, overlubrication caused by temperature variation and equipment adjustment led to wheel slippage on ascending or descending grades. In other cases, underlubrication resulted from placing the lubricator at the wrong location in the spiral or using the wrong lubricant. In addition, maintenance of the equipment was complicated by poor weather, need for seasonal adjustment, and many minor features that made wayside equipment less than perfect. The problems were often so great that one employee per railroad division was designated exclusively to fill and maintain the lubricators. Other considerations in the evaluation of the use of wayside equipment include

- The maximum number of application points to provide coverage throughout the curve and associated spiral;
- Advantages and disadvantages of lubricating the low rail;
- Limitations to the ability to distribute state-of-the-art wayside lubricants because of the maximum quantity that can be applied at the oiler without risking contamination onto the rail head while spreading it longitudinally; and
- Influence of lubricant qualities that permit achieving a dispersed film thickness that will provide adequate lubrication.

Extensive research continues into the use of wayside lubrication. The new-generation lubricator is electronically controlled to regulate the flow of grease, handle variations of speed, sense train direction, and maximize the distribution of lubricant with an improved wiping bar. The potential also

exists to limit the lubrication output through a centralized control system.

In the early 1980s, major railroads began looking for a means to replace or supplement the wayside systems with some type of "on train" or "on track" system. The more publicized of these was a boxcar-mounted system that sensed curves and sprayed grease on the gage side of the high rail. At a time when a great deal of effort was being spent to eliminate the cabooses, it did not appear practical to add another car to a train, with the resultant switching, operating, and maintenance costs. An absence of savings in the wear rates of locomotive wheel flanges was an additional disadvantage. As a matter of interest, the reduction in locomotive wheel wear rates was the precise and only reason that lubrication was added to locomotives on European railroads.

Another method that was tried and tested was the use of a hi-rail vehicle to lubricate either rail while track inspections were being performed. Hi-rail (non-train-mounted mobile) systems must apply an amount of grease that will be adequate until the next available application cycle. This often causes overlubrication just following application and very little lubrication just before the next cycle. In concept, this system works well in medium-density lines, but it is not as effective with heavy traffic because the hi-rail vehicles interfere with train operations. Its effectiveness on low-density lines is also reduced, because of the lack of trains to benefit from the lubricant before it deteriorates. Two commercially available hi-rail vehicles were deemed appropriate for applications and cost-effective.

The potential energy savings available caused most Class I railroads to focus on on-board lubrication. Several types of locomotive-mounted hardware are available that transfer some type of lubricant (oil or grease) from a nozzle or roller directly to the wheel flanges of locomotives. From a hardware standpoint, the following factors must be considered:

- Operation environment,
- Installation cost,
- Frequency of application,
- Reservoir type and size,
- Grease replenishment,
- Maintenance,
- Crew acceptance,
- Curve sensing capability, and
- Purchase price.

When Conrail made a commitment to equip its road locomotives, the selection of hardware was limited. Flange lubricators developed and used in Europe were investigated, because they had been used for many years to prevent wheel climbs and reduce locomotive wheel flange wear. In spring 1984, two Willy Vogel wheel flange lubrication systems were procured. The available "timer" type control was replaced with a Conrail-designed distance-measuring control circuit to activate the lubricators. These two systems were installed on General Motors Electromotive Division SD50 and SD40-2 locomotives. The spray nozzles were mounted to lubricate the leading axle of each locomotive, regardless of operating direction. Over-the-road tests were then conducted to determine whether fuel savings could be detected in typical railroad

service. The initial tests were conducted in central Pennsylvania with a unit coal train. The encouraging results led to a second series of tests between New Jersey and Illinois in high speed piggyback freight service. Unavoidable variations in train configuration and speed profiles made the results of these tests statistically contestable.

Nevertheless, in all of the tests conducted by the Conrail Technical Services Laboratory, the use of on-board lubrication produced an energy savings. These positive results were obtained regardless of problems encountered with lubrication rates, grease type, system reliability, crew variance, train weight differences, train type, or geographical considerations. On the basis of these indications, a corporate decision was made to equip 120 road locomotives with on-board systems and enjoy the inherent fuel savings until a more precise series of tests could be conducted to improve the accuracy of the savings estimation.

A third series of tests was specifically designed and conducted to determine how much fuel would be saved if the entire locomotive fleet were equipped with on-board lubrication. This test series was conducted between Albany, New York, and Boston, Massachusetts, with a dedicated test train consisting of 18 open-top hoppers loaded with stone ballast and instrumented to record test parameters on Conrail's research car. Test results, when transferred to a mathematical model of the entire Conrail system, indicated that the potential savings would approximate a 7 percent reduction in the amount of energy required to power Conrail trains.

Existing on-board systems are highly flexible, but they may have lubricant volumetric limitations that will require dispersal of lubrication points throughout a very long train. Limitations seem to be maximum grease line length or pumping pressure available, or both. A need to find better lubricants is evident. The potential to vary spray or discharge frequency may help solve the need to apply more lubricant in curves than on tangent track to achieve the desired benefit. Research in this field is also progressing at a very rapid rate. There are now six manufacturers of hardware conducting research to provide the optimum product for railroad use. In addition, a number of Class I railroads are in the process of conducting involved tests to evaluate hardware and the optimum lubricant. Equally important is the necessity to accurately determine the potential cost benefits.

LUBRICANTS

Petroleum and mineral oils have been used for centuries as a means of reducing the friction between sliding and rolling steel (iron) surfaces. Late in the last century, grease, which is an oil thickened by the addition of soaps (the salts of fatty acids) was introduced. The intent of such thickening was to lessen the tendency of the oil to flow. In other words, the grease had to stay where it was needed. The primary user of such materials was the steel industry, which needed to lubricate the bearings in hot rolls or other machinery.

The last several decades have brought improvements in the ability to resist flow (loss) due to temperature, wash-off from water (used extensively in steel mills), and tackiness or cling. All such improvements, normally attributed to the soaps

(calcium, sodium, lithium, and to some extent boron), have raised the useful temperature and reduced the tendency to wash off.

In recent years, other additives, such as graphite, lead, molybdenum disulfide, and Teflon, have been used to improve the ability of grease to resist higher pressures. In other words, these additives are necessary to resist squeeze-out and provide some greater ability to prevent scuffing or scoring.

All such improvements increase cost but will, it is hoped, provide the surface protection that has always been the major way to reduce friction. There is no question that the type of grease selected for any hardware is the "secret ingredient" that will maximize the resulting savings. The following are considered the characteristics of a good wheel flange lubricant:

1. Transferability by wiping from wheel to rail to maximize dispersal throughout the train;
2. Sufficient tackiness to resist fling-off;
3. Low-viscosity change with a change in temperature to stay on a hot wheel and remain pumpable;
4. Resistance to washing off by rain;
5. Resistance to bleed (i.e., separation of soap or additives) due to pressure, temperature, and long periods of storage;
6. Resistance to aeration during pumping action from the reservoir to the nozzle;
7. Environmental safety;
8. Finely milled constituents to be compatible with the close tolerance of machined parts found in most dispensing nozzles;
9. Cost-effectiveness to achieve maximum benefits; and
10. Distinguishable features to determine, from a test standpoint, the dispersal through the entire train.

Development of the characteristics is left to the grease manufacturers. Present laboratory testing methods are limited in duplicating the railroad environment, but newer and better

testing methods are being developed along with new qualification tests. The final choice will be based on individual field demonstration results because of geographic differences in weather or environmental conditions on the various user railroads.

CONCLUSION

Conrail currently has approximately 1,500 wayside lubricators covering 13,700 route miles. Approximately 80 percent of the 68.7 billion ton-miles of freight carried by Conrail in 1986 was accomplished with 600 locomotives applying 0.05 cm³ of grease every 25 wheel revolutions. Wayside lubricators are used in areas of high curvature and placed on tangent track before the spiral. Route-specific location decisions are made by Division Engineers on the basis of their experience and wear patterns for a particular curve. These criteria will undoubtedly change with design changes in the new generation of lubricators. The precise location, nozzle size, frequency of application, and amount of each spray for locomotive-mounted lubricators continue in the experimental stage. It can readily be seen that the use of lubrication to reduce the maintenance and resulting cost of minimizing delays to revenue trains is more of an art than it is a science. When hardware decisions are made, the single most important element—the grease itself—is still very much in the developmental stage.

At this time, Conrail is in the process of preparing test plans to evaluate the effects of various greases used in both wayside and on-board lubricators. It is Conrail's belief that the grease currently being used with on-board lubrication does not persist throughout the length of a normal train. Therefore, the potential savings available are not being fully used. The use of the correct lubricant is the bottom line in advancing this technology to a point at which the entire industry can maximize the savings of energy, wheel wear, and rail wear and reduce the number of derailments. This technological improvement, along with continued research on all types of lubrication, will improve the competitive posture of the railroad industry.

Report from FAST—Recent Test Experiences

R. P. REIFF

Recent results from accelerated rail testing performed at the Transportation Test Center are reviewed. This includes rail wear and rail fatigue experiments. Results are from full-scale field tests performed at the Facility for Accelerated Service Testing (FAST). These data represent performance under fully loaded hopper cars of 130 tons each load on the rail. Wear information for standard, alloy, and head-hardened rails under dry conditions is presented. The data allow curve wear life comparisons to be made for rails with differing chemistry and manufactured by different processes. Rail life was extended by reduction of wear through the use of lubrication to evaluate fatigue resistance. In this evaluation program, different lubrication levels were maintained to demonstrate the effect of various wear rates on defect occurrence and growth. Eliminating rail wear increased the defect rate significantly. Rail of higher hardness, in the range of 300 BHN and higher, offered an improvement over softer rails in fatigue resistance.

The Facility for Accelerated Service Testing (FAST) is located at the Transportation Test Center (TTC) near Pueblo, Colorado. The FAST program generates wear and fatigue information on railroad components through the operation of a 9,800-ton train made up of conventional cars and locomotives. The FAST track has been in operation since late 1976, with total applied tonnage to date exceeding 950 million gross tons (MGT). In 1985 the main FAST loop was shortened from 4.78 mi to just over 2.77 mi in an effort to increase the rate of applying tonnage for a given amount of train operation. This increases the MGT application rate in support of track-related tests. The new loop, which incorporates portions of the original FAST loop, is designated the High Tonnage Loop (HTL), as shown in Figure 1.

Rail tests have played a primary role in all FAST/HTL operations. Early tests were aimed at monitoring and reporting basic rail wear information (1). To aid in obtaining wear information, the FAST program has developed a number of improved measurement tools that increase the accuracy and efficiency of these tests. As the data base of rail wear information increased, other rail testing programs, including rail profile grinding and fatigue testing, were incorporated into the program (2).

Currently, two major rail-oriented tests are being conducted. These tests are aimed at monitoring rail wear and fatigue under fully lubricated and dry conditions. This paper will address recent developments from these two tests, as well as review the measurement policies and other controls incorporated into the project.

CURRENT TESTS

The final configuration selected for the HTL was in part to satisfy requirements of the defect occurrence and growth (DOG) test, and allow continued monitoring of the rail wear and fatigue (RWF) test, which is to be operated under dry conditions.

DOG Test

As the name suggests, in the DOG test rail life is examined for defect occurrences; when defects are located, the growth rate of each is determined. The defect occurrence rate is controlled in part by different types of rail quality and different levels of lubrication. The test train direction is controlled so that lubrication, which is applied by a trackside lubricator, will always be significantly greater in one area of the loop and less in another area. Figure 2 provides details of the HTL loop along with the locations of the wayside lubricators. The wear and fatigue of nearly identical test rails located in these areas are monitored for a 150-MGT period.

RWF Test

The RWF test obtains similar information, but rail life is generally limited by wear instead of fatigue. Items such as low-rail crushing and high-rail spalling are observed and documented.

USE OF DATA

With the increase in the number of railroads using or improving their lubrication programs, the replacement criteria for rails may not always be a function of wear. At locations where rail wear is a critical factor, the use of lubrication can extend the service life considerably. By examining FAST tests and comparing them with various locations in revenue service, the data obtained can be used to assist in selecting proper rails to best fit a particular situation.

LUBRICATION

Background

Before examination of the detailed wear and fatigue results, a brief review of the lubrication controls and methods is needed. Lubrication has been shown to be the single most influential item that can be used to increase rail life (3). Wear at the gage

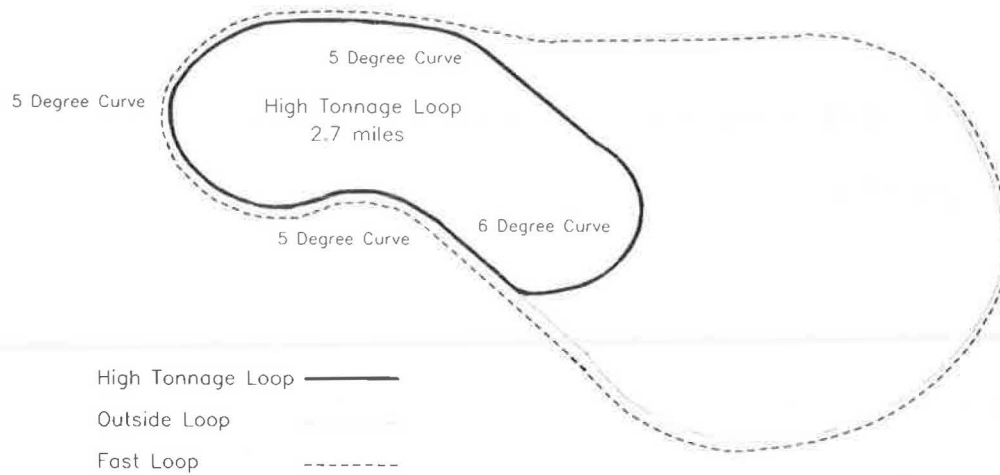


FIGURE 1 FAST loop with HTL layout.

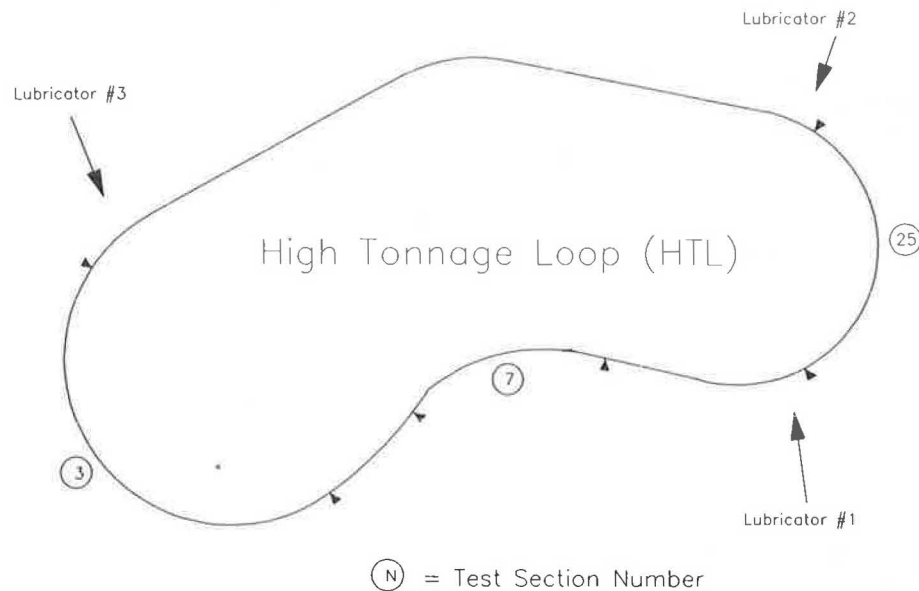


FIGURE 2 HTL loop showing lubricator locations.

face of standard carbon rail can be decreased by a factor of over 80 times by use of lubrication. (A more detailed explanation can be found in a later section of this paper.) A number of lubrication studies have been performed or are in progress to document various methods of lubrication control and application (4, 5).

Control of Wear

During the third rail experiment at FAST, lubrication was used to control the life of test wheels during evaluation of premium trucks. Full rail lubrication was maintained for periods of 40 MGT, followed by 10- to 15-MGT periods of dry operation. The dry periods were operated to allow accelerated wheel wear under controlled conditions. Thus, a 50-MGT block of operation was created and repeated five times for a 250-MGT test period (2). The results indicated significant savings in rail wear during periods of lubrication, and after evaluation of fuel purchases, a dramatic reduction in fuel consumption was also noted during the lubrication periods.

Evaluation of the data indicated, however, that a wide range of rail life could be obtained, depending on the effort applied to maintain proper lubrication. For standard carbon rail, gage face wear of 0.0251 in./MGT to 0.0016 in./MGT was observed. In addition, virtually no rail defects were observed during this 250-MGT test period. This was in sharp contrast to the previous 180-MGT period of FAST, which had been operated with virtually full lubrication from the time of rail installation and obtained a very high defect rate.

Another item added to this matrix includes a period of 107 MGT that was operated after the completion of the third rail experiment (immediately following the 250-MGT period with alternating lubricated and dry conditions). During this 107-MGT period the rail was again subjected to full lubrication under very tight controls. Absolutely no operation was permitted without gage face lubrication. Although predictions of a high defect rate were made, not one surface or subsurface defect was generated during this period. In addition, virtually no measurable wear was recorded.

The major difference between the second rail experiment and the extension of the third appears to be the condition of the

rail at the time that full lubrication was initiated. In the case of the second experiment, new rail was installed and immediately lubricated, with no dry operations of any great amount. During the extension of the third experiment, rail that had already been worn to a conformal profile with the FAST wheels was in place. Unfortunately, rail of the two periods was from a variety of manufacturers and chemistries, because the original intent of these tests was, of course, to study rail wear. To better study the effect of lubrication on rail fatigue, the DOG test was proposed and is being operated.

The lubrication, rail installation, and defect pattern observed are summarized in Table 1.

Control of Defects

The use of lubrication appeared to have a direct effect on development of rail defects. The DOG test was designed to provide fatigue occurrence information on a range of rails of controlled chemistry and manufacturing processes under a variety of steadily maintained levels of lubrication. Information would be used by the analyst to determine the relationship of defect occurrence with rail type and lubrication.

As of May 1987 this test had been subjected to just over 108 MGT of traffic. The defect occurrence rate has been extremely high, and will be reviewed in a later section.

WEAR RESULTS

Measurement Techniques

FAST has developed a series of instruments designed to obtain precision wear data at selected locations on the rail head. The wear rates of the gage face and head can be determined very accurately by precise (+0.003 in.) gages. Rail profiles are utilized to determine rail shape and head area loss, but are not sufficiently precise to be used for normal wear-rate determination in a short time period (40 to 60 MGT). With the use of these precision measurement tools, accurate wear rates for high wear-rate rails (>0.005 in./MGT) can be determined in 35 MGT or less, whereas low wear-rate rails (<0.005 in./MGT) generally will require a period of 50 to 60 MGT to obtain statistically significant wear rates.

Wear information is gathered every 10 to 12 MGT from all rails located in test curves operated with no lubrication. The

TABLE 1 GAGE FACE WEAR RATES AND FIGURES OF MERIT

Metallurgy	MGT in Service	GFW (With Both Rails Dry) Wear Rate	GFW FM	GFW (With Low Rail Lubricated) Wear Rate	GFW FM
STD 289	35-111	.007132		.002082	
STD 300	35-111	.007522		.001852	
BHN 300 Avg*	--	.007327	1.0	.001967	1.0
CrMo-A	0-111	.004191	1.7	.001754	1.1
CrMo-B	0-111	.004393	1.6	.001221	1.6
CrMo-C	0-71	.003652	2.0	---**	---
HH-A	0-111	.002874	2.5	.001309	1.5
HH-B clean	0-111	.003240	2.2	.001167	1.6
HH-C reg.	0-111	.003300	2.2	.001177	1.7
HH SiCr	0-111	.002537	2.8	.001278	1.5
HH CrSiV	71-111	***	---	.002175	.90
MnSiCrV	0-71	.006204	1.2	**	---
STD 248	0-35	.00887	.82	***	---
Low Mn	86-111	***		.005421	.36

Note: Wear rates are in inches per MGT.

*Replaced Standard Carbon rail at 35 MGT as baseline rail.

**Insufficient wear to obtain statistically significant wear rate.

***Removed/Not in place during this phase of test.

GFW - Gage Face Wear Rate

FM - Figure of Merit - Std. BHN 300 Rail - FM 1.0

HH - Head Hardened Rail

data are evaluated using standard linear regression techniques to determine a rate of change per MGT of applied traffic.

Wear-rate information is highly variable between different sites; thus most FAST data reports avoid presenting only wear-rate data, electing to rank results by a figure-of-merit (FM) process. The FM rating allows one to compare the net improvement (or reduction) in the particular wear parameter of interest with that of a given standard. For example, if at a given location the baseline rail is a standard carbon rail with a gage face wear rate of 0.0012 in./MGT, this is used as the baseline rate. The FM of the standard rail is 1.0. If CrMo and head-hardened (HH) rails in the same curve have wear rates of 0.0009 and 0.0006 in./MGT, respectively, the FM of CrMo rail would be 1.33 and that of HH rail would be 2. This would permit the reviewer to determine that under similar conditions of lubrication, a CrMo rail could be expected to last 1.33 times as long as standard rail, whereas HH rail would last about 2.0 times as long as standard.

The actual wear rate obtained at any given location is highly dependent on field conditions (lubrication, unbalance speed, etc.). However, the FM allows one to judge what improvement in rail life can be expected of a premium rail over that of the baseline rail.

For FAST data, standard carbon rail [most recently, standard rail with a Brinell Hardness Number (BHN) of 285] is used as the baseline rail and by default has a FM rating of 1.0. All other rails are then compared with the standard rail.

Recent Results

The current rail wear test is located in Section 7 of the HTL track (Figure 3). Section 7 consists of a 5-degree curve 1,000+ ft long with 4 in. of superelevation on a -0.05 percent grade in the direction of predominant traffic. Train direction for the test period has been very uniform, 44 to 45 mph for the 0- to 61-MGT period and 40 mph from 61 MGT to the present (170 MGT). Almost all trains consist of four 4-axle locomotives

and 70 to 80 loaded hopper cars with 100-ton capacity. A few empty cars have been periodically placed in the consist. Track is constructed with wood ties spaced at 19½ in. on center using conventional cut spikes and tie plates with timber cross ties on slag ballast 18 in. deep.

Test rails are 136/132 lb/yd American Railroad Engineering Association (AREA) section. The initial rail profile usually disappears within 5 MGT of dry operation and takes on a uniform worn profile similar to that of all FAST current rails; thus profile and section differences are not addressed in this test.

The most recent results from the dry wear portion of the HTL track are presented in Tables 1–3. As will be discussed in the next section, the change in the operation of the FAST loop to the HTL loop was a significant difference in rail wear rates. The effect of mild contamination on the low rail of the curve from lubrication of the outside rail of the HTL for defect studies was a significant reduction in the gage face wear of the high rail.

Tables 1–3 present wear rates and FM's for rails evaluated during dry high rail tests. Results for gage face wear are presented, as well as high-rail and low-rail head height loss.

Because standard carbon 248-BHN rail is no longer considered a baseline rail (generally being replaced by 285- to 300-BHN rail by the railroad industry), all data after 35 MGT are compared with 300-BHN rail. As can be seen in Table 1, under dry rail operation the 300-BHN rail provides about 20 percent more gage face rail life than standard 248 BHN. The head height loss rate for the 300-BHN rail is higher than that for 248-BHN rail, however, indicating that the rail has not sufficiently work hardened after the relatively short MGT period that these data represent. The dry, uncontaminated data for the 300-BHN rail are based on only the initial 25 MGT of traffic. A longer test period would have been desirable to obtain more statistically significant wear rates. The wear rates were relatively low, generally 1/10 of the gage face rates, resulting in data with somewhat less statistical significance than the gage

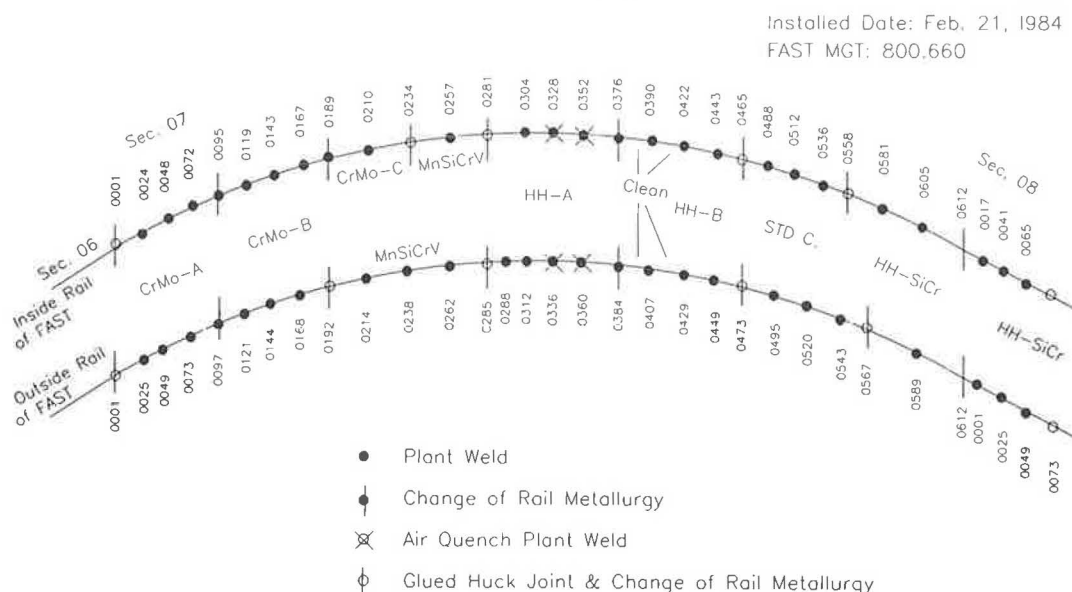


FIGURE 3 Rail wear layout—Section 7: rail metallurgy layout in relation to ties.

TABLE 2 HIGH RAIL HEAD HEIGHT WEAR RATES AND FIGURES OF MERIT

Metallurgy	MGT in Service	HL (With Both Rails Dry) Wear Rate	HL FM	HL (With Low Rail Lubricated) Wear Rate	HL FM
STD 289	35-111	.002580		.001344	
STD 300	35-111	.002201		.001053	
BHN 300 Avg*	--	.002393	1.0	.001199	1.0
CrMo-A	0-111	.000626	3.8	.000715	1.7
CrMo-B	0-111	.000871	2.7	.000884	1.4
CrMo-C	0-71	.000835	2.8	**	---
HH-A	0-111	.000283	8.4	.000242	4.9
HH-B clean	0-111	.000634	3.7	.000332	3.6
HH-C reg.	0-111	.000551	4.3	.000358	3.3
HH SiCr	0-111	.000183	13.0	.000163	7.4
HH CrSiV	71-111	***	---	.000112	1.1
MnSiCrV	0-71	.001239	1.9	**	---
STD 248	0-35	.001992	1.2	***	---
Low Mn	86-111	***	---	.001717	0.70

Note: Wear rates are in inches per MGT.

*Replaced Standard Carbon rail at 35 MGT as baseline rail.

**Insufficient wear to obtain statistically significant wear rate.

***Removed/Not in place during this phase of test.

HL - Head Height Loss Wear

face wear data. Figure 4 shows the overall test sequence in a bar chart format.

Low-Rail Contamination

The initial 61 MGT of traffic over this test zone was operated with both rails dry. At the start of HTL operations, the outside rail of the HTL was lubricated by trackside lubricators. Because the RWF section is a reverse curve, the high rail remained dry, and the low rail received some mild lubrication contamination. Measurements using a tribometer to determine the top-of-rail coefficient of friction indicated typical coefficients as follows:

Rail Location	Top-of-Rail Friction	Occur- rence (%)	Notes
High	0.49-0.51	98	Dry
High	0.35-0.45	2	Some contamination when train is turned
Low	0.35-0.45	80	Contaminated
Low	0.20-0.25	15	Excess lubrication; misadjusted lubricator
Low	0.49-0.51	5	Dry, during dry down for rail flaw inspections

Because about 80 percent of the operation after 61 MGT is with a contaminated low rail, a separate wear rate for all rails was computed for all operation after 61 MGT. The effect of this contamination is dramatic (Table 4). In this case, FM numbers compare the same rail metallurgy between different test periods. The gage face wear for standard rail was reduced by up to a factor of 3.7, even though a very mild level of lubrication was present only on the low rail.

DEFECT STUDIES

General

Rail located on severely curved track generally will be replaced because of wear before failure from internal defects. To combat this wear, lubrication or the use of profile grinding, or both, has been suggested. At FAST, lubrication has been shown to extend rail life; however, little documented information on the effects of profile grinding on long-term rail life at FAST is available.

A profile grinding experiment, operated for 20 MGT, was performed under dry conditions in order to accelerate the wear rates. The results of this test indicated that a significant reduction in high-rail gage face wear rates can be achieved. However, the duration of the test was insufficient to determine whether fatigue problems could also be controlled. The ground profiles generally remained fully effective for only 10 MGT

TABLE 3 LOW RAIL HEAD HEIGHT WEAR RATES AND FIGURES OF MERIT

Metallurgy	MGT in Service	HL (With Both Rails Dry) Wear Rate	HL FM	HL (With Low Rail Lubricated) Wear Rate	HL FM
STD 289	35-111	.002248		.000246	
STD 300	35-111	.001791		.000243	
BHN 300 Avg*	--	.002091	1.0	.000245	1.0
CrMo-A (136)	0-111	.000726	2.7	.000244	1.0
CrMo-A (132)	0-111	.000846	2.4	.000111	2.2
CrMo-B	0-111	.000855	2.4	.000233	1.0
HH-A	0-111	.000329	6.1	.000141	1.7
HH-B clean	0-111	.000623	3.2	.000006	40.7**
HH-C reg.	0-111	.000600	3.3	.000093	2.6
HH SiCr	0-111	.000369	5.7	.000117	2.0
HH CrSiV	71-111	***	---	.000076	3.2
Mn SiCrV	0-71	.000769	2.6	**	---**
STD 248	0-35	.001754	1.2	***	---
Low Mn	86-111	***	---	.000542	0.45

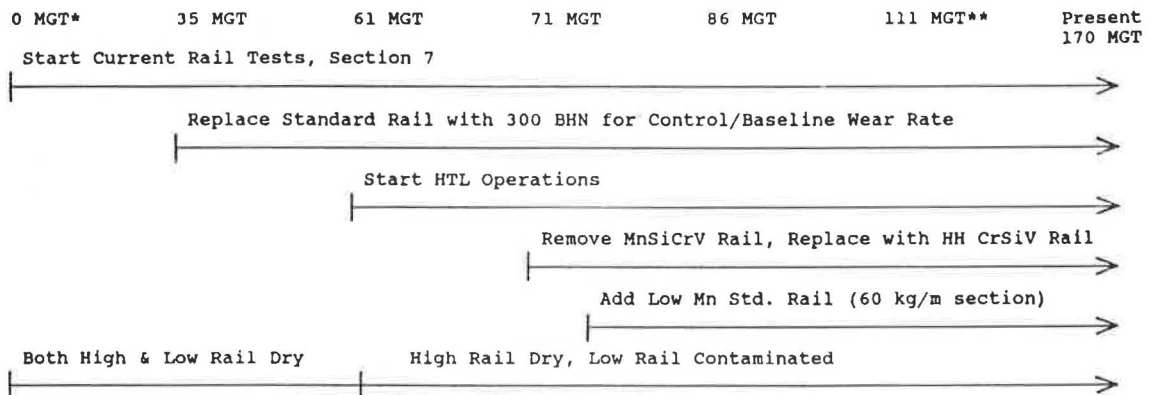
Note: Wear rates are in inches per MGT.

*Replaced Standard Carbon rail at 35 MGT as baseline rail.

**Insufficient wear to obtain statistically significant wear rate.

***Removed/Not in place during this phase of test.

HL - Head Height Loss Wear



*0 MGT Rail Test = 800 MGT overall FAST MGT.

**Data for this report current to 111 MGT.

FIGURE 4 Sequence of FAST/HTL operations—rail wear test.

and were completely removed after 20 MGT (dry operation); therefore the long-term effects were not addressed. A possible repeat of part of this experiment during lubricated operation has been suggested.

The danger of rail fatigue is that its effects are generally hidden from view, and inspections require specialized tech-

niques such as ultrasonic inspection. The use of ultrasonics is widespread in the railroad industry, but has several drawbacks. Paramount among these is that the rail-ultrasonic probe interface must be clean. Excess lubrication, dirt, or grease will interfere with normal signals and could hide potentially dangerous flaws.

TABLE 4 EFFECT OF LOW RAIL LUBRICATION ON WEAR DATA FIGURES OF MERIT

Metallurgy	High Rail GFW	High Rail HL	Low Rail HL
STD 289	3.4	1.9	9.1
STD 300	4.0	2.1	7.4
BHN 300 Avg*	3.7	2.0	8.2
CrMo - A(136)			2.9
CrMo - A(132)	2.3	.87	7.6
CrMo - B	3.5	.98	3.7
HH - A	2.2	1.2	2.3
HH - B clean	2.7	1.9	103.9**
HH - C reg	2.8	1.5	6.4
HH - SiCr	2.0	1.1	3.2
HH - CrSiV	---	---	---
MnSiCrV	---	---	---
STD 248	---	---	---
Low Mn	---	---	---

Note: FM is comparison of dry to contaminated wear rate periods.
Baseline is dry period, e.g., FM = (GFW : Dry) (GFW : Lubricated).
Wear rates in Table 3 were utilized for these FM values.

*Replaced Standard Carbon rail at 35 MGT.

**Data Scatter results in statistically insignificant wear rate.

Only Rails in place for sufficient time to obtain significant wear rates during both periods are shown.

GFW - Gage Face Wear

HL - Head Height Wear

Rail defects that are monitored by the FAST/HTL program fall into two broad categories: surface defects (visible to the eye) and subsurface defects. Surface defects generally include spalls, chips, cracks, and severe metal flow. Shells, even when visible, are catalogued as subsurface defects; their origin is almost always below the surface. Major subsurface flaws include shells, transverse defects, and detail fractures.

Rail Fatigue—Dry Wear Test Zone

An important aspect of rail life is its fatigue limit. Wear life is but one limiting factor used when deciding when to replace rail. The dry regime is intended to accelerate the wear rate of rail; however, some test rails have developed surface fatigue discontinuities such as chips, spalls, and head checks before wearing out. As of this date these defects have not led to rail fatigue failure in the dry wear test Section 7 nor do they warrant removal of the rail; nevertheless, the defects are being monitored. No subsurface defects other than weld failures have been discovered in the current dry wear test to date.

Surface fatigue defects have been observed on the high rail of 300-BHN rail (after about 60 MGT of service), the low rail of SiCr-HH rail (after about 85 MGT of service), and the high

rail of the CrSiVd rail. The following field observations were made:

- 300-BHN Rail—The surface conditions of concern are 45-degree head checks approximately $\frac{5}{8}$ to $\frac{3}{4}$ in. long located entirely on the gage corner of the high rail. No lubrication has ever been applied here. Coalescence of the head checks caused a significant amount of gage corner flaking over about 20 ft of the total 160-ft-long installation.
- SiCr-HH Rail—The surface conditions of concern are severe spalling and metal flow located on top of one of the low rails near the gage corner. Approximately 15 ft of the rail located in the spiral is affected.
- CrSiVd-HH Rail—Surface conditions on the top center of the high rail indicate severe spalling after about 75 MGT of service. Approximately 40 ft of spalling has developed.

Lubricated-Rail Defect Rates

The DOG test was purposely laid out to develop internal rail defects. In this respect, the experiment has been an unqualified success; after 100 MGT more than 100 internal defects have been discovered and monitored in 3,600 ft of test rail. Data

collected during this test will allow the history of many flaws to be documented in detail, with post-test flaw examination and analysis. The information presented in Tables 5 and 6 indicates the effects of differential lubrication on wear and flaw generation during the initial 100 MGT of this test for a total of about 1,800 ft of track.

Table 5 provides information as to gage face wear rates of standard carbon 248-BHN rail operated dry, and from the three areas of controlled lubrication in the DOG test. Segments A, B, and C are from the 6-degree (Section 25) outside rail, whereas the dry wear data are from Section 7, a 5-degree curve. The improvement in life of 248-BHN rail from dry to moderately lubricated in this case is a factor of 74; full, continuous lubrication resulted in an improvement of at least 445 times. These are net improvements in gage face wear only.

As can be seen, rail near the lubricator has virtually no measurable wear in 100 MGT of exposure. A total of about 0.00002 in. of metal has been removed from the gage face, which is less than can accurately be measured with the TTC gages. The other rails, located farther away from the lubricator, show significantly more wear but are still much more protected than rail in the dry wear test.

Table 6 shows the total number of shells and transverse defects (TDs) discovered on the test rails that are located near and far away from the lubricator during the initial 80 MGT of testing; Table 7 shows the totals for the 110-MGT period.

Most of these rails are similar to the 285- to 300-BHN rails in wear rates, as shown in Table 5. The middle segment (B) is not included here because the gage corner of this segment was ground, and the effects of lubrication and grinding are mixed.

Tables 6 and 7 indicate that mild wear (0.00012 in./MGT) had a dramatic effect in reducing the number of shells. The TD development rate is somewhat low, but data during the most recent 30 MGT indicate that this defect rate is now increasing. It should be noted that the standard rail, located in Section 7, had a wear rate of about 0.0089 in./MGT. This rail was removed from the test after 35 MGT of traffic because almost 0.33 in. of actual gage face wear had been experienced. At the

wear rate observed in the lubricated test, over 2,500 MGT would be required to obtain the same hypothetical 0.33 in. of gage face wear. Obviously, the rail fatigue life has replaced the wear life limit in this case.

In both lubricated cases, the rail metallurgy, manufacturer, and heat are identical or nearly identical (when available rail from identical heats was selected); thus the major variable has been reduced to lubrication/rail wear.

The standard carbon rail is a 248-BHN rail left over from earlier FAST tests. This and all other rail for the DOG test were new when installed. The 248 rail was installed as a control and, having been rolled in 1979, is not considered state of the art as far as rail quality. The FAST program has always utilized this type of rail, and it was selected for placement to act as a control and provide a benchmark to compare with past rail data.

Table 8 shows the head height loss wear rates for the same rails. The wear rates for the outside rail show some difference between ends of the curve, but the difference is too small to be statistically significant.

DISCUSSION

Only a small portion of the entire DOG test data base being collected has been reviewed here. A major study is also being conducted in this same area to assess the effect of grinding. Of the data presented, an overriding observation is that there is a definite difference in rail behavior between the heavily lubricated and less lubricated areas. The results initially lead one to deduce that lubrication is detrimental and brings about relatively rapid flaw occurrence in rails. The history of FAST does not necessarily agree with this, however, because rails at the end of the third metallurgy experiment were subject to the same lubrication pattern, but only after several dry periods totaling 10 to 30 MGT, depending on rail type. Table 9 gives defect history from rail lubrication.

The current DOG test is scheduled to continue a fully lubricated operation until a total of 150 MGT has been applied. At that time, significant changes in the operation of the

TABLE 5 GAGE FACE WEAR RATES OF 248-BHN RAIL

<u>Rail Conditions</u>	<u>Wear Rate</u>	<u>FM Based on Dry</u>
Dry*	.0089	1
Fully lubricated-near lubricator	.00002	445
Fully lubricated-1500' from lubricator**	.00006	15
Fully lubricated-2800' from lubricator	.00012	74

Wear Rate expressed in inches/MGT.

* 5 degree curve - all others 6 degree curve.

**Rail with gage face profile grinding.

TABLE 6 EFFECT OF LUBRICATION ON RAIL DEFECTS, 6-DEGREE CURVE: 80-MGT DATA

Rail Metallurgy	Low Wear Rate Area*			High Wear Rate Area*		
	Lubrication Always Present On Top of Rail/Gage Face (High Lube Level)			Lubrication Only On Gage Face (Low Lube Level)		
	No. of Shells	No. of T.D.'s	No. of Surface Defects	No. of Shells	No. of T.D.'s	No. of Surface Defects
Std. 248	13	2	5	1	0	0
Std. 264	0	0	0	0	0	0
Std. 269A	0	0	0	0	0	0
Std. 269B	0	2	2	0	0	1
Std. 269C	1	1	0	0	0	0
Std. 264D	0	0	0	0	0	0
Std. 272	0	0	0	0	0	0
Std. 273	1	1	0	0	0	1
Std. 280	0	0	0	0	0	0
Std. 283	0	0	0	0	0	0
Std. 285	0	0	0	0	0	0
Std. 289	0	0	1	0	0	1
Std. 300	0	0	0	0	0	0
Std. HH	1	0	0	0	0	0
TOTAL	16	6	8	1	0	3

*GFW of High Wear Rate : 258 Std. Rail 0.00012"/MGT

GFW of Low Wear Rate : 248 Std. Rail 0.00002"/MGT

HTL will occur, the most dominant being a change to a heavy axle load (HAL). The current limit of 33 kips per wheel will be increased to 39 kips per wheel. This will be accomplished by obtaining a new set of cars and simulating a load of what has been generically referred to as a 125-ton capacity car. Selected rails currently part of the DOG test will remain in test, and a number of new rails will also be installed.

Data analysis of flaw occurrence during the initial 150-MGT phase will be performed to determine defect origins and provide information as to rail quality required for operation in the low wear mode.

The rail wear and fatigue test will continue, with emphasis on rail life under the HAL environment. Rail wear and surface fatigue under a nonlubricated condition are expected to suffer

from the HAL, especially in the head-crushing and metal-flow mode. An increase in these rates could lead to increased failures because surface anomalies turn into the rail head and cause severe spalls and chips.

FIELD CORRELATION

General

TTC has been involved with a number of field correlation studies. These sites have been offered by host railroads as locations to evaluate rail wear in the field under revenue service conditions. To date, two such studies have been completed, and the results of the most recent study indicate significant correlation with FAST results, both in the relative ranking of wear and the effects of lubrication.

TABLE 7 EFFECT OF LUBRICATION ON RAIL DEFECTS, 6-DEGREE CURVE: 110-MGT DATA

Rail Metallurgy	<u>Low Wear Rate Area*</u> Lubrication Always Present On Top of Rail/Gage Face (High Lube Level)			<u>High Wear Rate Area*</u> Lubrication Only On Gage Face (Low Lube Level)		
	No. of Shells	No. of T.D.'s	No. of Surface Defects	No. of Shells	No. of T.D.'s	No. of Surface Defects
Std. 248	48	2	12	24	0	9
Std. 264	0	0	5	0	0	0
Std. 269A	1	0	0	0	0	4
Std. 269B	0	3	4	0	1	5
Std. 269C	1	5	2	0	0	0
Std. 269D	0	0	0	0	0	0
Std. 272	0	0	0	0	0	0
Std. 273	6	1	2	0	0	3
Std. 280	0	0	0	0	0	0
Std. 283	0	0	0	0	0	0
Std. 285	0	0	1	0	0	2
Std. 289	4	0	2	0	0	1
Std. 300	0	0	2	0	0	0
Std. HH	1	0	0	0	0	0
TOTAL	61	11	30	24	1	24

*GFW of High Wear Rate : 258 Std. Rail 0.00012"/MGT

GFW of Low Wear Rate : 248 Std. Rail 0.00002"/MGT

TABLE 8 HEAD HEIGHT WEAR RATES OF 248-BHN RAIL

<u>Rail Condition</u>	<u>High Rail</u>	<u>Low Rail</u>
Dry*	.002	.0018
Fully Lubricated - Near lubricator	.00038	.0024
Fully Lubricated - 1500' from lubricator	.00047	.002
Fully Lubricated - 2800' from lubricator	.00041	.002

*5 degree curve - all others 6 degree curves.

Wear Rates are expressed in inches/MGT.

TABLE 9 QUALITATIVE DEFECT OCCURRENCE PATTERN—RAIL TESTS

Approximate Time Period	MGT of Test	Rails and Type of Lubrication	Defect History
1978-1979	180	Installed new rails. Full lubrication from onset of rail lubrication.	High rate of occurrence.
1979-1981	250	Installed new rails. Alternating periods of lubrication (40 MGT) and dry (10 MGT).	Very low rate.
1982	107	Same rails as above but ran only Fully Lubricated.	No defects.
1985-Present	110 & ongoing	Installed new rails. Full lubrication at all times.	High rate of occurrence.

Western Railroad Correlation

A site was offered on a western railroad that contained two 4-degree curves; seven metallurgies were installed on each curve (6). The overall goal of this test was to evaluate the rails as well as to determine the effect of lubrication.

Details of this test are included in the Association of American Railroads (AAR) report (7). The basic ranking of the rails is presented here. The eastbound curve of this test was evaluated for a total period of 42 MGT, during which the initial 23 MGT was operated dry and the final 19 MGT was operated lubricated. The test results indicated that lubrication was not fully effective; however, even the small amount applied had a dramatic effect on rail life, especially for the high wear-rate rails (standard 285 BHN). Table 10 shows the gage face wear rates of the eastbound curve for the dry and lubricated periods. As can be seen, the FMs of the dry period are considerably higher than those of the lubricated period, which follows the FAST results, in which lubrication tends to make different rails more equal in gage face wear.

Table 11 shows the effect of lubrication on gage face wear for the eastbound curve test rails. As can be seen, the standard 285-BHN rail received the most benefit. The improvement in gage face wear life with proper lubrication has been documented in the range of 10 to 80. The improvement seen at this site indicates that only marginal lubrication was present. The fact that the premium rails received little or no improvement confirms this conclusion. The overall ranking of rail fits the general trend observed at FAST, as follows:

1. Best: heat-treated rails,
2. Second: alloy rails, and
3. Worst: standard rails.

The site controls of this particular revenue service test were such that no more detailed ranking than that above can be

stated with any confidence. The differential wear between ends of the curve, due to a variation in train speed and lubrication, was so great that actual numbers derived from the data cannot be utilized directly for ranking. Depending on the test period, one end of the curve or the other indicated a 25 to a -12 percent wear differential. These data are obtained from the control rail measurements obtained at each end of the test zone. The control rail gage face wear rates for the entire 42-MGT test period and the dry test period are as follows:

	Entire Test	Dry Period Only
West end	0.003121	0.005043
East end	0.003509	0.004041
Differential (West/East) (%)	-12	25

The results of this field service test indicate that lubrication does indeed have a dramatic effect on rail life but that to obtain valid data for rail assessment, controlled conditions are essential. The advantage of FAST is that train speed and lubrication conditions are controlled as well as documented, so that assessment of rail performance can be made with the proper statistical background.

SUMMARY AND CONCLUSIONS

FAST tests to date have provided a wealth of rail wear and fatigue data. The relative merits of different rail types have been documented under a variety of operating conditions. Ranking of rail has been standardized and compared with normal 285-type rail, allowing the user to determine the optimum rail for various conditions. The effect of lubrication has been documented. It has a dramatic effect on wear life and, if not properly controlled, can extend rail life to the point at which fatigue becomes the dominant replacement criterion.

TABLE 10 EASTBOUND DATA, GAGE FACE WEAR: WEAR RATES AND FM VALUES FOR DRY AND LUBRICATED PERIODS

Metallurgy	Dry Period		Lubricated Period	
	Wear Rate	FM	Wear Rate	FM
1) STD 285 BHN	.008466	1.0	.002958	1.0
2) Chrome Moly A	.002442	3.5	.002075	1.4
3) Flame Head Hardened	.000756	11.2	.000989	2.9
4) Chrome Moly B	.002978	2.8	.002039	1.5
5) Chrome Vanadium	.004698	1.8	.002971	1.0
6) Induction Head Hardened	.001631	5.2	.001202	2.4
7) Fully Heat Treated	.002716	3.1	.001773	1.7
8) East Control	.004041	2.0	.002566	1.2
9) West Control	.005043	1.7	*	*

Note:

Wear data expressed in inches of gage face wear at 5/8" below top of rail running surface.

*Insufficient wear to determine statistically significant wear rate.

TABLE 11 EASTBOUND CURVE DATA ON EFFECT OF LUBRICATION: FM VALUES FOR LUBRICATED VERSUS DRY PERIODS

1) STD 285 BHN	2.9
2) Chrome Moly A	1.2
3) Flame Head Hardened	.8
4) Chrome Moly B	1.5
5) Chrome Vanadium	1.6
6) Induction Head Hardened	1.4
7) Fully Heat Treated	1.5
8) East Control	1.6
9) West Control	*

*Insufficient data to determine statistically significant wear rate.

Limited field correlation tests validate the basic results of FAST tests but generally are difficult to interpret because of a variety of uncontrolled influences that are part of revenue service train operation.

Future FAST/HTL rail testing will be directed at monitoring the effects of HAL on rail of different profiles operated under a variety of lubrication patterns for extended periods of traffic.

REFERENCES

1. *Proceedings, FAST Engineering Conference 1981*. Report FRA/TTC-82/01. Federal Railroad Administration, U.S. Department of Transportation, 1982.
2. R. K. Steele and R. P. Reiff. *Rail—Its Behavior and Relationship to Total System Wear*, Paper 82-HH-24. Proceedings of the Second International Heavy Haul Railway Conference, Sept. 1982.
3. R. P. Reiff. Lubrication Applications Systems Tests at FAST. Presented at Winter Annual Meeting, American Society of Metallurgical Engineering, New Orleans, Dec. 1984.
4. K. C. Rownd and R. P. Reiff. *Illinois Central Gulf Tangent Track Lubrication Test*. AAR Report R-623. Association of American Railroads, Washington, D.C., Oct. 1985.
5. Conrail Rail/Wheel Lubrication Study Savings. *AAR Energy News*, No. 6, July 1984.
6. R. P. Reiff. Measuring Rail Wear the FAST Way. *Railway Track Structures*, Sept. 1983.
7. R. P. Reiff. Union Pacific Rail Wear Lubrication Demonstration Project. AAR Report. Association of American Railroads, Washington, D.C., 1987.